Mara Lisa Miranda Marques

Licenciada

Monotherapy and combined therapy of new potential antitumor compounds: antiproliferative activities and biological targets

Dissertação para obtenção do Grau de Mestre em

Genética Molecular e Biomedicina

Orientador: Prof. Doutora Maria Alexandra Núncio de Carvalho Ramos Fernandes, FCT/UNL

Presidente de Júri: Prof. Doutor José Paulo Nunes de Sousa Sampaio

Arguente: Doutor Pedro Miguel Martinho Borralho

Vogal: Prof. Doutora Maria Alexandra Núncio de Carvalho Ramos Fernandes

FACULDADE DE CIÊNCIAS E TECNOLOGIA
UNIVERSIDADE NOVA DE LISBOA

Dezembro 2014

Mara Lisa Miranda Marques

Licenciada

Monotherapy and combined therapy of new potential antitumor compounds: antiproliferative activities and biological targets

Dissertação apresentada na Faculdade de Ciências e Tecnologias da Universidade Nova de Lisboa para a obtenção do Grau de Mestre em Genética Molecular e Biomedicina

Orientador: Professora Maria Alexandra Núncio de Carvalho Ramos Fernandes, FCT/UNL

Presidente de Júri: Prof. Doutor José Paulo Nunes de Sousa Sampaio

Arguente: Doutor Pedro Miguel Martinho Borralho

Vogal: Prof. Doutora Maria Alexandra Núncio de Carvalho Ramos Fernandes

Universidade Nova de Lisboa

Faculdade de Ciências e Tecnologias

Departamento de Ciências da Vida

Monte de Caparica

Dezembro 2014

Thesis publication

Review article

Martins, P., Marques, M., Coito, L., Pombeiro, A.J.L., Baptista, P.V., Fernandes, A.R. 2014. Organometallic Compounds in Cancer Therapy: Past Lessons and Future Directions. Anti-cancer Agents in Medicinal Chemistry 14. PMID: 25173559.

Monotherapy and combined therapy of new potential antitumor compounds: antiproliferative activities and biological targets.

Acknowledgments

I would like to express my gratitude to my supervisor, Professor Alexandra Fernandes, whose expertise and assistance in writing this thesis added considerably to my graduate experience. I appreciate her vast knowledge in this field, and I would like to thank Professor Alexandra Fernandes for taking time out from her busy timetable to help me with this work.

I must also acknowledge Joana Silva for her guidance and presence along this year, supporting me with her experience and knowledge in the laboratory.

I would like to thank Catarina Rodrigues and Luís Raposo for their guidance in proteomics and, in alphabetical order, Ana Mendo, Carmen Gomez, Lídia Coito and Pedro Martins for their accessibility and exchanges of knowledge.

I would also like to thank to the Glycoimmunology Group of the Faculty of Medical Sciences in Lisbon, the Photochemistry and Supramolecular Chemistry Research Group and NanoTheranostics Group in FCT/UNL for their empathy and support, providing facilities for some experiments of this thesis.

Finally, I would like to express my gratitude and admirance to my closest relatives for all the support and advices given during all my life.

Abstract

The *in vitro* antiproliferative potential of three new oxorhenium complexes in particular compounds 1 ($[ReO_3(PTA)_2][ReO_4]$) and 2 ($[ReO_3(HMT)_2][ReO_4]$) bearing the 1,3,5-triaza-7-phosphaadamantane (PTA) and the hexamethylenetetramine (HMT) ligands, respectively, and compound 3 ([ReO(Tpms)(HMT)]) bearing the tris(pyrazol-1-yl)methanesulfonate (Tpms) and HMT ligands, was evaluated in several cancer cell lines and fibroblasts. Compound 4, which is in a pending patent, bearing the trimeric polythiophene acetic acid (tPTAA) ligand, was also evaluated.

The rhenium compound 2 showed the best results on the colorectal cancer cell line with a relative IC_{50} of 88.6 +/- 7.1 μM.

Combined therapy using compound 2 and doxorubicin lead to a reduction of ~1.5x in the percentage of cell viability compared to doxorubicin alone. The combined therapy with compound 4 and cisplatin lead to a reduction of almost 3x in the percentage of cell viability compared with cisplatin alone.

Based on the spectroscopic titration with calf thymus DNA and the results of the electrophoretogram with plasmid DNA is proposed that compound 2 interacts weakly with ct-DNA and it has a non-covalent mode of binding. Furthermore, the low binding constant ~10^5 suggests that the interaction between the metal complex and DNA might not be intercalative in nature.

The fluorescence quenching assay of Human Serum Albumin showed a relatively moderate interaction between compound 2 and Human Serum Albumin with an average value of binding constant of the protein-quencher complex of 3.10 (+/- 1.2) x 10^3 M^{-1}.

According to the comparative proteomic results, colorectal cancer cells exposed to compound 2 were more sensitive and prone to cell death due to alterations in the relative abundance of some heat shock proteins, a small GTPase and tubulin. On the other hand, Ezrin protein was more abundant on colon cancer cells exposed to compound 2 what could be an adaptive response inhibiting apoptosis. Proliferation-associated protein 2G4 overexpression might indicate that compound 2 triggers cell death by cell cycle arrest.

Tumor cell death was also evaluated. According to the results of fluorescence microscopy, compound 4 was more effective in killing tumour cells than compound 2. Apparently, apoptosis is not the main mechanism of cell death for compound 2 with 4.15 +/-1.16 % of apoptotic cells by Hoechst staining assay and 1.4% of early apoptotic cells and 13.3% of late apoptotic cells for cells exposed to compound 2 in the flow citometry.

Keywords: Cancer, Cisplatin, Citotoxicity, Combined Therapeutics, Doxorubicin, Rhenium

Table of contents

List of figures

List of tables

Abreviations

1433z	14-3-3 protein zeta
acac	acetylacetonate
ACTG	Actin Gamma 1 protein
AMPL	Cytosol aminopeptidase
ANXA2	Annexin A2 protein
APC	Adenomatous polyposis coli
ATCC	American Type Culture Collection
Bak	Bcl-2 homologous antagonist/killer
Bax	Bcl-2-like protein 4
Bcl-2	B-cell CLL/lymphoma protein 2
Bcl-x_L	Bcl-2-like protein 1 isoform
Bim	Bcl-2-like protein 11
CALR	Calreticulin protein
c-MET	Hepatocyte growth factor receptor
CSCs	Cancer Stem Cells
Ct-DNA	Calf Thymus-DNA
DHE3	Glutamate dehydrogenase
DMEM	Dulbecco's Modified Eagle Medium
DMSO	Dimethylsulfoxide
DTT	Dithiothreitol
ECM	Extracellular Matrix
EDTA	Ethylenediamine tetraacetic acid
EGF	Epidermal Growth Factor
EMT	Epithelial–mesenchymal transition
ENOA	Alpha-enolase protein
ENPL	Endoplasmin
EZRI	Ezrin protein
FDA	Food and Drug Administration
GLUT1	Glucose transporter 1 protein
GRP75	75 kDa glucose regulated protein
HER	Epidermal growth factor receptor
HMT	Hexamethylenetetramine
HSA	Human Serum Albumin
HSP	Heat Shock Protein
HSP7C	Heat shock cognate 71 kDa protein
IARC	International Agency for Research on Cancer
IC_{50}	Half maximal inhibitory concentration
IEF	Isoelectric focusing
IGF-1R	Insulin-like growth factor 1 receptor

IF4A2	Eukaryotic initiation factor 4A-II
KRAS	Kirsten Rat Sarcoma viral oncogene
MALDI-TOF	Matrix Assisted Laser Desorption/Ionization-Time of Flight
MAPK	Mitogen-Activated Protein Kinase
MAPs	Microtubule-associated proteins
MMP-9	Matrix Metalloproteinase-9
MTS	3-(4,5-dimethylthiazol-2-yl)-5-(3-carboxymethoxyphenyl)-2-(4-sulfophenyl)-2H-tetrazolium
MYC	v-myc avian myelocytomatosis viral oncogene homolog
MW	Molecular Weight
Nd-YAG	Neodymium-doped yttrium aluminium garnet
NF1	Neurofibromin 1 tumour suppressor
NF2	Neurofibromin 2 gene (Merlin)
NSCLC	Nonsmall cell lung cancer
P4HB	Prolyl 4-hydroxylase beta polypeptide
PA2G4	Proliferation-associated protein 2G4
PBS	Phosphate buffered saline
PDIA3	Protein disulfide isomerase family A member 3
PI3K	Phosphatidylinositol-3 Kinase protein
PIK3CA	Phosphatidylinositol-4,5-bisphosphate 3-kinase, catalytic subunit alpha
PMS	Phenazine methosulfate
PMSE1	Proteasome activator subunit 1 protein
PMSF	Phenylmethanesulfonyl fluoride
PTA	1,3,5-triaza-7-phosphaadamantane
PTEN	phosphatase and tensin homolog tumour suppressor
PUMA	Bcl-2 binding component 3
PUR9	Bifunctional purine biosynthesis protein
RAF	Raf-1 proto-oncogene, serine/threonine kinase
RANG	Ran-specific GTPase-activating protein
RAPTA	Ruthenium(II)−Arene PTA Complexes
RAS	Retrovirus associated sequence oncogene
RB	Retinoblastoma-associated protein
Re	Rhenium
RPM	Rotations per Minute
ROS	Reactive Oxygen Species
RSSA	40S ribosomal protein SA
RTK	Receptor tyrosine kinase
SDS-PAGE	Sodium Dodecyl Sulfate-Polyacrylamide Gel Electrophoresis
TNF-α	Tumor Necrosis Factor

SCLC	Small cell lung cancer
SEM	Standard Error of the Mean
SGTA	Small glutamine-rich tetratricopeptide repeat-containing protein alpha
SHC	Src Homology 2 Domain Containing pathways
SI	Selectivity Index
SSCs	Semicarbazones
STIP1	Stress-induced-phosphoprotein 1
TBA1B	Tubulin alpha-1B chain protein
TCPG	T-complex protein 1 subunit gamma
TEMED	Tetramethylethylenediamine
TGF-α	Transforming Growth Factor
TP53	Tumor Protein p53
Tpms	Tris (pyrazol-1-yl)methanesulfonate
tPTAA	trimeric polythiophene acetic acid
TSP-1	Thrombospondin- 1 protein
VEGF	Vascular Endothelial Growth Factor
VHL	von Hippel-Lindau tumor suppressor
WHO	World Health Organization

1 Introduction

1.1 Cancer in numbers

Cancer is one of the main causes of death. According to the World Health Organization, 8.2 million people worldwide died from cancer in 2012, although the chemotherapeutic agents available (International Agency for Research on Cancer (IARC), 2012). The trend for the Estimated Global Cancer Burden, according to the data since 1980 (**Figure 1.1**), is a considerable increase, even though the public health action by governments and health practitioners. In addition, current chemotherapeutic agents are highly toxic. This indicates the need of new pharmaceuticals with reduced toxicity and more effective therapeutics.

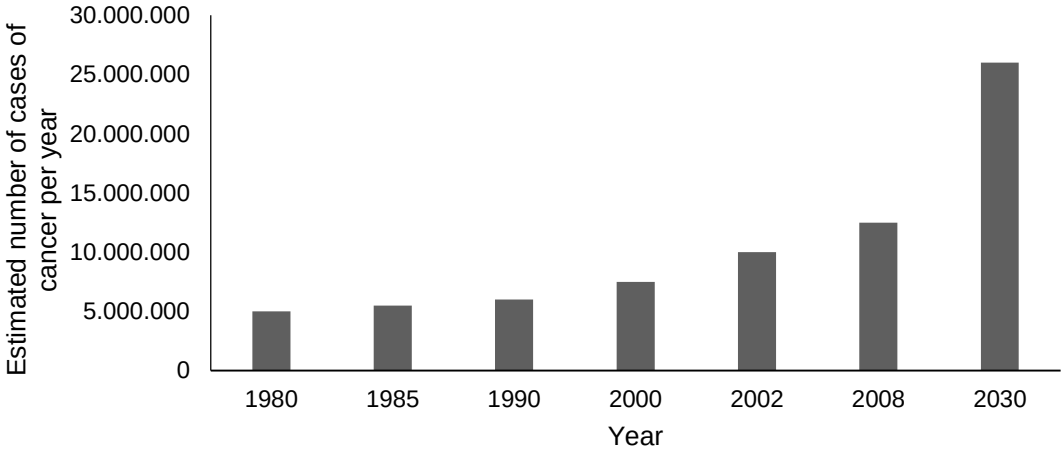

Figure 1.1 Estimated Global Cancer Burden: number of new cases of cancer per year (adapted from IARC, 2008). The figure shows data from 1980, 1985, 1990, 2000, 2002, 2008 and a prevision for 2030 (IARC, 2008).

The difference between developed and developing countries is reflected on the incidence of specific types of cancer. Richer countries have incidence rates of cancer more than the double in relation to developing countries. Europe and America are the regions with the highest incidence of all forms of cancer. Lung (1.59 million deaths, 19.4% of the total), liver (745.500 deaths, 9.1% of the total), stomach (723.000 deaths, 8.8% of the total), colorectal (694.000 deaths, 8.5% of the total), breast (522.000 deaths) and prostate (307.000 deaths) cancers cause most of the deaths, worldwide. Lung Cancer is the most common and the deadliest cancer in the world mainly due to tobacco smoking, being women less affected by this particular type of cancer due to cultural reasons. Colorectal cancer is the third most common cancer in men (10 % of the total) and the second in women (9.2 % of the total) worldwide, and the deadliest type of cancer in Portugal (3797 deaths, 15.7% of the total) (see **Figure 1.2**).

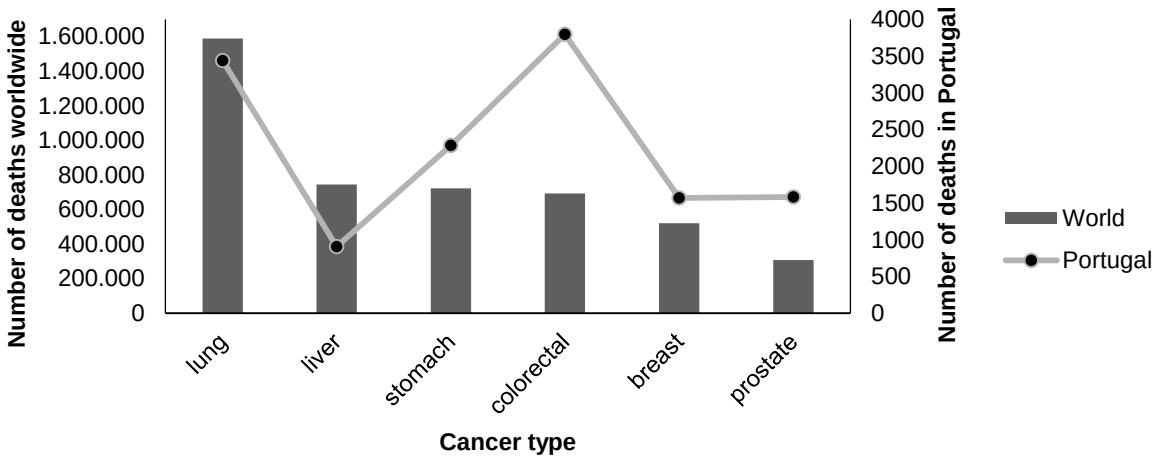

Figure 1.2 Estimated cancer mortality worldwide (columns) and in Portugal (line) (adapted from IARC, 2012).

1.2 Cancer etiology

Cancer is not a modern disease. However, the world is facing a situation without precedent as the proportion of older people and life expectancy increase throughout the world, what makes chronic diseases such as cancer more common nowadays. It is also important to observe that the potential economic and social costs of cancer rise sharply with age (WHO, 2011). This link between aging and cancer has been studied and some reasons were pointed. An increase in mutations is proposed as an aging mechanism mainly due to the accumulation of mutations in the nuclear genome (Kennedy *et al*., 2012). The genomic instability generates random mutations, chromosomal rearrangements and dysregulation of epigenetic mechanisms that promote tumor progression (Berdasco and Esteller, 2010). Some authors indicate the disruption of the correct functioning of telomerase and telomere length as other cause. Tumor cells can prevent the loss of telomeres by telomerase upregulation due to alterations in the function of proteins that interact or interfer with the telomeres at the level of chromatin (Blasco, 2005). Other links between aging and cancer are described elsewhere (Campisi, 2013; Finkel *et al*., 2007).

In addition, there is an increased exposure to etiological agents. External factors as well as internal factors (inherited mutations, hormones, immune conditions and mutations resulting from metabolism) may act together or in sequence to initiate cancer development (WHO, 2013). Tobacco smoke influence on lung cancer incidence and mortality was already mentioned before (see 1.1). Other examples are the bacterium *Helicobacter pylori* that predisposes to stomach cancer (Jemal *et al*., 2010) and the human papilloma virus that is responsible for infections that can originate cervical cancer (Subramanya *et al*., 2008). Additional causes are based on the eating habits and physical activity. It is estimated that one in every ten cancers in Western populations are due to an inadequate intake of vegetables and fruit and excessive consumption of red meat (Daniel *et al*., 2011; IARC, 2003). Other studies corroborate these causes (Bao *et al*., 2013; Bravi *et al*., 2013; Kandaswami *et al*., 2005). Pollution of air, soil and water (Berman *et al*., 2008; Abnet, 2007; Chen *et al*., 2004; Desai *et al*., 2004) and ionizing radiation (Robertson *et al*., 2013; Sethi *et al*., 2012; Krewski *et al*., 2005; Shinji *et al*., 2004; Pavia *et al*., 2003;) are other well known causes of cancer as described elsewhere.

1.3 Cancer biology and therapeutics

There are several different kinds of cancer that can be included in four main groups: carcinoma, sarcoma, lymphoma/leukemia and cancers derived from cells of the nervous system. Both carcinomas and sarcomas are solid tumours. Carcinomas are solid malignant lesions originating in the epithelial tissue. Sarcomas are solid tumours of the connective tissue, such as bone and muscle. Leukemia and lymphoma are malignancies originating in haematopoeitic or immune cells that are found throughout the vascular system (Alberts *et al*., 2008).

All groups of cancer have in common an abnormal cell proliferation that gives rise to a neoplasm, but not all give rise to a mass of cells, e.g. leukemia (Hutter, 2010). Malignant neoplasms show a high level of anaplasia (lack of differentiation), the ability of invading neighbouring structures and to spread through the lymphatic system and bloodstream to other organs originating secondary tumors through a process called metastazation (Alberts *et al*., 2008).

The human tumorigenesis is considered a multistep process. Sustaining proliferative signaling, growth suppressors' evasion, cell death resistance, replicative immortality, angiogenesis induction, invasion activation and finally metastasis formation are considered the main steps. They are acquired in different tumor types via distinct mechanisms and at different points during the course of the tumorigenesis. The tumor progression can be viewed as a sequence of clonal expansions, each of which is triggered by the accidental acquisition of somatic mutations that confers selective advantage. This advantageous mutant genotype enables their outgrowth and an eventual dominance in a local tissue environment (Hanahan and Weinberg, 2011).

In terms of therapeutics, cancer can be treated by surgery, radiation, chemotherapy, hormonal therapy, and targeted therapy. An early detection of cancer results in a less expensive treatment and better results. While surgical resection and adjuvant therapy can cure well confined primary tumors, metastatic disease is largely untreatable because of their systemic nature and the resistance of tumor cells to existing therapeutic agents (Gupta and Massagué, 2006). However, molecular and cell-biological details of the tumour progression process are emerging and influencing the therapeutics available (Valastyan and Weinberg, 2011). Surgery and radiotherapy dominated the field of cancer therapy into the 1960s until new data showed that combinating chemotherapy could cure patients with various advanced cancers (Vincent T. *et al*., 2008).

Some important features in cancer biology and therapeutics will be briefly addressed.

1.3.1 Mutation acquisition

The development of tumours from single cells that begin to proliferate abnormally, called tumour clonality, is one important characteristic of cancer. Although this single cell origin, some fundamental changes are needed in order to develop cancer. The development of cancer is viewed as a multistep process involving mutation and selection for cells with progressively increasing capacity for proliferation, survival, invasion, and metastasis (Hanahan and Weinberg, 2011; Cooper, 2000).

Studies of colon carcinomas provide an example of tumour progression during the development of cancer (see **Figure 1.3**).

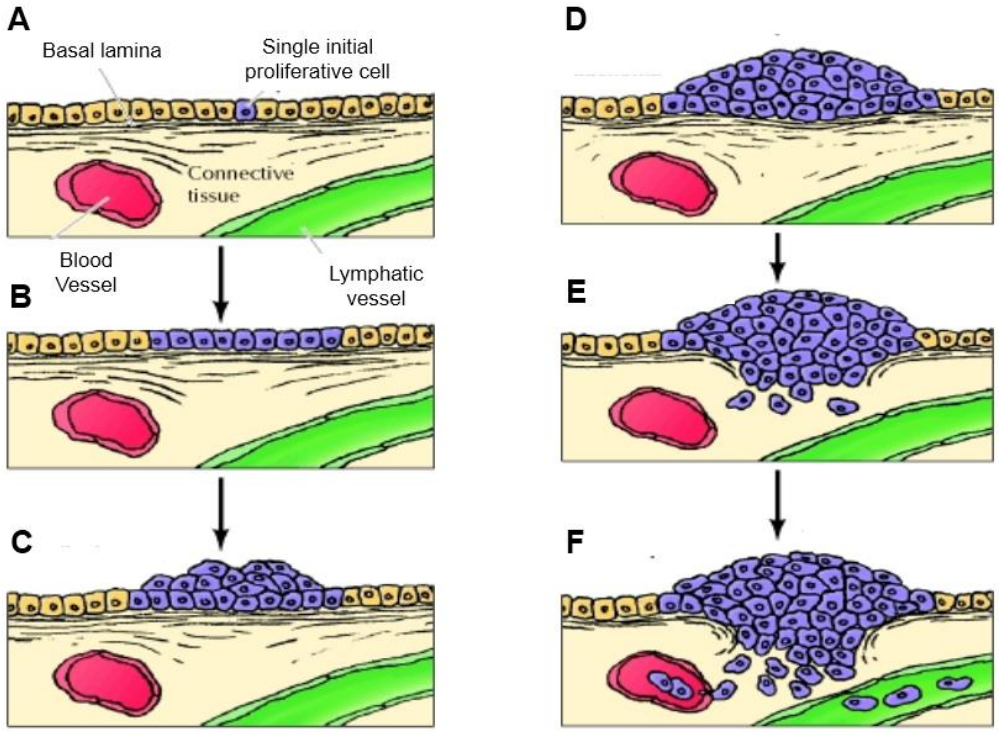

Figure 1.3 Development of colon carcinomas (Adapted from Cooper, 2000). A single initially altered cell (A) begins to proliferate and gives rise to a proliferative cell population (B), which progresses first to benign adenomas (C) of increasing size (D) and then to malignant carcinoma (E and F). In this phase, cancer cells invade the underlying connective tissue and penetrate blood and lymphatic vessels, spreading throughout the body.

The earliest stage of colon cancer is increased proliferation of colon epithelial cells (Cooper, 2000). Tumour initiation, is thought to be the result of a genetic alteration leading to abnormal proliferation of a single cell. Cell proliferation leads to the development of a population of clonally derived tumour cells, such as a benign neoplasm (an adenoma or polyp in colon cancer). Tumour progression continues by additional mutations that occur within cells of the population of clonally derived tumour cells that leads to the growth of adenomas of increasing size and proliferative potential (Hanahan and Weinberg, 2011; Alberts, 2008; Cooper, 2000). Some considered pathways of genomic instability in colorectal cancer are mutations in DNA mismatch repair genes, leading to a DNA microsatellite instability phenotype; mutations in Adenomatous polyposis coli (*APC)* and other genes that activate Wnt pathway, characterized by chromosomal instability phenotype, and global genome

hypermethylation, resulting in switch off of tumor suppressor genes, indicated as CpG island methylator phenotype (Bogaert and Prenen, 2014; Mojarad *et al*., 2013).

Some of these mutations confer a selective advantage to the cell, e.g. more rapid growth, and by a process called clonal selection, the descendants of this cell will consequently become dominant within the tumour population. Clonal selection during tumour development, also aids tumours becoming increasingly malignant (Hanahan and Weinberg, 2011; Alberts, 2008; Cooper, 2000).

Malignant carcinomas then arise from the benign adenomas characterized by invasion of the tumour cells through the basal lamina into underlying connective tissue. In the connective tissue of the colon wall cancer cells continue to proliferate and spread. Then, the cancer cells penetrate the wall of the colon and invade other abdominal organs. In addition, the cancer cells invade blood and lymphatic vessels, allowing them to metastasize throughout the body (Cooper, 2000). In a molecular level, Epithelial-mesenchymal transition (EMT, see section 1.3.8) is an important early event involved in invasion and metastasis of colorectal cancer. Some alterations in EMT include vimentin hyperexpression that iniciates the molecular program, and genes involved in invasion such as N-cadherin with a decrease expression of genes involved in epithelial cell adhesion such E-cadherin, and even its loss. Progression in colon cancer is also characterized by activating mutations in Ras genes and tumor growth factor action (Todosi *et al*., 2012).

1.3.2 Proliferation barriers: oncogenes, cell senescence and tumor suppressors

Genes important for cancer development can be grouped into two main classes. Genes in which a gain-of-function mutation promotes cancer are called proto-oncogenes. The mutant forms are called oncogenes. Oncogenes are cancer-promoting genes. Many of them are involved in the mitogenic signaling pathways. Genes of the second group are called tumour suppressor genes. A loss-of-function mutation in a tumour suppressor gene can contribute to cancer (Alberts, 2008).

Oncogene signaling deregulation is important for cell proliferation however there is no universal response to an increasing expression of oncogenes. In contradiction with the notion that elevated expression of oncogenes increases cancer cells proliferation and thus tumor growth, some studies indicates that excessively elevated signaling by RAS (Retrovirus associated sequence oncogene), MYC (v-myc avian myelocytomatosis viral oncogene homolog), and RAF (Raf-1 proto-oncogene, serine/threonine kinase) oncoproteins can provoke induction of cell senescence and/or apoptosis (Collado and Serrano, 2010). Other function for oncogenes operating within tumor cells, such as *Ras* and *Myc*, is upregulating the expression of angiogenic factors that promote angiogenesis.

Cell senescence is a protective barrier to neoplastic expansion. Senescence is a cell nonproliferative but viable state characteristic of premalignant tumor stages, but it is absent from malignant tumors. Tumor suppressors can induce or prevent senescence. Deletion of tumor suppressors *PTEN* (phosphatase and tensin homolog), *VHL* (von Hippel-Lindau), *NF1* (neurofibromin 1) and *RB* (retinoblastoma-associated) leads to excessive proliferative signaling and ultimately to senescence (Collado and Serrano, 2010).

There are dozens of tumor suppressors, including, two tumor suppressors that encode the P53 and the RB proteins. They transduce growth-inhibitory signals that originate inside the cell and

the RB protein also integrates signals from extracellular sources. The ‘‘guardian of the genome’’, TP53 (Tumour protein P53), is involved in preserving genomic integrity. Depending of the context, P53 can stop the cell-cycle progression or trigger apoptosis, the last one in case of irreparable damages (Jackson and Bartek, 2009). Although P53 and RB absence permits persistent cell proliferation they are not essencial. There are studies that reflect a functional redundancy that restrict replication of cells lacking these proliferation suppressors. Tumor suppressor genes, in addition to their cell-cycle progression interference, can also contribute to contact inhibition that is abolished in cancer cells. For example, the protein Merlin, the product of the gene *NF2*, by sequestering growth factor receptors, limits its ability to efficiently emit mitogenic signals (Curto et al., 2007). In this way, Merlin absence promotes cancer cells proliferation.

As stated before, many oncogenes are involved in mitogenic signaling pathways. *p38α* is a tumour suppressor gene and is a mediator of Mitogen-activated protein kinase pathway, involved in resistance to cisplatin, irinotecan and 5-fluorouracil chemotherapy in colorectal cancer patients. Despite its tumour suppressor activity in some tissues, the p38α pathway may also acquire an oncogenic role involving cancer related-processes such as cell metabolism, invasion, inflammation and angiogenesis (Grossi *et al*., 2014).

There are some suggestions of therapeutic exploration of the pathways involving oncogenes and tumor supressors described by other authors (Shanker *et al*., 2011; Luo *et al.*, 2009).

1.3.3 Apoptosis, autophagy and necrosis

Apoptosis, in which a cell contracts and is consumed by neighbors, is triggered by diverse stresses as signaling imbalances resulting from elevated levels of oncogene signaling and DNA damage. Apoptosis is divided into two pathways: the extrinsic apoptotic pathway (death receptor), involving the Fas ligand/Fas receptor that receives extracellular death-inducing signals and the intrinsic pathway (mitochondrial) that integrates a variety of signals of intracellular origin as those originated during radio- and chemotherapy. Apoptosis is tightly regulated by the balance between pro- and antiapoptotic proteins. In human cancers, overexpression of antiapoptotic proteins such as Bcl-2 (B-cell CLL/lymphoma 2) and Bcl-x_L (Bcl-2-like protein 1 isoform), or downregulation of proapoptotic factors such as Bax (bcl-2-like protein 4), Bim (Bcl-2-like 11) and Puma (Bcl-2 binding component 3) is observed (Bai and Wang, 2014).

As stated before, Bcl-2 is an antiapoptotic protein. However, Zeestraten and co-workers reported that from studies on colorectal cancer patients to determine Bcl-2 expression, upregulation of Bcl-2 was related with better survival. The explanations rised for this is the fact that Bcl-2 can also exert a distinct negative influence on cell cycle progression, which can eventually slow down tumor growth. The role of Bcl-2 may also depend on disease stage (Zeestraten *et al*., 2013).

Autophagy appears to represent another barrier that needs to be avoided during tumor development (White and DiPaola, 2009). However, nutrient starvation, radiotherapy, and certain cytotoxic drugs can induce elevated levels of autophagy that could be cytoprotective for cancer cells (White and DiPaola, 2009; Apel *et al*., 2009). The autophagic program enables cells to break down cellular organelles, such as ribosomes and mitochondria, allowing the resulting catabolites to be

recycled and thus used for biosynthesis and energy metabolism. Autophagy machinery has both regulatory and effector components (Levine and Kroemer, 2008) and there is a link between autophagy and apoptosis. Mice bearing inactivated alleles of the *Beclin-1* gene or of certain other components of the autophagy machinery exhibit increased susceptibility to cancer (White and DiPaola, 2009; Levine and Kroemer, 2008). Beclin-1 is a member of the BH3-only subfamily of apoptotic regulatory proteins, and its BH3 domain allows it to bind the Bcl-2/Bcl-xL proteins. Stress-sensor-coupled BH3 proteins can displace Beclin-1 from its association with Bcl-2/Bcl-xL, enabling the liberated Beclin-1 to trigger autophagy, much as they can release proapoptotic Bax and Bak (Bcl-2 homologous antagonist/killer) to trigger apoptosis.

In contrast to apoptosis and autophagy, necrotic cells swollen and explode releasing proinflammatory signals into the local tissue microenvironment, and in some circumstances under genetic control (Galluzzi and Kroemer, 2008). Necrotic cells can recruit immune inflammatory cells and promote cell proliferation given that immune inflammatory cells are capable of promoting angiogenesis, cancer cell proliferation, and invasiveness. Additionally, necrotic cells can release bioactive regulatory factors, such as IL-1a, which can directly stimulate neighboring viable cells to proliferate (Grivennikov *et al*., 2010). Consequently, necrotic cell death can also stimulate cell proliferation. Other authors show that although this contradictory effects, necrosis could have a fundamental role in tumor clearance by stimulating the innate immune response (Guerriero *et al*., 2008).

In relation to anticancer therapeutics, apoptosis, necrosis, mitotic catastrophe, senescence, and autophagy are the main types of cell death and cytostatic mechanisms described so far (Guerriero *et al*., 2008). There are studies about some compounds to modulate the activity of Bcl-2 family members or inhibit negative regulators of caspases such anticancer peptidic compounds that induce apoptosis of tumor cells (Barras and Widmann, 2011). Other review highligths the development of small-molecule inhibitors targeting three major classes of antiapoptotic proteins (Bai and Wang, 2014). New drugs could be designed for targeting the major players in autophagy however more studies are needed to better understand the relationship between autophagy and cancer (Lisiak *et al.*, 2014).

1.3.4 Inflammatory cells in tumor progression

Although cancer cells actively evade from elimination by the immune system (Bindea *et al*., 2010; Ferrone and Dranoff, 2010), inflammation can contribute to tumor progression. Tumor-promoting inflammatory cells include macrophage subtypes, mast cells, and neutrophils, as well as T and B lymphocytes (Egeblad *et al*., 2010; DePalma *et al*., 2008; Johansson *et al*., 2008; Murdoch *et a*l., 2008). Some of the signaling molecules released by inflammatory cells with tumor-promoting activity are the Epidermal Growth Factor (EGF), the angiogenic Vascular Endothelial Growth Factor (VEGF), chemokines, cytokines, proangiogenic and/or proinvasive matrix-degrading enzymes, including Matrix Metalloproteinase-9 (MMP-9), cysteine cathepsin proteases and heparanase (Qian and Pollard, 2010; Murdoch et al., 2008). Targeting regulators and mediators of inflammation is thought as one strategy for cancer treatment (Sun and Karin, 2014).

1.3.5 Cell energy metabolism changes

In cancer cells some metabolic changes occur in order to support continuous cell growth and proliferation (Wu and Zhao, 2013; Negrini *et al*., 2010). Even in the presence of oxygen, cancer cells can limit their energy metabolism to glycolysis. As cancer cells obtain less energy with glycolysis compared to mitochondrial oxidative phosphorylation, they upregulate glucose transporters such as Glucose transporter 1 (GLUT1), which increases glucose import into the cytoplasm (Jones and Thompson, 2009; DeBerardinis *et al*., 2008). Glycolytic fueling has been shown to be associated with activated oncogenes (e.g., RAS, MYC) and mutant tumor suppressors (e.g., TP53) (Jones and Thompson, 2009; DeBerardinis *et al*., 2008) whose alterations in tumor cells have been selected primarily for their benefits in promoting tumour progression. Other studies show tumours with two subpopulations of cancer cells that function symbiotically: one subpopulation consists of glucose-dependent (‘‘Warburg-effect’’) and other subpopulation of cells that preferentially import and utilize the lactate produced by the first group (Kennedy and Dewhirst, 2010; Feron, 2009; Semenza, 2008).

Some antineoplastic agents that have been used in the clinic for a long time – such as 5-fluorouracil, methotrexate and gemcitabine – inhibit metabolic enzymes. This leads to the idea that some drugs that are currently licensed by the US Food and Drug Administration (FDA) for use in patients with metabolic disorders may exert antineoplastic effects. Other possible antineoplastic agents indicated are metformin, phenformin and fibrates (Galluzzi *et al*, 2013).

1.3.6 Growth-promoting signaling and division deregulation

Cancer cells have the ability of continual proliferation. The growth-promoting signals bind to cell-surface receptors, typically containing intracellular tyrosine kinase domains, to regulate the cell growth and division. Cancer cells can deregulate the growth-promoting signals by autocrine proliferative stimulation. Structural alterations in the receptor molecules or the constitutive activation of components of signaling pathways operating downstream of the receptors (that can happens by somatic mutations) can also facilitate chronic proliferation. Some tyrosine-kinase inhibitors have been introduced in cancer therapeutics (Leeuwen *et al*., 2014). Cancer cells may also send signals to their microenvironment (see 1.3.9) to stimulate normal cells within the supporting tumor-associated stroma supplying cancer cells with growth factors (Hanahan and Weinberg, 2011).

Some authors also observed that members of the mitogen-activated protein kinase (MAPK) and phosphatidylinositol-3 kinase (PI3K) cascades are good targets for anticancer therapeutics, as some of these proteins are involved in the cell survival mechanisms (Mester and Redeuilh, 2008).

Other protein alterations have been associated with several cancer types. These alterations can be useful as therapeutic targets. Among the heat shock proteins (HSP), HSP27, HSP70 and HSP90 are the most studied stress-inducible HSPs. In particular, Hsp90 aids in the conformational development of more than two hundred proteins which are associated with all main steps of cancer (Audisio *et al*., 2014). Heat shock proteins are a family of conserved chaperones induced by cell stress such as that provoked by chemotherapeutic drugs or heat, between other physiological and environmental insults (Horváth and Vígh, 2010; Blank and Goodman, 2009). In cancer cells, the expression and/or activity of those three heat schok proteins is atypically high, and is associated with

increased tumorigenicity, metastatic potential of cancer cells and resistance to chemotherapy. When associated with some apoptotic factors, some heat shock proteins become anti-apoptotic proteins with the ability to block the cell death process (Horváth and Vígh, 2010; Multhoff and Hightower, 2011).

However, some treatments can trigger the cell membrane accumulation of heat shock proteins and promote anti-tumour T cell response (Kroemer *et al*., 2013; Krysko *et al*., 2013). Altogether, HSP27, HSP70 and HSP90 are emergent targets for anticancer therapeutics.

Other relevant target in anticancer therapeutics is the tubulin/ microtubule system due to its role in cell division. Drugs that interfere with microtubule function inhibit the proliferation of cancer cells by preventing the correct formation of the mitotic spindle (Pasquier and Kavallaris, 2008). Alterations in expression of tubulin isotypes, in the tubulin post-translational modifications, and in the expression of microtubule-associated proteins (MAPs) are thought to influence cellular responses to chemotherapeutics (Parker *et al*., 2014).

Besides mitotic spindle assembly, Ran also regulates nuclear envelope formation and cell cycle checkpoint control. Ran is a small ras-related GTPase that controls the nucleocytoplasmic exchange of macromolecules across the nuclear envelope, and is overexpressed in a range of tumors, such as breast and renal. Oncogenic KRAS (Kirsten Rat Sarcoma viral oncogene) or PIK3CA (phosphatidylinositol-4,5-bisphosphate 3-kinase, catalytic subunit alpha) mutations makes some tumors addicted to Ran expression. Decreasing the endogenous levels of Ran in the cell could have anti-mitotic effects and consequently contribute to the development of an effective cancer therapeutic (Matchett *et al*., 2014).

Other possible targets are among the purine ring de novo synthesis pathways. The synthesis of the purine ring de novo is required when DNA is replicated. The requirement to synthesize new purines in differentiated cells is smaller because the salvage pathway “recycle” nucleotides to the everyday needs.In this way, de novo synthesis of the purine ring is low in differentiated cells. This all together make inhibitors of the purine de novo synthesis effective drugs against cancer (Adam T., 2005).

1.3.7 Angiogenesis

Angiogenesis is activated early during the development of invasive cancers, causing normally quiescent vasculature to continually sprout new vessels that help sustain expanding neoplastic growths. Tumor neovasculature is marked by premature capillary sprouting, distorted and enlarged vessels, leakiness, and abnormal levels of endothelial cell proliferation and apoptosis (Nagy *et al*., 2010). In addition, tumors exhibit diverse patterns of neovascularization depending on the interactions between cancer cells and the associated stromal microenvironment (Baeriswyl and Christofori, 2009).

Angiogenesis is controlled by the level of inducing and opposing angiogenesis factors (Baeriswyl and Christofori, 2009). The most-known angiogenesis regulators and/or target proteins are vascular endothelial growth factor-A (VEGF-A), transforming growth factor (TGF)-α, TGF-β and tumor necrosis factor (TNF)-α as inducers, and thrombospondin- 1 (TSP-1), angiotensin, caveolin-1, -2 endostatin and interferon-alpha as inhibitors (Hanahan and Weinberg, 2011). Some therapeutic peptides have been derived from these endogenous regulators (Rosca *et al*., 2011). Other regulators

include dominant oncogenes operating within tumor cells, such as *Ras* and *Myc* that can upregulate the expression of angiogenic factors, whereas in others, such inductive signals are produced indirectly by immune inflammatory cells (Wang and Miao, 2013; Hanahan and Weinberg, 2011).

1.3.8 Metastasis formation

Metastasis remains the major cause of mortality in patients with cancer. After angiogenesis and local invasion, distant metastasis formation is another step towards a higher grade of malignancy. The invasion-metastasis cascade is characterized by the invasion of epithelial cells of primary tumors into surrounding extracellular matrix and stromal cell layers (local invasion), entry into the lumina of blood vessels, transport through the vasculature (physical dissemination through lymphatic and hematogenous systems) and arrest at distant organ sites and into the parenchyma of distant tissues. In these distant sites the epithelial cells from the primary tumor form micrometastases, and in certain conditions re-initiate their proliferative programs, generating macroscopic tumors clinically detectable (Fidler, 2003).

There are three types of invasiveness known: “mesenchymal”, “collective invasion” and “amoeboid” form of invasion. During the invasion-metastasis cascade cancer cells typically developed alterations in their shape as well as in their attachment to other cells and to the extracellular matrix (ECM). The Epithelial-Mesenchymal Transition (EMT) program regulates a particular type of invasiveness that has been named ‘‘mesenchymal’’. EMT is a program that can be activated transiently or stably, and to differing degrees (Hanahan and Weinberg, 2011). The transcriptional regulators Snail, Slug, Twist, and Zeb1/2 that are normally expressed during embryogenesis are also expressed in various combinations in the EMT program during tumor development. They are responsible for the loss of adherens junctions and associated conversion from a polygonal/epithelial to a spindly/fibroblastic morphology, expression of matrix-degrading enzymes, increased motility, and heightened resistance to apoptosis (Hanahan and Weinberg, 2011). Several of these transcription factors can directly repress E-cadherin (a cell-to cell adhesion molecule) gene expression, favoring invasion and metastasis (Peinado *et al*., 2004). Other forms of invasion are described elsewhere (Madsen and Sahai, 2010; Sabeh *et al*., 2009).

Most of the studies on cancer are done in primary tumors even though primary tumors and metastases can differ in expression profiles. Targeting the outgrowth at a distant site (metastatic colonization), by targeting the metastatic cancer cell or the host cell, or by interrupting reciprocal interactions between tumor cells and the microenvironment are considered the most relevant therapeutics. Some target candidates are pointed elsewhere (Steeg and Theodorescu, 2008).

1.3.9 Tumor Microenvironment

Many human tumors are histopathologically heterogeneous, with various degrees of differentiation, proliferation, vascularity, inflammation, and/or invasiveness. In most tumors a subclass of neoplastic cells with varying abundance, named cancer stem cells (CSCs) are present (Cho and Clarke, 2008). Increasing evidence in a variety of tumor types suggests that cells with properties of CSCs are more resistant to various commonly used chemotherapeutic treatments (Singh and

Settleman, 2010). Being considered responsible for cancer initiation, progression, metastasis, recurrence and drug resistance, they are actracting attention for the development of new anticancer therapies (Chen *et al.*, 2013).

Other concerns are described elsewhere, such as “cancer-associated fibroblasts”, “cancer-associated adipocytes” (Dirat *et al*., 2010; Pietras and Ostman, 2010; Rasanen and Vaheri, 2010; Shimoda *et al*., 2010) and dozens of microRNAs which are implicated in various tumor phenotypes and have been considered emerging targets in anticancer therapy (Garzon *et al*., 2010).

1.4 Metallic compounds and doxorubicin

Metals are essential cellular components with unique characteristics that include redox activity, variable coordination modes, and reactivity towards organic substrates what makes the coordination complexes with a metal ion, good candidates for anticancer agents (Frezza *et al*., 2010).

The type of metal bonded to carbon subdivides metallic compounds in two distinct types. One type involves compounds containing the main group elements such as the alkali and alkaline earth metals, and the more metallic elements in the zinc, boron, carbon, nitrogen, and oxygen vertical groups in the periodic table. The other type includes compounds containing transition metal elements. One of the features of transition metal chemistry that is not shared by main group elements is the potential for formation of metal-metal multiple bonds. This property of transition metals resulted in the foundation of coordination complexes with variable coordination modes (Martins *et al.*, 2014; Hartinger and Dyson, 2009).

To date, practically all transition and main group metals have been tested for antitumor properties. The antineoplastic potential of compounds of several metals such as gallium, ruthenium and titanium was recognized more than two decades ago. The number of metal compounds in current clinical use for the cancer therapy is extremely limited (Jakupec *et al*., 2008). Platinum drugs are still the most used chemotherapeutic drugs (see section 1.4.1). Doxorubicin is not a metallic drug, but is also a reference chemotherapeutic drug (see section 1.4.2).

1.4.1 Cisplatin

Although the potential of the diverse metals in periodic table, cisplatin (**Figure 1.4**) impact influenced the antitumor agents development towards platinum compounds (Jakupec *et al*., 2008).

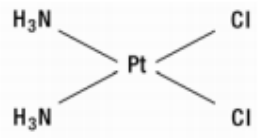

Figure 1.4 The anticancer drug cisplatin (Adapted from Food and Drug Administration, 2011).

Platinum complexes such as cisplatin are clinically used as adjuvant therapy of cancers. Cisplatin is used to treat cancers including: sarcoma, small cell lung cancer, germ cell tumors, lymphoma, and ovarian cancer. Other platinum drugs include carboplatin, a drug with fewer and less severe side effects introduced in the 1980s, and oxaliplatin, a drug which is part of the FOLFOX (5-FU, leucovorin, and oxaliplatin) treatment for colorectal cancer. Cisplatin is frequently given as part of a combination chemotherapy regimen with other drugs and it continues to find uses, especially as it is synergistic with other agents (Florea and Büsselberg, 2011).

Cisplatin damages tumors via inhibition of DNA synthesis and repair that might result in cell cycle arrest and therefore apoptosis will be induced. Neither cytotoxicity nor apoptosis are exclusively induced in cancer cells, thus, cisplatin might also lead to diverse side-effects such as neuro- and/or renal-toxicity or bone marrow-suppression. Other problem is that cancer cells could become cisplatin-

resistant. To minimize or avoid this, combinatorial therapies are being developed (Florea and Büsselberg, 2011).

1.4.2 Doxorubicin

Doxorubicin (**Figure 1.5**) is an anthracycline antiobiotic without a metallic center but has shown great treatment potential, being regarded as one of the most potent of the Food and Drug Administration-approved chemotherapeutic drugs. The drug is a nonselective class I anthracycline, possessing aglyconic and sugar moieties (Tacar *et al*., 2012).

Doxorubicin is given to treat non-Hodgkin's lymphoma, multiple myeloma, acute leukemias, Kaposi sarcoma, Ewing sarcoma, Wilm tumor, and cancers of the breast, adrenal cortex, endometrium, lung, ovary, and other sites. There are also some studies on colorectal cancer cell lines (Tacar *et al*., 2012).

Doxorubicin acts by binding to DNA-associated enzymes, such as topoisomerase enzymes I and II, and it can intercalate the base pairs of the DNA's double helix. By binding to her targets a range of cytotoxic effects occurs in conjunction with the antiproliferative role, however this effect is limited by its toxicity on normal cells, being cardiotoxicity the major concern regarding the use of doxorubicin (Tacar *et al*., 2012). New therapies are needed to minimize the doxorubicin dose used in cancer treatment.

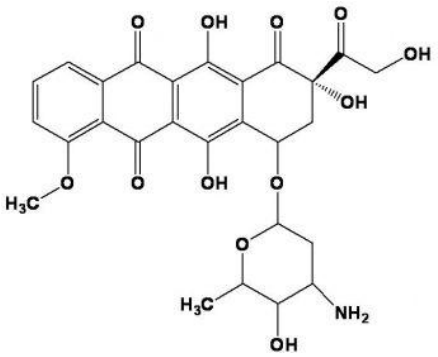

Figure 1.5 The anticancer drug doxorubicin (Adapted from Inspiralis, 2006).

1.4.3 Rhenium compounds

In line with these problems, rhenium compounds have been studied for some imaging and therapeutic applications, (Bertrand *et al*., 2014; Lecina *et al*., 2014; Smilkov *et al*., 2014; Hanson *et al.*,2012; Wuest *et al*., 2012), including anticancer therapeutics.

The chemistry of rhenium permits the existence of a large number of oxidation states ranging from +I to + VII. Current activity in the study of rhenium coordination chemistry has increased mainly due to radiopharmaceuticals. Some examples are the rhenium(V) complex of dimercaptosuccinic acid and mercaptoacetyltriglycine (MAG3) technetium system used as an agent for the treatment of a relatively rare medullary thyroid carcinoma (Yumata, 2010) and as an imaging agent for renal function, respectively. Other rhenium radiopharmaceuticals have been designed for various cancer tumours by labelling the radionuclide to steroids (Dilworth and Parrot, 1998).

The biodistribution and targeting ability of a compound are determined by a number of factors, such as the oxidation state of the metal, as well as the charge, polarity and lipophilicity of the complex. Some rhenium compounds are transported as perrhenate (ReO4-), which is the most stable, water-soluble rhenium oxide in the +VII oxidation state (Yumata, 2010).

Besides radiopharmaceuticals are derivatives of a nontoxic luminescent probe of rhenium applied for biological imaging that were discovered to have antitumor properties when irradiated at a suitable wavelength. Replacing just the 2,2'-bipyridine in 4 with 2-(2'-pyridyl)indolato and its derivatives (1–3) changes the physicochemical and biological properties of such rhenium(I) complexes (see **Figure 1.6**) making them toxic for cancer cells (Dieckmann et al., 2013).

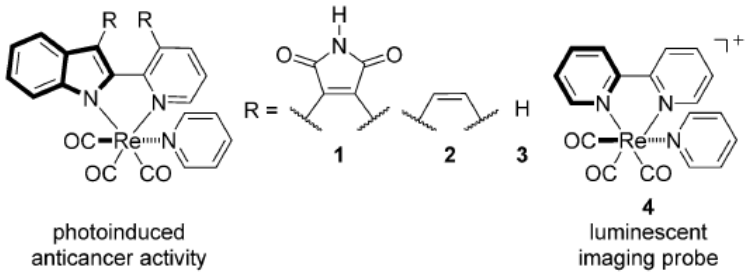

Figure 1.6 From luminescent (4) to light-induced anticancer Re complexes (adapted from Dieckmann *et al*., 2013).

Other rhenium compounds studied for their anticancer properties and lowest toxicity are described elsewhere (Collery *et al*., 2014; Kitanovic *et al*., 2014; Pracht *et al.*, 2013; Wang *et al*., 2013; Collery *et al*., 2012; Martínez-Lillo *et al*., 2011) and provide a strong body of evidence that rhenium complexes could be effective anticancer agents, alone or in combination with other well established therapeutics.

1.5 Work subject and objectives

Cisplatin, oxaliplatin, related metallodrugs as well doxorubicin are extensively used in the treatment of a diversity of cancers. However these drugs are highly toxic and tumor becomes drug-resistance (Holohan *et al*., 2013). On the other hand, in addition to drug resistance there are also complicated side effects (Tacar *et al*., 2012). These facts indicate the need for cytotoxic agents with less toxicity, more tumour specific and devoid of drug resistance. New metallic compounds that could be more selective to cancer cells could fulfil these requirements.

The present work is based on the latest studies of rhenium compounds and their anticancer therapeutic properties with alternative mechanisms of action and possible uses in combined therapeutics (Collery *et al*., 2014; Kitanovic *et al*., 2014; Pracht *et al.*, 2013; Wang *et al*., 2013; Collery *et al*., 2012; Martínez-Lillo *et al*., 2011).

The cytotoxic potential of three new rhenium compounds $[ReO_3(PTA)_2][ReO_4]$ (PTA = 1,3,5-triaza-7-phosphaadamantane), $[ReO_3(HMT)_2][ReO_4]$ (HMT = hexamethylenetetramine) and [ReO(Tpms)(HMT)] (Tpms = tris(pyrazol-1-yl)methanesulfonate) designated from here on by 1, 2 and 3, and compound 4 was evaluated in several cancer cell lines and fibroblasts. The structure of compound 4, bearing the trimeric polythiophene acetic acid (tPTAA) ligand, can not be revealed due to a pending patent. The compounds 2 and 4 were also tested in combination with cisplatin and doxorubicin in tumor cell lines. Flash photolysis was used to assess transient species formation that could increase the anticancer potential (Dieckmann *et al*., 2013).

The other objective was to deduce the mechanism of action and possible targets. For this, it was also analysed the capacity of the compound 2 to interact with Calf Thymus and plasmid DNA and Human Serum Albumin. The Two-dimensional Protein Electrophoresis technique was used to analyse the proteic extract of tumor cells after treatment with the compounds.

2 Materials and Methods

2.1 Metalic compounds

Rhenium compounds tested for antitumoral activity (see **Table 2.1)** were synthesized by Martins and collaborators (2013). They were prepared from the Re (VII) oxide Re_2O_7, which is a relatively inexpensive, accessible, and highly reactive material, and characterized by Infrared and Nuclear Magnetic Ressonance spectroscopies, elemental analysis and electrochemical properties as described by Martins and collaborators (2013). The same authors also have shown that the oxorhenium compounds are soluble in water, an ambivalent behavior which is characteristic of certain 1,3,5-triaza-7-phosphaadamantane (PTA) Renhium complexes.

Table 2.1 Oxorhenium complexes bearing the water-soluble tris(pyrazol-1-yl)methaneulonate, 1,2,5-triaza-7-phosphaadamtane or related ligands. These organometallic compounds have been prepared from the Re(VII) oxide Re_2O_7 (Martins *et al*., 2013). In this table are represented from left to right: code (the number used in this thesis to refer a particular rhenium compound), formule, structure and molecular weight.

Code	Formule/ Structure	Molecular Weight ($gmol^{-1}$)
1	$[ReO_3(PTA)_2][ReO_4]$ (PTA = 1,3,5-triaza-7-phosphaadamantane) 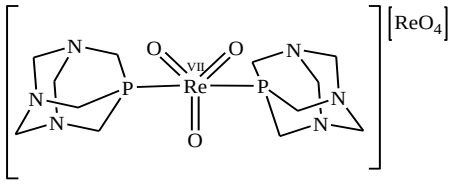	830.8
2	$[ReO_3(HMT)_2][ReO_4]$ (HMT = hexamethylenetetramine) 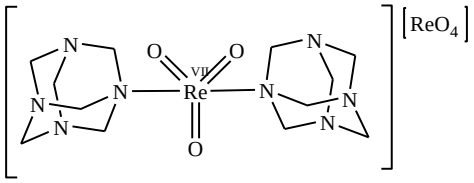	796.8
3	[ReO(Tpms)-(HMT)] (Tpms = tris(pyrazol-1-yl)methanesulfonate) 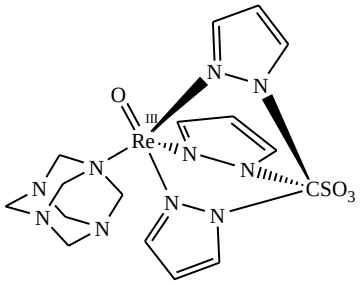	635.7

The stock solutions of compounds 1 (12 036.6 µM), 2 (12 550.2 µM) and 3 (15 730.7 µM) were prepared by weighting 10 mg (Mettler Toledo, Greifensee, Switzerland) of each compound and dissolving them in 1 mL of dimethyl sulfoxide (DMSO, Sigma, St. Louis, United States of America), an organic solvent. Then they were divided in aliquots of 100 µL each. DMSO is the most common solvent used due to its good solvating ability for compounds, relative chemical inertness, and relatively

high boiling and freezing points. DMSO is also known by its antimicrobial activity, thereby avoiding the need for sterilization and autoclaving before use. The samples in DMSO can be stored either at room temperature or in a frozen state and thawed when needed (Cheng *et al*., 2003). In this work the aliquots were stored at -20ºC.

Compound 4 was synthesized in University College of Dublin by Grace Morgan Group and its structure can not be revealed due to a pending patent. Compound 4 (4502.0 µM) was stored at 4ºC.

2.2 Combined therapeutics

The stock solution of cisplatin (3332.9 µM, Teva Parenteral Medicines, Inc., Teva Pharmaceuticals, Sellersville, United States of America) used in combined therapy with compound 2 (see 2.1) was prepared by dissolving 1 mg of cisplatin USP and 9 mg of NaCl, in 1 mL of distilled water, pH 5.5, and stored at room temperature. Compound 4 was used in combined therapy with cisplatin and doxorubicin (8621.0 µM) separately. Doxorubicin was stored in aliquots of 100 µL at 4ºC.

2.3 Cell lines

2.3.1 Tumour cell lines

In this work eight tumour cell lines of *Homo sapiens* origin (see **Table 2.2**) were used (American Type Culture Collection (ATCC) nomenclature).

Table 2.2 Tumoral cell lines that are used in this work. From left to right: the name, morphology, culture properties and cell line derivation and other informations.

Tumoral Cell Lines	Morphology	Culture properties	Derivation
A549[(1)]	epithelial	adherent	Initiated in 1972 through explant culture of lung carcinomatous tissue from a 58-year-old caucasian male.
H1650[(2)]	epithelial	adherent	Derived from stage 3B adenocarcinoma, in particular, bronchoalveolar carcinoma. The tissue donor was a 27-year-old caucasian male.
H1975[(3)]	epithelial	adherent	Established in July 1988 and is from an adenocarcinoma; non-small cell lung cancer. The tissue donor was a female non-smoker.
HCT116[(4)]	epithelial	adherent	This cell line is from colorectal carcinoma. The tissue donor was an adult male.
HepG2[(5)]	epithelial	adherent	This cell line is from hepatocellular carcinoma. The tissue donor was a 15-year-old caucasian male.
K562[(6)]	lymphoblast	suspension	The continuous cell line K-562 is from the pleural effusion of a 53-year-old female with chronic myelogenous leukemia (CML) in terminal blast crisis.
MCF-7/GFP[(7)]	epithelial	adherent	MCF-7 was isolated (1970) from a malignant adenocarcinoma from the breast of a 69-year-old woman. The cell line MCF-7/GFP expresses GFP.
MNT-1[(8)]	epithelial	adherent	This is a melanotic cell line from skin enriched with mature stage III and IV melanosomes.

Legend: More information in (accessed in November 29, 2013):
[(1)]http://www.lgcstandards-atcc.org/Products/All/CCL-185.aspx#generalinformation;[(2)]http://www.lgcstandards-atcc.org/products/all/CRL-5883.aspx?geo_country=pt;[(3)]http://www.lgcstandards-atcc.org/Products/All/CRL-5908.aspx#generalinformation;[(4)]http://www.lgcstandards-atcc.org/Products/All/CCL-247.aspx;
[(5)]https://www.lgcstandards-atcc.org/Products/All/CRL-10741.aspx;[(6)]https://www.lgcstandards-atcc.org/Products/All/CCL-243.aspx;[(7)]https://www.cellbiolabs.com/sites/default/files/AKR-211-gfp-mcf-7-cell-line.pdf; [(8)] http://www.lifetechnologies.com/pt/en/home/technical-resources/cell-lines/m/cell-lines-detail-545.html

2.3.2 Normal cell line culture

One normal cell line of *Homo sapiens* origin composed of adherent dermal fibroblasts from foreskin of a neonatal African American was used in this work (ATCC). The morphology is spindle-shaped and cells are bipolar and refractile (http://www.lgcstandards-atcc.org/Products/All/PCS-201-010.aspx).

2.4 Cell lines culture and harvesting

Cell lines were cultured in Complete Culture Medium constituted by Dulbecco's Modified Eagle Medium (DMEM; Invitrogen, New York, United States of America) supplemented with 10% (v/v) fetal bovine serum (FBS, Invitrogen, New York, United States of America), 1% (v/v) streptomycin-penicillin (Pen-Step+Antimycotic; Invitrogen) in culture flasks of 25, 75 and 175 cm^2 (BD Biosciences, New Jersey, EUA). The culture flasks were incubated at 37℃ in a humidified atmosphere of 99% and 5% CO_2. For the tumoral cell line HepG2 and dermal fibroblasts 1% (v/v) of MEM nonessential amino acids (100x, Invitrogen, New York, United States of America) were added to the Complete Culture Medium.

When cells were near the end of exponential growth (roughly 80% confluent), they were harvested with 6 mL, 4 mL or 1 mL of TrypLE (Gibco, Thermo Fisher Scientific, Waltham, United States of America), a replacement of Trypsin, (for 175 cm^2, 75 cm^2 or 25 cm^2 flasks, respectively). After ten minutes TrypLE is neutralized with the same volume of Complete Culture Medium and cells were centrifugated at 1500 RPM for 5 minutes at 20ºC. Then the medium with TrypLE was aspirated and added new Complete Culture Medium, 1 or 2 mL to dissolve the pellet. The cell lines were subcultured at a 1:10 split ratio.

2.4.1 Cell counting

Cells were counted by the *Trypan* blue exclusion method in a hemocytometer (Hirschmann, Eberstadt, Germany) from a mixture of 350 µL of complete culture medium, 100 µL of Trypan blue at 0.4 % (v/v) (Sigma, St. Louis, United States of America) and 50 µL of cellular suspension obtained during the subculturing process (see 2.4). A hemocytometer consists of a thick glass microscope slide with a grid of perpendicular lines etched in the middle. The grid has specified dimensions so that the area covered by the lines is known. The area under the coverslip fills by capillary action. The load volume is about 10 µL. The number of cells per ml is obtained by multiplying the number of total cells counted, the volume of the hemocitometer (10^4 mL^{-1}) chamber and the dilution factor (10) divided by the number of squares counted, as represented in equation (1).

$$(1)\quad \text{Total cells/mL} = \frac{\text{Total cells counted x } 10^4 \text{ x } 10}{\text{number of squares}}$$

2.5 Cell Viability assays

To assess cell drug inhibition, 7500 cells per well were seeded in 96-well plates and incubated during 24 hours at 37ºC in a humidified atmosphere of 99% and 5% (v/v) CO_2 in air. Drugs were added 24 hours later at established concentrations (between 0.1 µM and 1000 µM). Control cells used have been growth in the presence of 0.1% (v/v) DMSO at 99.5% (Sigma, St. Louis, United States of America). The 96-well plates were then incubated for 48 hours at 37ºC in a humidified atmosphere of 99% and 5% (v/v) CO_2.

Cell viability was measured using the colorimetric method *CellTiter 96® AQ_{ueous} Non-Radioactive Cell Proliferation Assay* (Promega, Madison, United States of America) in 96-well assay plates. In this assay 3-(4,5-dimethylthiazol-2-yl)-5-(3-carboxymethoxyphenyl)-2-(4-sulfophenyl)-2H-tetrazolium (MTS) is bioreduced by intracellular dehydrogenases present in metabolically active cells in the presence of the electron coupling reagent phenazine methosulfate (PMS) into a formazan

product that is soluble in tissue culture medium. The quantity of formazan product measured by the amount of 490nm absorbance is directly proportional to the number of living cells in culture.

After 48 hours after drug addition, medium was aspirated from 96-well plates and 100 µL of a solution mixture of complete culture medium, MTS and PMS (100:20:1) were pipetted to each well. The 96-well plates were incubated at 37ºC and after 40 minutes the absorbance at 490 nm was read in a microplate reader (Tecan infinite F200, Männedorf, Switzerland). An illustrative scheme is shown in **Figure 2.1**.

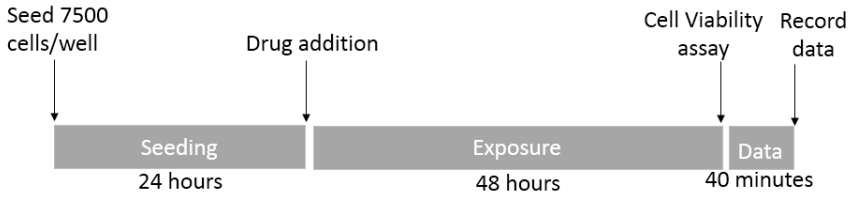

Figure 2.1 Illustrative scheme of cell viability assays. 7500 cells per well (0.75 x 10^5 cells/mL) were seeded in 96-well plate at 37ºC, humidified atmosphere of 99% and 5% (v/v) CO_2, and 24 hours later the cells were exposed to compounds for more 48 hours in the same conditions. Then, each well was aspirated and 100 µL of a solution mixture of complete culture medium, MTS and PMS (100:20:1) were pipetted to each well. After 40 minutes of incubation the absorbance at 490nm was read in a microplate reader.

Data were treated by the equation (2) and the half maximal inhibitory concentration (IC_{50}) determined by *GraphPadPrism 6*:

$$(2)\text{Cellular viability }(\%) = \frac{\text{Absorbance 490nm (sample)}}{\text{Absorbance 490nm (control)}} \text{ x } 100\%$$

2.6 Flash photolysis

Laser Flash Photolysis experiments were carried out at room temperature on LKS.60 Nanosecond Laser Flash Photolysis Spectrometer (Applied Photophysics, Surrey, United Kingdom) in two different solvents (distilled water solutions and deaerated distilled water solutions for at least 5 minutes with oxygen-free nitrogen and methanol (99.9%, Sigma, St. Louis, United States of America)). The concentrations are adjusted to yield an absorbance of 0.2 at the excitation wavelength. Samples were excited by the 4th harmonic (λ_{EXC} = 266 nm, laser energy around 10 J) of a neodymium-doped yttrium aluminium garnet (Nd-YAG) laser. Light excitation was carried out using a medium pressure mercury arc lamp. Filters (Oriel, Bozeman, United States of America) were placed in the light path to narrow the spectrum and remove wavelengths inferior to 305 nm. Transient absorption spectra were recorded after the laser pulse (ten shots at each wavelength, with an interval of ten nanometers).

Stock solutions of quenchers in the energy transfer assays were prepared so that it was only necessary to add microliter volumes (see **Table 2.3**) to the sample cell in order to reach appropriated quencher concentration. Benzophenone (10^{-4} mol/L) used in energy transfer assays was acquired from Merck, Whitehouse Station, United States of America. Data were acquired and analysed with the Applied Photophysics software.

Table 2.3 Energy transfer assay table with volumes of compound 2 stock added to the quartz cuvette with benzophenone during the titulation.

volume (µL)	final concentration (M)
0	0
5	2.09×10^{-5}
10	4.17×10^{-5}
20	8.31×10^{-5}
30	1.24×10^{-5}
40	1.65×10^{-4}
50	2.06×10^{-4}

DNA interaction assays

2.7 Study of the interaction between compounds and pUC18 plasmid DNA

2.7.1 *Escherichia coli* culture and DNA extraction

Plasmid DNA (pDNA) extraction from pUC18 (Thermo Scientific, Waltham, United States of America), was done from *Escherichia coli* DH5α culture. Transformed cells stored at -80ºC were inoculated (20 µL) in an erlenmeyer (50 mL) with 20 mL of Luria-Bertani medium and 100 µg/mL of ampicillin (100 mg/mL, Bioline, Humber Road, United Kingdom). The culture was grown for sixteen hours with orbital agitation of 250 RPM at 37ºC.

The NZYMiniprep kit (Nzytech, Lisbon, Portugal) was used to extract pUC18 pDNA. The procedure was followed according to manufacturer's instructions, however some exceptions were performed: centrifugation times of 30 seconds was doubled for 1 minute and the elution step was made with 30 µL of Tris-HCl buffer (50 mM Tris-HCl (Merck, Whitehouse Station, United States of America), 10 mM NaCl (Panreac, Barcelona, Spain), pH 7.0) pre-warmed at 70ºC.

The resulting pDNA was quantified by spectrophotometry at 260 nm (NanoDrop2000*,* Thermo Scientific, Waltham, United States of America). DNA purity is evaluated with the ratios Abs_{260}/Abs_{280} and Abs_{260}/Abs_{230}. Values of Abs_{260}/Abs_{280} bellow 1.8 indicate protein contamination and above 2.0 RNA presence. Values of Abs_{260}/Abs_{230} bellow 2.0 indicate mainly alcohol contamination, and this ratio must be between 2.0 and 2.2. DNA integrity was assessed by agarose gel electrophoresis at 0.7 % (w/v) in TAE 1x (composition for 1 L of TAE 10x: 48.4 g of Tris-base, 3.72 g of EDTA, 11.42 mL of acetic acid, pH 8.0) with 1 % (v/v) GelRed (10000 x, Biotarget, Lisboa, Portugal).

2.7.2 Plasmid DNA Electrophoretic procedure

Each sample (20 µL) was prepared by mixturing 200 ng of pDNA pUC18, with the compounds (concentration between 0 and 200 µM) and Tris-HCl buffer (50 mM Tris-HCl, 10 mM NaCl, pH 7.0). Compounds were diluted in the same buffer before adding to the samples. A pDNA sample with 1.6 % (v/v) DMSO, instead of compound, was prepared as control. A sample of 200 ng of pDNA pUC18 was linearized with 0.5 µL of EcoRI (10 U/µL, Fermentas, Maryland, United States of America), 2 µL of EcoRI buffer (Fermentas, Maryland, United States of America) and destilled water until 20 µL.

Samples were incubated during 24 hours at 37ºC. Then, they were deposited on an electrophoresis agarose gel 0.7 % (p/v) in TAE 1x buffer and run at 70 V during 90 minutes in a horizontal electrophoresis system. The DNA size marker used was λ DNA/HindIII (Fermentas, Maryland, United States of America). The agarose gel was stained in a solution of 100 mL of distilled water with ethidium bromide (Invitrogen) 0.04 % (v/v) during 15 minutes with agitation and visualized and images acquired with BioRad equipment and Quantity One software (BioRad, California, United States of America). Gel images were analysed by GelAnalyzer 2010 (http://www.gelanalyzer.com/).

2.8 Spectrophotometric assays

For compound-DNA interaction assessment absorption spectroscopy was done. The solution of DNA used was prepared by dilution (1:100) of Calf Thymus-DNA (Ct-DNA, Invitrogen, Carlsbad,

United States of America) stock in Tris-HCl buffer (50 mM Tris-HCl (Merck, Whitehouse Station, United States of America), 10 mM NaCl (Panreac, Barcelona, Spain), pH 7.0). Ct-DNA was quantified by spectrophotometry at 260 nm (*NanoDrop2000,* Thermo Scientific, Waltham, United States of America).

Samples of different concentrations of Ct-DNA (2 µM to 84 µM) were prepared by pippeting diferent volumes from the stock solution (1:100). Then 200 µM of compound 2 or 1 µM of 4 or DMSO were added. 70 µL of Tris-HCl buffer and destiled water was added to make up 100 µL. DMSO absorbance was discounted from the obtained data. Samples were incubated during 24 hours at 37ºC. Then the U.V./Visible spectrum was acquired between 230 nm and 500 nm (UVmini-1240 UV-Vis Shimadzu spectrophotometer, Kyoto, Japan) for 80 µL of each sample.

Protein interaction assays

2.9 Human Serum Albumin interaction assays

Human Serum Albumin (HSA, Sigma, St. Louis, United States of America) stock solution was prepared diluting 100 mg of HSA in 10 mL of phosphate buffer (39 mL of 0.2 M monobasic sodium solution (Merck, Whitehouse Station, United States of America), 61 mL of 0.2 M dibasic sodium solution (Sigma, St. Louis, United States of America) and 100 mL of distilled water) with 0.15 M NaCl (VWR, Radnor, Pennsylvania), pH 7, incubating 1 hour at room temperature for full rehydration. Samples were prepared with 35 µM of HSA and varying the concentration of compound 2 (0 µM to 720 µM). Then phosphate buffer was added to make up 100 µL. Samples were incubated during 24 hours at 37ºC. The U.V./Visible spectrum was acquired between 230 nm and 500 nm (UVmini-1240 UV-Vis Shimadzu spectrophotometer, Kyoto, Japan) for 80 µL of each sample and an emission spectrum between 300 nm and 500 nm after excitation at 295 nm (Varian Cary Eclipse Fluorescence Spectrophotometer, Agilent Technologies, Santa Clara, United States of America).

2.10 Proteomic assay

2.10.1 Cell culture and lysis

Two-dimensional electrophoresis was used in this work for the analysis of protein mixture extracted from HCT116 cells after compound treatment. The technique allows to separate proteins according to two independent chemical properties in two steps: first Isoelectric focusing (IEF, see 2.10.5), which separates proteins according to their isoelectric points, and the second step Sodium Dodecyl Sulfate-Polyacrylamide Gel Electrophoresis (SDS-PAGE, see 2.10.6), which separates them according to their Molecular Weights (MW).

In a 175 cm^2 culture flask, HCT116 cells (2 x 10^5 cells/mL) in Complete Culture Medium were incubated during 24 hours at 37ºC in a humidified atmosphere of 99% and 5% (v/v) CO_2 in air for cell adherence. After 24h compounds were added after aspirating the medium and cells were incubated for 48 hours at 37ºC in a humidified atmosphere of 99% and 5% (v/v) CO_2. As a control cells were incubated in the presence of 0.1% (v/v) DMSO (99.5%, Sigma, St. Louis, United States of America).

After the 48 hours of incubation cells were harvested (see 2.4) to microcentrifuge tubes (1.5 mL) and washed 2 times with PBS 1x. Lysis buffer (see Annex, **Table 6.1**) was applied in a proportion of 100 µL for 1 x 10^6 cells/mL. Cell lysis was accomplished with the aid of a sonicator (Hielscher UTR200, Teltow, Germany). First, five cycles of five pulses at 60% amplitude, second ten cycles of ten pulses at 70% amplitude and finally ten cycles of fifteen pulses at 80% amplitude, all of them at 0,5 cycles and 30 seconds of interval on ice between each group of pulses. Afterwards, lysated samples were seen at microscope to confirm the lysis. In the end, samples were centrifugated first at 500 xg during 5 minutes at 4ºC to remove debris. The supernatant was recovered to a new microcentrifuge tube to centrifugate again at 9000xg during 10 minutes at 4ºC and stored at -80ºC.

2.10.2 Protein extract purification

On the following day, samples were thawed on ice and about 8 hours later, 2-D Clean-up Kit (GE Healthcare, Little Chalfont, United Kingdom) was used to purify the samples, according to manufacturer's instructions, but with some exceptions. 1 mL of cold (-20ºC) acetone was added to the pellet that was then dissolved by the aid of the vortex during 2 hours each 15 minutes. Afterwards, samples were left overnight at -20ºC. On the following day, the pellet was recovered at 12000 RPM during 15 minutes at 4ºC. Then 1 mL of cold (-20ºC) acetone was added. The pellet was dissolved with the aid of the vortex for 2 hours and recovered at 12000 RPM during 15 minutes at 4ºC. Pellet was left to dry and remove acetone at room temperature during 5 minutes.

For protein rehydration 100 µL of rehidration buffer were used (see Annex,**Table 6.2**). Then it was thawed at room temperature and added prior use 0.1% DTT (10%, Promega, Madison, United States of America) and 1 mM PMSF (100 mM, Sigma, St. Louis, United States of America). Samples in rehidration buffer stayed at room temperature for 2 hours. Samples were then centrifugated at 14000xg during 15 minutes to recover the supernatant where the soluble protein extract was.

2.10.3 Total protein quantification

For total protein quantification Pierce 660nm Protein Assay (Thermo Scientific, Waltham, United States of America) was used. The assay is based on the binding of a deprotonated dye-metal complex to positively charged amino acid groups in proteins, in acidic conditions, causing a shift in the dye's absorption maximum measured at 660nm. This dye interacts mainly with basic residues in proteins. 5 µL of each protein extract, 45 µL of distilled water, and 750 µL of Pierce reagent (Thermo Scientific, Waltham, United States of America) were mixed by the aid of a vortex. The absorbance of each sample was read at 660 nm (Nanodrop2000, Thermo Scientific, Waltham, United States of America) and compared to a standard curve (125 to 1000 µg/mL of Bovine Serum Albumin, BSA, Thermo Scientific, Waltham, United States of America).The volume corresponding to 200 µg of total protein was added to a new microcentrifuge tube.

2.10.4 SDS-PAGE for assessment of compound quantification

Compound interference in Pierce quantification was assessed by comparing the SDS-PAGE results of samples with or without compound treatment.

The volume corresponding to 20 µg of total protein was mixed with a solution of 1x SDS loading buffer (4%, see Annex, **Table 6.3**) and 0.1% of DTT (10%, Promega, Madison, United States of America) and left overnight at room temperature. On the following day, the supernatant was recovered at 10000xg during 15 minutes. The samples were loaded in a poliacrilamide gel (see Annex, **Table 6.4**) and run at 130V (BioRad, California, United States of America, see **Table 6.5**) until the bromophenol blue arrived at the end of the gel.

Gels were stained in a 100 mL solution of comassie blue R-350 (see Annex, **Table 6.6**). Gels in this solution were warmed in the microwaves during 2 minutes at 450 W, and rested 30 minutes on low horizontal agitation. In order to remove the excess of staining, the staining solution was substituted by Milli-Q water. This process was repeated until the excess is removed.

2.10.5 First dimension: IEF

0.5 % (v/v) of DeStreak Reagent (GE Healthcare, Wilmington, United States of America) and 0.5 % (v/v) of IPG pharmalyte pH 3-10 (GE Healthcare, Wilmington, United States of America) were added to 200 ng of protein in 125 µL of rehydration buffer.These samples were loaded on a ceramic support with an Immobiline DryStrip pH 3-10 NL of 7 cm (GE healthcare, Wilmington, United States of America). Afterwards, about 750 µL of Drystrip Cover Fluid (GE Healthcare, Wilmington, United States of America) were added. Samples were placed in Ettan IPGphor3 IEF System (GE Healthcare, Wilmington, United States of America) running the program in the **Table 2.4**:

Table 2.4 Conditions of the Isoelectric Focusing program in Ettan IPGphor3 IEF System. Other parameters are 50 µA per strip and 20 ºC.

Step number	Volts (V)	Time (hour)
1	30	14
2	100	0,5
3	500	0,5
4	1000	0,5
5	5000	1

2.10.6 Second dimension: SDS-PAGE

After Isoelectric Focusing, strips were placed in 5 mL of an equilibration solution (see Annex, **Table 6.7**) with 1% (p/v) of DTT (Promega, Madison, United States of America) during 15 minutes and then with a new equilibration solution with 2.5% (p/v) of iodoacetamide (GE Healthcare, Wilmington, United States of America) for more 15 minutes.

Strips were placed in 12% poliacrilamide gels (see Annex, **Table 6.4**) and sealed with a solution of 0.5 % (p/v) of agarose (Fisher Scientific, Waltham, United States of America) in electrophoresis buffer with bromophenol blue traces (Riedel-de Haën, Saint Louis, United States of America).

The same procedure that was described before (see 2.10.4) was used to run the samples, excepting the use of catodic buffer (1x of electrophoresis buffer (10x, see **Table 6.5**), 0.5% SDS (10%, p/v, Riedel-de Haën, Saint Louis, United States of America) and Milli-Q water) between the gels. 30 V were applied to ease protein transfer and then 80 V until the end of the gel. Gels staining procedure was described before (see 2.10.4).

2.10.7 Gel Analysis

The analysis of the protein abundancy levels was done by Melanie 7.0 software (Genebio, Geneva, Switzerland). First, spots were detected automatically and confirmed manually. Then, the match was made between spots of different gels. Each spot has a relative volume (% vol) obtained by Melanie 7.0 software. The abundancy level for each spot to DMSO (0.1%) control was calculated as shown in equation (3).

$$(3)\quad \frac{\text{media of the relative volume of each spot on compound gels}}{\text{media of the relative volume of each spot on control gels}}$$

If abundancy level is equal or greater that 1.5 it indicates more protein abundancy than the control, and if it is equal or less than 0.7 it indicates less protein abundancy. Spot identification was made by comparison with a reference gel, where some spots were previously identified by Matrix Assisted Laser Desorption/Ionization-Time of Flight (MALDI-TOF) Mass Spectrometry (at ITQB as collaboration).

Apoptotic potential assessment

2.11 Hoechst 33258 staining

Hoechst 33258 nucleic acid stain is a fluorescent probe that emits blue fluorescence (461 nm) when bound to dsDNA. Apoptotic potential was assessed for compounds 2 and 4 in the HCT116 carcinoma cell line. Culture plaques of 35 mm^2 with a square microscope slide cover glass in the center were seeded with 2 mL of 0.75 x 10^5 cells/mL solution and incubated during 24 hours with 37ºC, 5% (v/v) CO_2 and 99% of relative humidity to allow cell adherence. Then, the medium was aspirated and the compounds or 0.1 % of DMSO (control) (diluted in 2 mL of complete culture medium) were added. After 48 hours of incubation in the presence of the compounds or DMSO, cells were washed 3 times with PBS 1x (Invitrogen, Carlsbad, United States of America), fixed by adding 1 mL of a cold solution of paraformaldehyde 4 % (v/v) in PBS 1x and incubated at room temperature during 10 minutes in the dark. Cells were washed with 1 mL of PBS 1x, three times. A staining solution in the proportion of 2 µL of Hoeschst 33258 (5 mg/ mL, Sigma, St. Louis, United States of America) in 1 mL of PBS 1x was prepared and added to each plaque and incubated at room temperature during 15 minutes in the dark. Cells were washed with 1 mL of PBS 1x, three times. Afterwards 10 µL of a glycerol solution in PBS 1x in the proportion of 1:3 (v/v) was added to a microscope slide, and the microscope slide cover glass mounted carefully on the top with the cells glass face down. The compound 2 preparation was observed at the Olympus DP50 BX51 fluorescence microscope (Olympus, Tokyo, Japan) and the images acquired with the Olympus software. The compound 2018-5-3 preparations were observed at the Leica DFC480 DMLB fluorescence microscope (Leica, Solms, Germany) and the images acquired with the IrfanView software.

2.12 Flow cytometry

Flow citometry was used in this work to assess cell death. HCT116 cells were plated into 35 mm dishes at 1.5x10^5 cells per plate. Culture medium was removed 24 h after platting and replaced with 2 mL of fresh medium in the following conditions 1 to 5: 0.1% (v/v) DMSO (vehicle control) or (1) 86.5 µM of compound 2 or (2) 0.25 µM or (3) 0.42 µM of doxorubicin, or (4 and 5) doxorubicin and afterwards compound 2 for more 24 h. Cells were incubated and then stained with fluorescein isothiocyanate (FITC) labeled annexin V and propidium iodide (PI) (Invitrogen, Carlsbad, United States of America) by the following procedure. After 48 hours of incubation, cells were harvested at 1500 RPM for 5 minutes and washed 2 times with PBS 1x.100 µL of 1x Anexin V binding buffer (10x) in distilled water, 5 µL of Anexin V FITC and 2 µL of propidium iodide were added to the pellet of all samples. Then, samples were incubated at room temperature in the dark during 15 minutes. 400 µL of 1x Anexin V binding buffer and 500 µL of PBS1x were added. Samples were read in a flow cytometer Attune® Acoustic Focusing Flow Cytometer (Life Technologies, Carlsbad, California), acquiring 10000 events per sample. The results were analysed with Attune v2.1 (Applied Biosystems) software.

3 Results and Discussion

3.1 Antiproliferative activities

The experimental work was initiated with the viability assays that are used to determine if the compounds have effect on cell proliferation or show direct cytotoxic effects that could lead to cell death (Riss *et al*., 2013). In order to assess cell viability in response to compound treatment, the metabolic MTS assay was chosen. This assay measures mitochondrial enzymatic activity that occurs only in viable and proliferating cells (McGowan *et al*., 2011).

The rhenium compounds were tested in nine different cell lines (**Figure 3.1** to **Figure 3.9**). The values of relative IC_{50} were calculated from the analysis of dose-response curves obtained with the data from the **Figure 3.1** to **Figure 3.9**. The relative IC_{50} is given by the compound concentration corresponding to the midpoint between the top and bottom plateaus of the dose-response curve. The bottom plateau is due to the background absorbance of the assay reagents at 490 nm and the calculus of relative IC_{50} is one way of overcome this technical interference. The values of absolute IC_{50} could be obtained directly from the data since it is the value that corresponds to 50% on the right axis (GraphPad, 2010).

Compared to compound 1 and 3, compound 2 showed a higher antiproliferative activity in all the cell lines tested (**Figure 3.1** to **Figure 3.9**) and in particular the most promising results were obtained in HCT116 (IC_{50} of 88.6 µM +/- 7.1) and MNT-1 (IC_{50} of 57.6 µM +/-9.1) cell lines (**Figure 3.1** and **Figure 3.9**, respectively). Interestingly, a smaller cytotoxic effect of compound 2 in normal fibroblasts was observed (**Figure 3.2**). Even at 88.6 µM (IC_{50} of HCT116) of compound 2, cell viability in fibroblasts is ~100% (**Figure 3.2**).

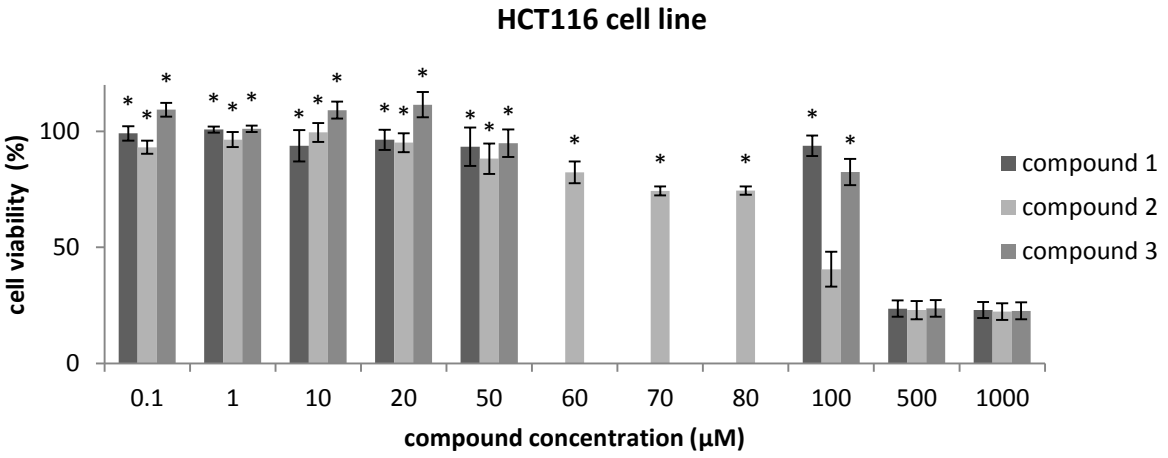

Figure 3.1 Cell viability assays in HCT116 cell line after 48 hours of treatment with compounds 1, 2 and 3. Cell viability was assessed by the MTS assay. The values shown correspond to media of three independent assays.The error bars correspond to the standard error of the mean (*p<0.05 in relation to 500 µM and 1000 µM of compound 1 and 3, and *p<0.05 in relation to 100 µM, 500 µM and 1000 µM for compound 2). Cell viability values were normalized to the control cells (no added compounds; presence of DMSO 0.1%).

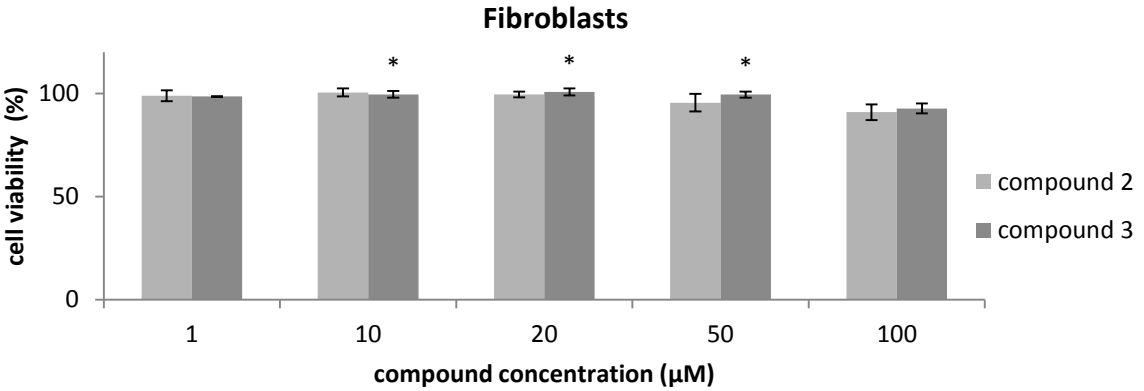

Figure 3.2 Cell viability assay in fibroblasts after 48 hours of treatment with compounds 2 and 3. Cell viability was assessed by MTS assay. The values shown correspond to media of three independent assays for compound 2 and two independent assays for compound 3. The error bars correspond to the standard error of the mean (*p<0.05 in relation to 100 µM of compound 3). Cell viability values were normalized to the control (no added compounds; presence of DMSO 0.1%).

In the present study, the Selectivity Index (SI) can not be calculated for compound 2. Selectivity Index is the result of the ratio between the IC_{50} of the compound in a normal cell line (fibroblasts) and the IC_{50} of the same compound in the cancer cell line (e.g. HCT116) (Badisa *et al*., 2010). The range of concentrations tested on fibroblasts was not enough to determine the corresponding IC_{50}. However could be expected a SI higher than 1. This is an important property for a chemotherapeutic drug since side-effects may be minimised.

Besides our results, Ho and co-workers synthesised $[ReBr(CO)_3(SSC)]$ [SSCs = semicarbazones] complexes that exhibited moderate to high cytotoxicities towards MOLT-4 cells from acute lymphoblastic leukemia (IC_{50} = 1–24 µM), and the majority of them were almost non-toxic against normal human fibroblasts. Displacement of the SSC ligand is probably not involved in the mechanism of cytotoxicity of rhenium salicylaldehyde semicarbazone complexes, but interaction with biomolecules after loss of bromide is plausible (Ho *et al.*, 2013).

It is worth of note the importance of the ligands in the antitumour complex antiproliferative activities. Comparing the results observed for compound 1 (IC_{50} of 213.9+/-15.9 µM), with the more hydrophilic 1,3,5-triaza-7-phosphaadamantane (PTA) ligand, and compound 2 (IC_{50} of 88.6+/-7.1 µM), with the same structure but instead of PTA with the ligand hexamethylenetetramine (HMT), it could be said that the HMT ligand is more effective in a antitumour compound than the PTA ligand. However, Scolaro and co-workers showed some promising results for compounds with PTA ligands by comparing the *in vitro* and *in vivo* activity and cytotoxicity of a series of RAPTA-type complexes bearing PTA ligands (Scolaro *et al*., 2005). It was demonstrated that these compounds are active and selective towards the metastasizing mouse cell line (TS/A) from mammary adenocarcinoma. Other compounds with PTA ligands such as $[C_5H_5Rh(PTA)Cl_2]$ and $[Os(\eta^6\text{-}p\text{-}C_{10}H_{14})Cl_2(PTA)]$ demonstrated cytotoxicity activity in the HT29 colon cell line. A possible explanation is as cancer cells display lower pH values (<6) than healthy ones, PTA would protonate at low pH values and hence showing selective DNA damage for cancer cells (Scolaro *et al*., 2005).

On the other hand, Scolaro and co-workers in other experiments showed that in some situations more hydrophilicity could be detrimental. The insertion of functional groups such as amines on the arenes of RAPTA-type compounds and formation of cationic complexes with BF_4 was tested in order to enhance hydrogen bonding with DNA. RAPTA-type compounds possess a modular structure comprising a ruthenium-bound arene, one PTA molecule and two halides and are known for their antitumour activity. Cell viability studies using the metastasizing mouse cell line TS/A from mammary adenocarcinoma were compared to the nonfunctionalized analogues. These structural alterations resulted in a decrease in toxicity towards cancer cells being a possible explanation the increasing hydrophilicity detrimental to drug uptake (Scolaro *et al*., 2006).

Those studies show that there must be a compromise between hydrophilicity and hydrophobicity to an effective antitumour effect and in the present study this is achieved by compound 2.

In addition to these observations, is known that the metal center of the complex, even with similar ligands, have an important role. The trans-platinum thiolate complexes bearing PTA or DAPTA ligands trans-$[Pt(SR)_2(P)_2]$ [P = PTA, SR = 2-thiopyrimidine, 2-thiopyridine; P = DAPTA, SR = 2-thiopyrimidine, 2- thiopyridine] and gold(I) complexes [Au(SR)(PR'3)] (SR = various thiolato derivatives; PR'3 = PTA, DAPTA) were tested for *in vitro* cytotoxicity against seven human cancer cell lines. Au(I) complexes showed low cytotoxicity, while the Pt(II) complexes demonstrated high cytotoxicity for almost the cells lines, including colon cancer cell line (Miranda *et al*., 2008). It would be interesting to study similar changes for the present rhenium compounds since it could better elucidate the structure-activity relationship and the importance of the metal center.

The results of cell viability assay in the chronic myelogenous leukemia cell line K562 after 48-hour treatment with the rhenium compounds are represented in **Figure 3.3**.

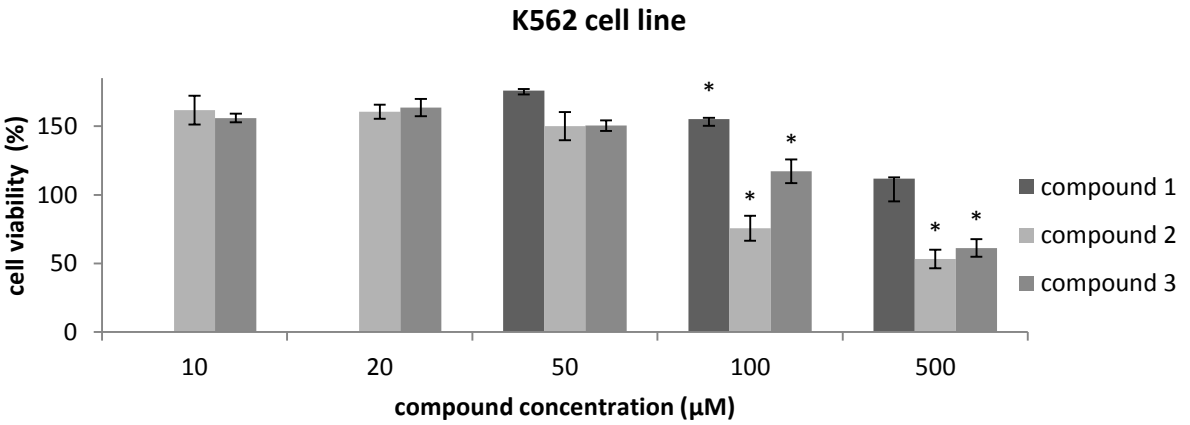

Figure 3.3 Cell viability assay in K562 cell line after 48 hours of treatment with compound 1, 2 and 3. Cell viability was assessed by MTS assay. The values shown correspond to media of three independent assays, excepting the cell viabilities for treatment with 10 and 20 µM concentrations of compound 1 and cell viabilities.The error bars correspond to to the standard error of the mean (*p<0.05 in relation to 50 µM of compound 1, *p<0.05 in relation to 10, 20 and 50 µM for compounds 2 and 3). Cell viability values were normalized to the control: (no added compounds; presence of DMSO 0.1%).

Although the unsatisfactory response of the chronic myelogenous leukemia cell line to the rhenium compounds in the present work, Parson and co-workers tested other rhenium compounds with promising results in which the rhenium atom is octahedrally coordinated to a chelated (bidentate)

polypyridyl ligand, three adjacent CO molecules, and a pentylcarbonate group [-OC(O)OC_5H_{11}] in a facial arrangement. According to the authors, the six drugs showed GI_{50} (GI_{50}, 50% cell-growth inhibition) around 3-4 μM and an efficacy against all the cancer cells treated, including myeloid leukemia cancer cells, at a lower dose than the cisplatin (Parson *et al*., 2013a). These studies show once again that the ligands around the metal atom play an important role in the antitumour properties.

The antiproliferative activities in lung adenocarcinoma cell lines (A549, H1650 and H1975) after 48-hour treatment with the rhenium compounds are represented on **Figure 3.4**, **Figure 3.5** and **Figure 3.6**.

Lung cancer is histologically classified into two major types, small cell lung cancer (SCLC) and nonsmall cell lung cancer (NSCLC). Approximately 85–90% of lung cancers are NSCLC being adenocarcinoma 40% of NSCLC (Gong *et al.*, 2011).

As far as the treatment of NSCLC is concerned, targeted therapies are mainly specific to the oncogenic tyrosine kinase pathways activated in tumour cells. For example, some receptor tyrosine kinase (RTK) pathway inhibitors, such as Sunitinib (Sutent) and Crizotinib are in clinical trials for NSCLC (Gong *et al.*, 2011).

The major problem in targeted therapy for NSCLC is to know the activated oncogenic pathways in the patient's tumor so that the appropriate inhibitor(s) can be chosen (Gong *et al.*, 2011). In this way there are a wide range of cell lines with different activated oncogenic pathways in order to study more efficacious treatments. H1975 shows a moderate activation of epidermal growth factor receptor2 (HER2), hepatocyte growth factor receptor (c-MET), and Src Homology 2 Domain Containing (SHC) pathways and a low activation of the insulin-like growth factor 1 receptor (IGF-1R) pathway. The metastatic bronchioalveolar carcinoma cell line H1650 shows a moderate activation of the HER1 and HER2 pathways.The large-cell carcinoma cell line A549 exhibits a moderate activation of the HER1 and IGF-1R pathways with a low activation of the c-MET and HER2 pathways (Gong *et al.*, 2011).

A549 cell line results for compound 2 (IC_{50} 197.8 μM), the one with best results, shows that it is not efficacious in this adenocarcinoma cell line. Our results in H1975 and H1650 cell lines show a similar outcome for rhenium compounds. Indeed, Vock and co-workers studied a serie of compounds of general formula [Ru($_6$-pcymene)(R_2acac)(PTA)][X] (R_2acac =Me_2acac, tBu_2acac, Ph_2acac, Me_2acac-Cl; X= BPh_4, BF_4) and demonstrated that tetrafluoroborate salts were less cytotoxic for A549 lung carcinoma than for the A2780 cells and the values of cytotoxicity were correlated to the lipophilicity parameters of the complexes (Vock *et al.*, 2008).

A549 cell line harbors the KRAS mutated gene. KRAS gene mutation is associated with resistance to HER1 tyrosine kinase inhibitors (Kobayashi *et al*., 2005; Paez *et al*., 2004). A549 don't respond to treatment with HER1 inhibitors but it is sensitive to the downstream Phosphoinositide 3-kinase (PI3K) inhibitor BEZ-235 (Gong *et al.*, 2011).

H1975, and H1650 lung tumor cell lines harbor the HER1 gene mutation and they are sensitive to HER1 inhibitor treatment. H1975 cells respond more effectively to a combination of HER1/2 RTK inhibitor BIBW-2992 with either MEK inhibitor PD-325901 or PI3K inhibitor BEZ-235 with almost 100% growth inhibition of this cell line at 10 *μ*M concentration. A synergistic inhibition of H1650

cell proliferation can be observed when it is treated with the irreversible HER1/2 inhibitor BIBW-2992 in combination with one of the downstream inhibitor BEZ-235 or a combination of the two downstream inhibitors, PD-325901 and BEZ-235 (Gong *et al.*, 2011).

Combined therapy is a more efficacious way of eradicate a tumour, as it is indicated by the responses of lung cell lines to this known inhibitors. In this way, it would be important to try compound 2 with an established drug on the lung cancer cell lines.

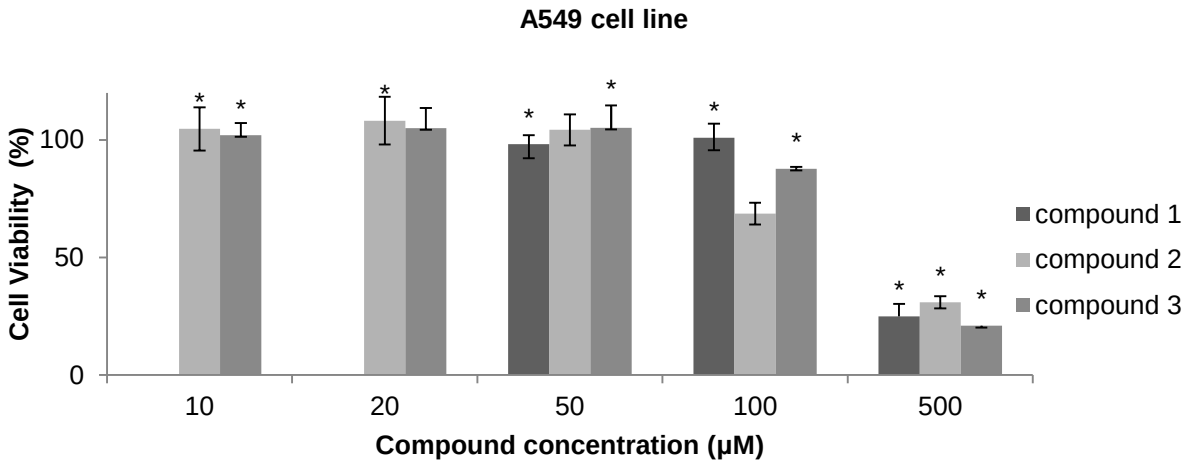

Figure 3.4 Cell viability assay in A549 cell line after 48 hours of treatment with compounds 1, 2 and 3. Cell viability was assessed by MTS assay. The values shown correspond to media of three independent assays, excepting the cell viabilities for treatment with 10 and 20 µM concentrations of compound 1.The error bars correspond to the standard error of the mean (*p<0.05 in relation to 500 µM of compound 1, 2 and 3). Cell viability values were normalized to the DMSO control: (no added compounds; presence of DMSO 0.1%).

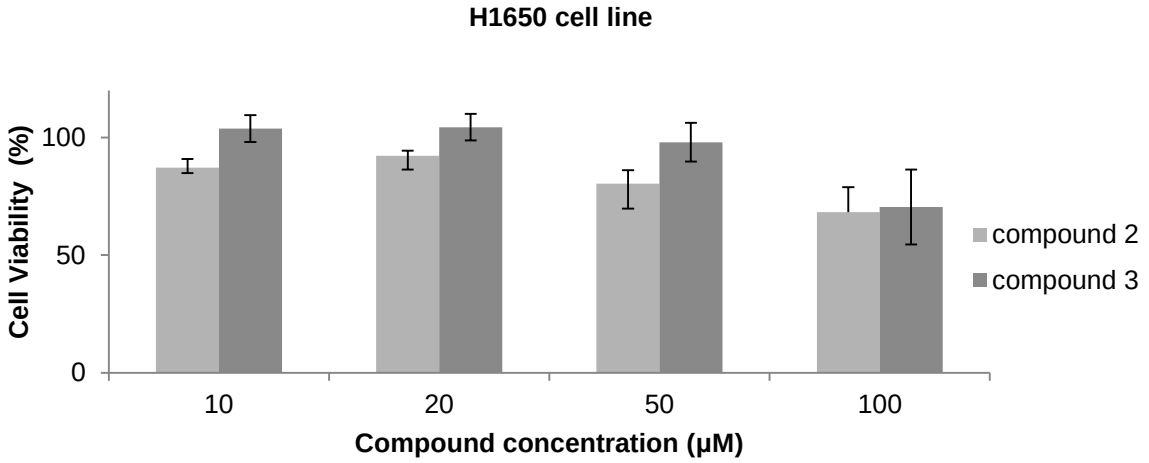

Figure 3.5 Cell viability assay in H1650 cell line after 48 hours of treatment with compounds 2 and 3. Cell viability was assessed by MTS assay. The values shown correspond to media of two independent assays.The error bars correspond to the standard error of the mean. Cell viability values were normalized to the DMSO control: (no added compounds; presence of DMSO 0.1%).

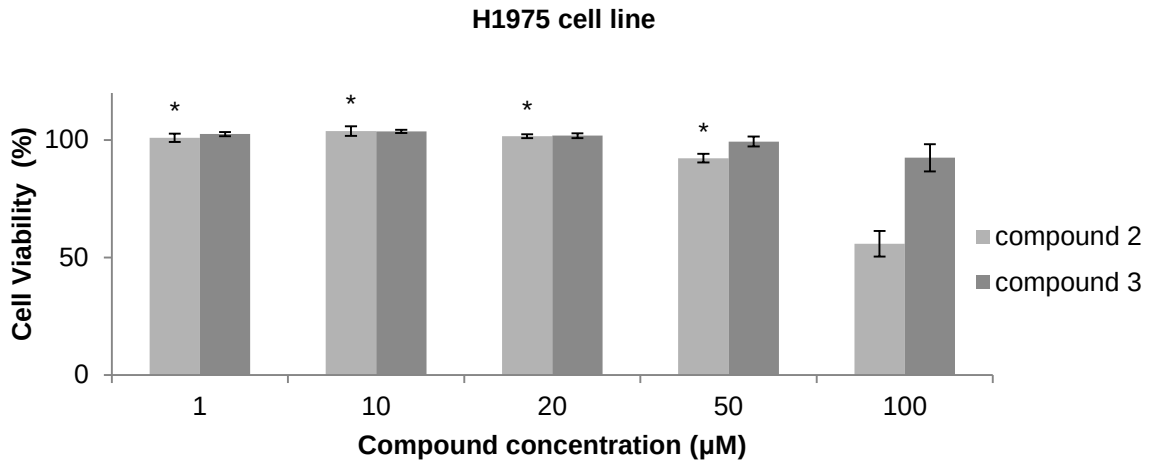

Figure 3.6 Cell viability assay in H1975 cell line after 48 hours of treatment with compounds 2 and 3. Cell viability was assessed by MTS assay. The values shown correspond to media of three independent assays. The error bars correspond to the standard error of the mean (*p<0.05 in relation to 100 μM of compound 2). Cell viability values were normalized to the DMSO control: (no added compounds; presence of DMSO 0.1%).

In **Figure 3.7** we show the antiproliferative activity results for the breast cancer cell line, MCF7, after 48-hour treatment with the rhenium compounds.

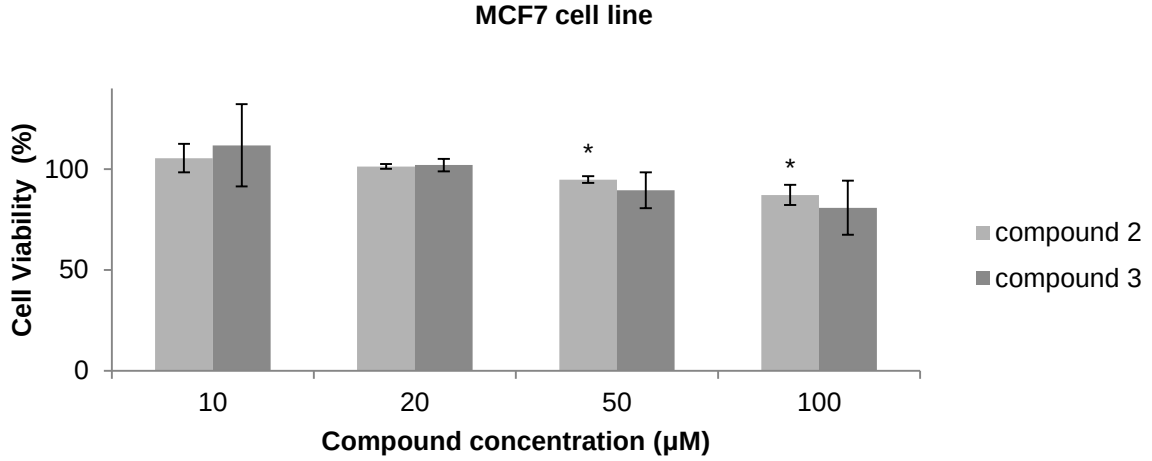

Figure 3.7 Cell viability assay of MCF7 cell line after 48 hours of treatment with compounds 2 and 3. Cell viability is assessed by MTS assay. The values shown correspond to media of three independent assays. The error bars correspond to the standard error of the mean (*p<0.05 in relation to 20 μM of compound 3). Cell viability values were normalized to the control: (no added compounds; presence of DMSO 0.1%).

Concerning the viability results in mammary carcinoma (MCF7) cell line no effective antiproliferative effect was observed (**Figure 3.7**). However, rhenium compounds could be studied in combined therapy with selenium compounds, as suggested by other authors.Collery and co-workers studied a water-soluble rhenium diseleno-ether compound (with one atom of Re and two atoms of Se) *in vivo* and they also investigated the uptake of Re into the nucleus of malignant cells in culture. It was observed that a compound combining Re and Se in a single molecule, is able to deliver them to the organism via an oral route, for cancer treatment. It was also demonstrated that exposure to Rhenium diseleno-ether induced a Re uptake in the nucleus and there was no efflux of Re after a post-exposure period of 48 hours in MCF-7 cells. The explanations appointed for the success of the Re

diseleno-ether compound is its amphiphilic nature. Its solubility in water makes it easy to administer and its lipophilic properties allow a great diffusion across cell membranes (Collery *et al*., 2014).

Other rhenium compounds were studied in MCF-7. Cabeza and co-workers studied complexes of rhenium(I) with some 5-nitrosopyrimidines with general formula $[ReCl(CO)_3L]$ that showed cytotoxic effects in all the cell lines used, including MCF-7(Cabeza *et al*., 2005). Other six novel rhenium pentycarbanato compounds were also presented by Parson and co-workers. The trypan blue assay revealed a significant cytotoxicity against the triple node negative breast cancer cell line HTB-132 and less toxicity than cisplatin in the Balb/c mouse kidney cell lines (Parson et *al.*, 2013b). Further studies are needed to discover the mechanism of action and structure-activity relationship of these rhenium compounds what could in addition explain the results of the compounds 2 and 3 in the MCF7 cell line.

Similar results to MCF7 cell line are shown in hepatocellular cancer cell line HepG2 (**Figure 3.8**). In contrast, besides the radioactive isotopes of rhenium, Wong and co-workers also studied the rhenium compound of formula $[Re(CO)_3(2\text{-appt})Cl]$ [2-appt = 2-amino-4-phenylamino-6-(2-pyridyl)-1,3,5-triazine] that exhibited moderate cytotoxicities toward several cancer cell lines, including HepG2 (Ma *et al*., 2007).

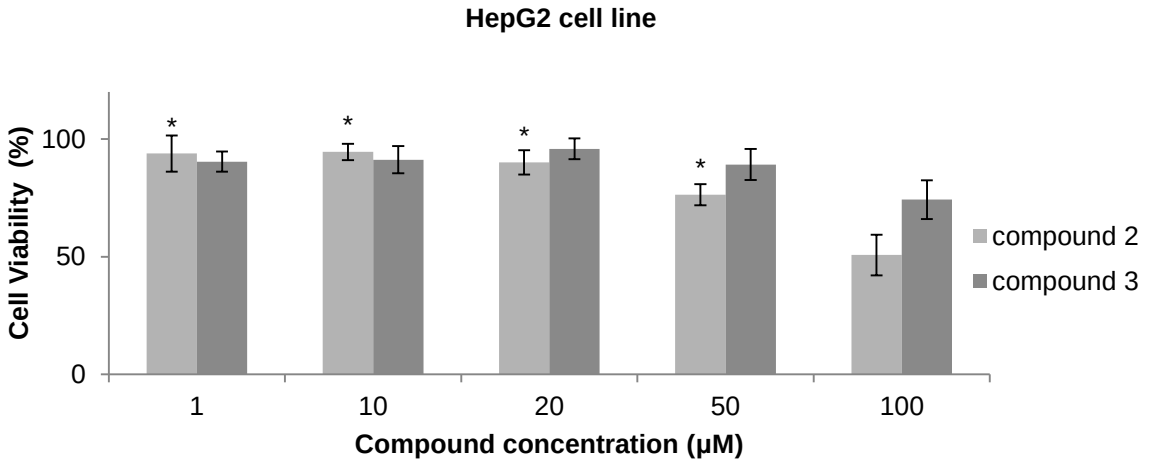

Figure 3.8 Cell viability assay in HepG2 cell line after 48 hours of treatment with compounds 2 and 3. Cell viability was assessed by MTS assay. The values shown correspond to media of three independent assays. The error bars correspond to the standard error of the mean (*$p<0.05$ in relation to 100 µM of compound 3). Cell viability values were normalized to the control: (no added compounds; presence of DMSO 0.1%).

As observed in the melanocitic cell line from the skin (MNT-1), the compound 2 with the hexamethylenetetramine (HMT) ligands show a better antitumour activity compared to compound 3 with the tris(pyrazol-1-yl)methanesulfonate (Tpms) ligand (**Figure 3.9**).

Malignant melanomas are intrinsically resistant to many conventional treatments, such as radiation and chemotherapy (Chen *et al*., 2009). There is a radioactive rhenium compound, ^{188}Re-6D2, in clinical trials for the treatment of melanoma. The data demonstrated that was well tolerated, localized in melanoma metastases, and had antitumor activity. The investigation is going on in patients with metastatic melanoma (Klein *et al.,* 2013).

Although the interesting antiproliferative potencial of compound 2 in MNT-1 cancer cell line, studies were not continued due to the possible interference of its dark color in the colorimetric cell viability assays.

The rhenium compound 1 with the PTA ligands was not tested on most of the cancer cell lines (HepG2, MNT-1, H1975, H1650). However, studies undertaken by Pettinari and co-workers with four silver(I) complexes of formulas [Ag(Tpms)], [Ag(Tpms)-(PPh3)], [Ag(Tpms)(PCy3)], and [Ag(Tpms)(PTA)] {Tpms = tris(pyrazol-1-yl)methanesulfonate, PPh3= triphenylphosphane, PCy3= tricyclohexylphosphane} showed antiproliferative activity, with IC_{50} between 0.42 μM and 12.35 μM, against human malignant melanoma (A375) with an activity often higher than that of AgNO3, which has been used as a control. The complex with less activity was [Ag(Tpms)(PTA)] whereas the other complexes without the PTA ligand showed higher cytotoxicity, even the complex [Ag(Tpms)] (Pettinari *et al*., 2011). Taking these results into consideration and our previous results in other cancer cell lines it is possible to expect that the rhenium compound 1 has lower cytotoxic potential.

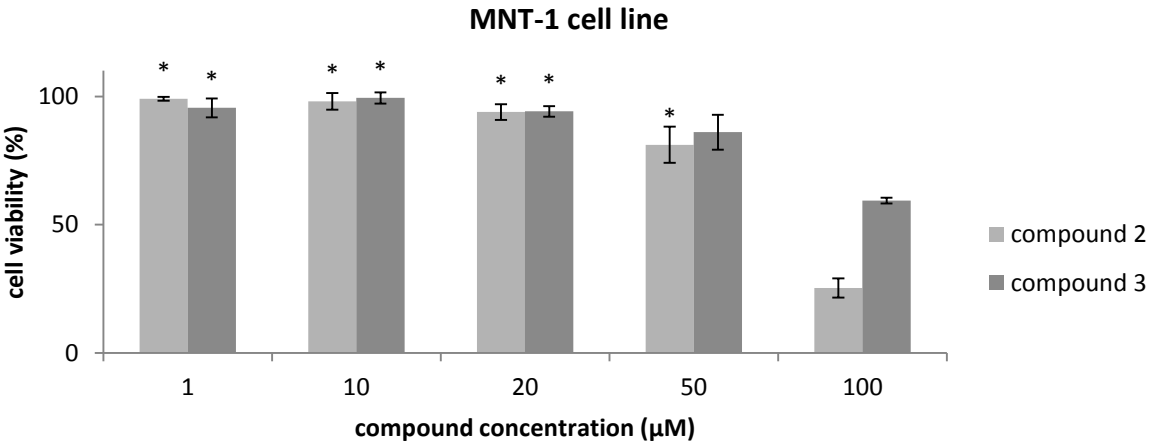

Figure 3.9 Cell viability assay in MNT-1 cell line after 48 hours of treatment with compounds 2 and 3. Cell viability was assessed by MTS assay. The values shown correspond to media of three independent assays. The error bars correspond to the standard error of the mean (*p<0.01 in relation to 100 μM of compound 2 and compound 3). Cell viability values were normalized to the control: (no added compounds; presence of DMSO 0.1%).

The results are summarized in **Table 3.1**.

Table 3.1 Cell viability assays results for rhenium compounds. The values shown correspond to media of three independent assays, excepting for H1650 cell line that are two independent assays. The IC_{50} value for compound 2 in HCT116 is representend as IC_{50} +/- SEM. Half maximal inhibitory concentration (IC_{50}) is determined by the software *GraphPadPrism 6*.

	IC_{50} (µM)		
Cell line	Compound 1	Compound 2	Compound 3
A549	>100	>100	>100
H1650	---	>100	>100
H1975	---	~100	>100
HCT116	>100	88.6 +/- 7.1	>100
HepG2	---	>100	>100
K562	>100	>100	>100
MCF-7/GFP	---	>100	>100
MNT-1	---	57.6 +/-9.1	>100
Fibroblasts	---	>100	>100

3.1.1 Combined therapeutics with compound 2 on colorectal cancer cell line

The majority of cases of colorectal cancer diagnosed are in advanced stage. Adenomas and early stage colorectal cancers are often asymptomatic but potentially curable if early detected and removed while symptomatic colorectal cancers are mostly likely in advanced stage when detected and treatment options more complicated specially in metastatic tumors (Carethers, 2008).Therapy for advanced colorectal cancer can be divided into colon and rectal cancer components, with surgery as the main component of therapy for both subtypes. Rectal cancers are treated surgically by low anterior resection or abdominal perineal resection, often in combination with 5-fluoruracil (5-FU)-based chemoradiation. All the stages of the disease are generally treated with adjuvant or neoadjuvant chemotherapy, excepting Stage I disease that is approached with wide surgical resection. In stage I, cancer has formed in the mucosa (innermost layer) of the colon wall and has spread to the submucosa (layer of tissue under the mucosa) (Winslow, 2014). For colon cancers, is normal to use adjuvant 5-FU-leucovorin or FOLFOX (5-FU, leucovorin, and oxaliplatin) especially in stage III patients and FOLFIRI for stage IV colon cancer (Carethers, 2008). In stage III cancer may have spread through the mucosa of the colon wall to the submucosa and muscle layer, and has spread to nearby lymph nodes or tissues near the lymph nodes. In stage IV cancer has spread through the blood and lymph nodes to other parts of the body, such as the lung, liver, abdominal wall, or ovary (Winslow, 2014). For this last stage, specific growth factor inhibitors, such as bevacizumab [antibody against VEGF] and cetuximab [antibody against EGFR] can also be added to the 5-FU-based chemotherapy. All of these treatments have diverse side effects and some of them are only for palliative care (Carethers, 2008).

As said before, new antitumour therapies are needed, including novel combinations with established chemotherapeutics. For this purpose is important to study drug combinations and administration schedules with more efficacies and less side-effects. In addition, the complexity of cancer and drug resistance requires a treatment that is able to target more than one biological component (Yap *et al*., 2013).

Some authors propose that the metal rhenium is more suitable for the treatment of cancer patients with anemia than iron (Collery *et al*., 2004). Rhenium, besides its possible antitumor potential, stabilizes the erythrocyte membrane by an antioxidant effect, protecting the erythrocytes against toxic agents that induce hemolysis (Shtemenko *et al.,* 2002). In this way, rhenium could be used in combination with other cytotoxic drugs, like cisplatin, in order to reduce side effects and improve the antitumour potencial (Collery *et al*., 2014). As stated before the use of HMT, the ligand of the compound 2, as an adjuvant to radiation and cisplatin in the treatment of the solid tumours with promising results was reported (Masunaga *et al*., 2010).

These observations potentiated to test the effect on HCT116 cell viability of the combined therapy with compound 2 and cisplatin (**Figure 3.10** and **Figure 3.11**). Besides the 48-hour treatment with cisplatin (IC_{50}) or compound 2 (IC_{50}) alone, the simultaneous administration of both compounds was analysed as well as the administration of cisplatin for 24h and then the administration of compound 2 for more 24h, and vice versa (**Figure 3.10** and **Figure 3.11**).

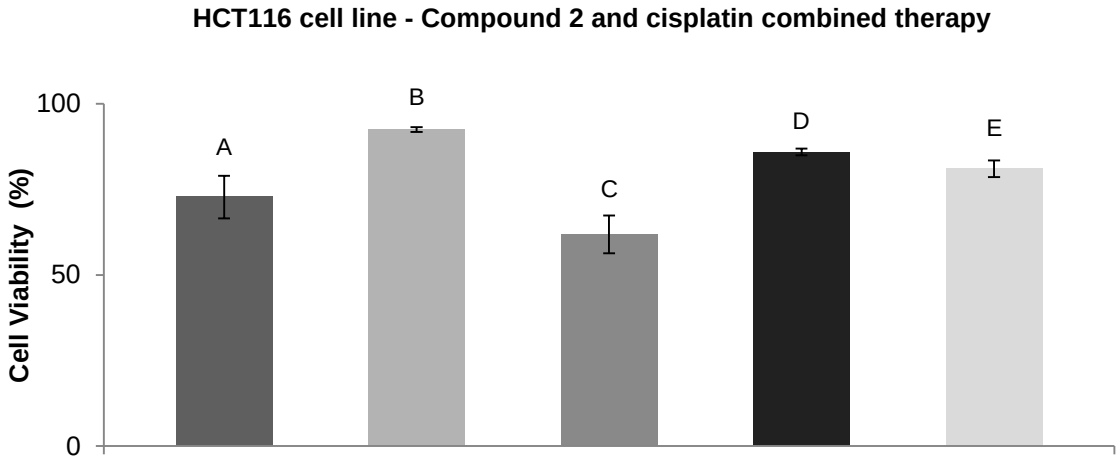

Figure 3.10 Cell viability in HCT116 cell line after combined therapy with compound 2 and cisplatin in the following conditions (A) to (E): (A) 15.3 µM of cisplatin for 48h, (B) 86.5 µM of compound 2 for 48h, (C) 15.3 µM of cisplatin for 24 hours and afterwards 86.5 µM of compound 2 for more 24h and (D) vice versa, and the (E) simultaneous addition of cisplatin (15.3 µM) and compound 2 (86.5 µM) for 48h. Cell viability was assessed by MTS assay. The values shown correspond to the media of three independent assays. The error bars correspond to the standard error of the mean ($p>0.05$, t-test). Cell viability values were normalized to the control cells (presence of DMSO 0.1%).

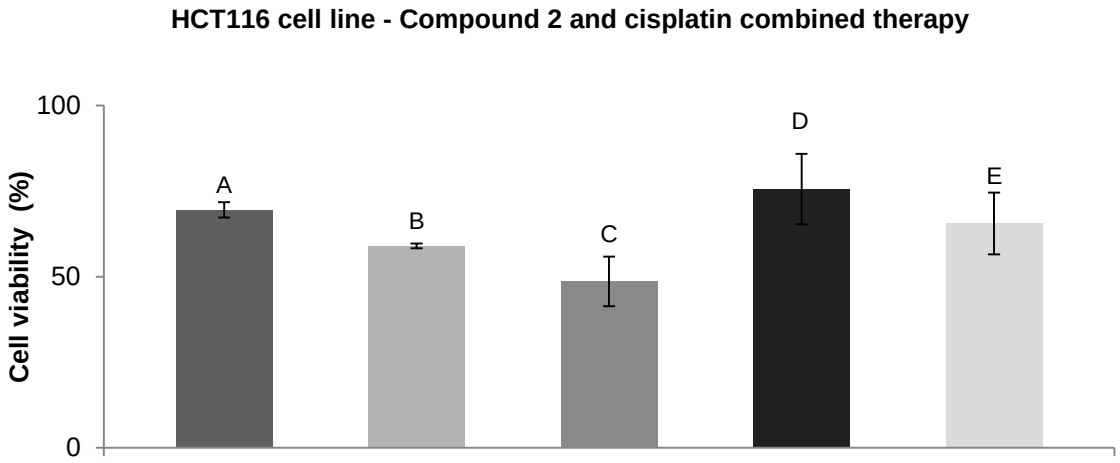

Figure 3.11 Cell viability in HCT116 cell line after combined therapy with compound 2 and cisplatin in the following conditions (A) to (E): (A) 15.3 µM of cisplatin for 48h, (B) 95 µM of compound 2 for 48h, (C) 15.3 µM of cisplatin and afterwards 95 µM of compound 2 for more 24h and (D) vice versa, and the (E) simultaneous addition of cisplatin (15.3 µM) and compound 2 (95 µM) for 48h. Cell viability was assessed by MTS assay. The values shown correspond to media of three independent assays. The error bars correspond to the standard error of the mean ($p>0.05$, t-test). Cell viability values were normalized to the control: (presence of DMSO 0.1%).

The best results were for the combined therapeutics where was administered cisplatin (15.3 µM) and then the compound 2 (+/-95 µM) for more 24 hours.

Ono and co-workers studied the administration *in vivo* of doxorubicin encapsulated into pegylated liposomes and the combination with hexamethylenetetramine (HMT), showing promising results (Masunaga *et al*., 2009). For this reason compound 2 was also tested with doxorubicin on the colorectal cancer cell line, with the same therapeutic schedule. The results are shown in **Figure 3.12** and **Figure 3.13**.

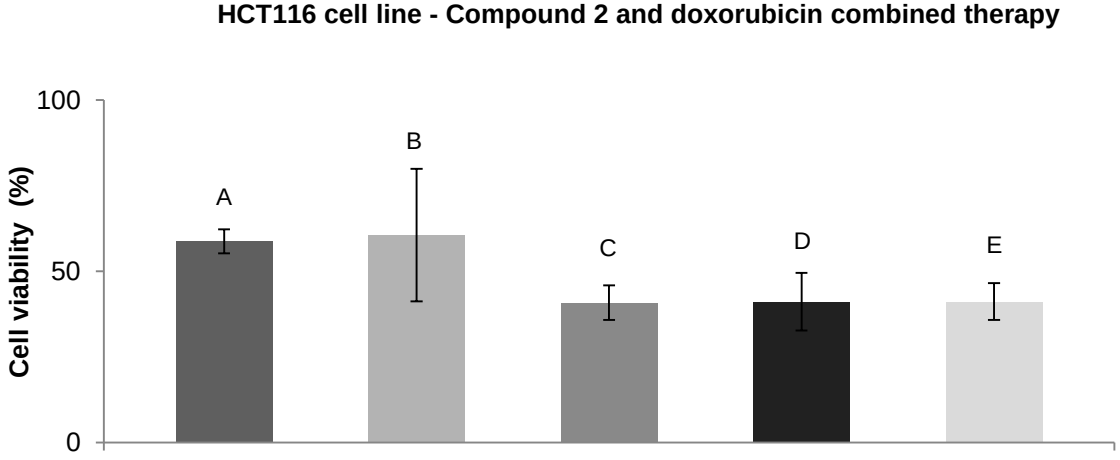

Figure 3.12 Cell viability assay in HCT116 cell line after combined therapy (48 hours) with compound 2 in the following conditions (A) to (E): (A) 0.42 µM of doxorubicin, (B) 95 µM of compound 2, (C) 0.42 µM of doxorubicin and afterwards 95 µM of compound 2 for more 24h and (D) vice versa, and the (E) simultaneous addition of doxorubicin (0.42 µM) and compound 2 (95 µM). Cell viability was assessed by MTS assay. The values shown correspond to media of three independent assays. The error bars correspond to the standard error of the mean ($p>0.05$, t-test). Cell viability values were normalized to the control: (presence of DMSO 0.1%).

In **Figure 3.13** the best combination of compound 2 and doxorubicin is analyzed in order to reduce the administred concentration of doxorubicin, and consequently reducing its side-effects. The

best results were observed for compound 2 administration and 24 hours later doxorubicin treatment, and vice versa, with a reduction of ~1.5x in the percentage of cell viability compared to doxorubicin alone.

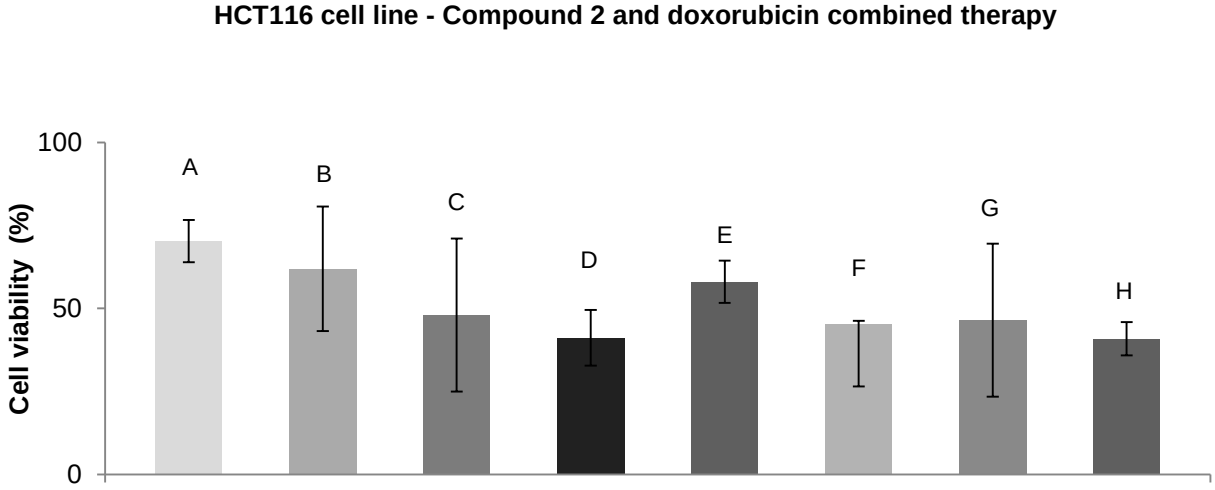

Figure 3.13 Cell viability in HCT116 cell line after combined therapy with compound 2 and doxorubicin in the following conditions (A) to (H): (A) 95 µM of compound 2 and then 0.25 µM of doxorubicin for more 24h, (B) 95 µM of compound 2 and then later 0.3 µM of doxorubicin for more 24h, (C) 95 µM of compound 2 and then 0.35 µM of doxorubicin for more 24h, (D) 95 µM of compound 2 and then 0.42 µM of doxorubicin for more 24h, (E) 0.25 µM of doxorubicin and then 95 µM of compound 2 for more 24h, (F) 0.3 µM of doxorubicin and then 95 µM of compound 2 for more 24h, (G) 0.35 µM of doxorubicin and 24 hours then 95 µM of compound 2 for more 24h, and (H) doxorubicin (0.42 µM) and then compound 2 (95 µM) for more 24h. Cell viability was assessed using the MTS assay. The values shown correspond to the media of three independent assays. The error bars correspond to the standard error of the mean ($p>0.05$, t-test). Cell viability values were normalized to control cells (presence of DMSO, 0.1%).

3.1.2 Compound 4

In **Figure 3.14** the antiproliferative potential of compound 4 in colonrectal carcinoma cell line was assessed after 48-hour of treatment. As we can observe there is a high loss of cell viability in the presence of this compound being the relative IC_{50} 0.2654 µM.

When compared to the relative IC_{50} of doxorubicin (0.42 µM) or cisplatin (15.3 µM) in this tumor cell line (Silva, 2012) this result is very promising. In order to understand if this result is due to the effect of the compound or the ligand trimeric polythiophene acetic acid (PTAA) we also have assessed the antiproliferative potential of the ligand in this cell line (**Figure 3.15**). It was obtained a relative IC_{50} of 0.6334 µM for the ligand tPTAA that is higher than the compound 4. This might indicate that the metallic center is also important for its antitumour properties.

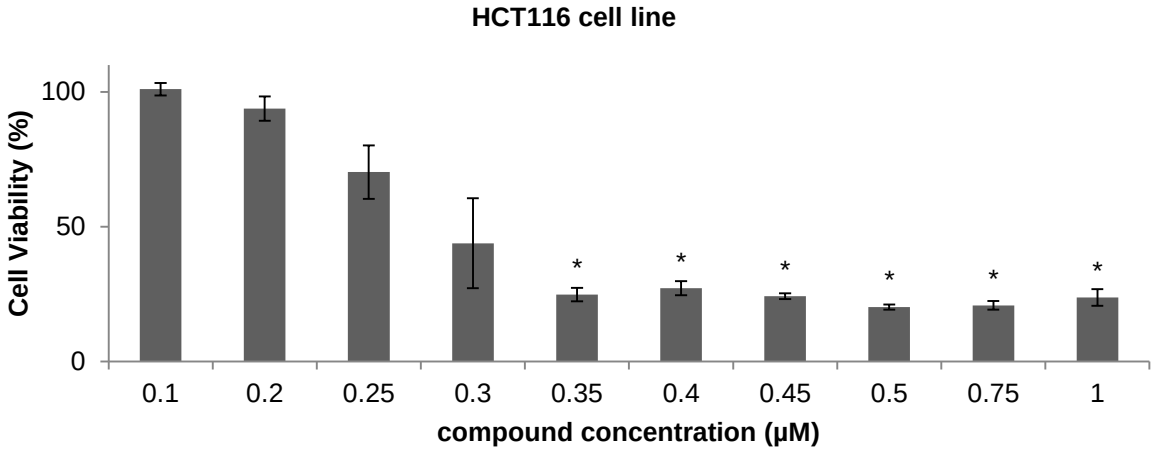

Figure 3.14 Cell viability in HCT116 cells after 48 hours of treatment with compound 4. Cell viability was assessed using the MTS assay. The values shown correspond to the media of three independent assays for the compound. The error bars correspond to the standard error of the mean (*p<0.01 in relation to 0.1 and 0.2 µM of compound 4). Cell viability values were normalized to the control cells (presence of DMSO 0.1%).

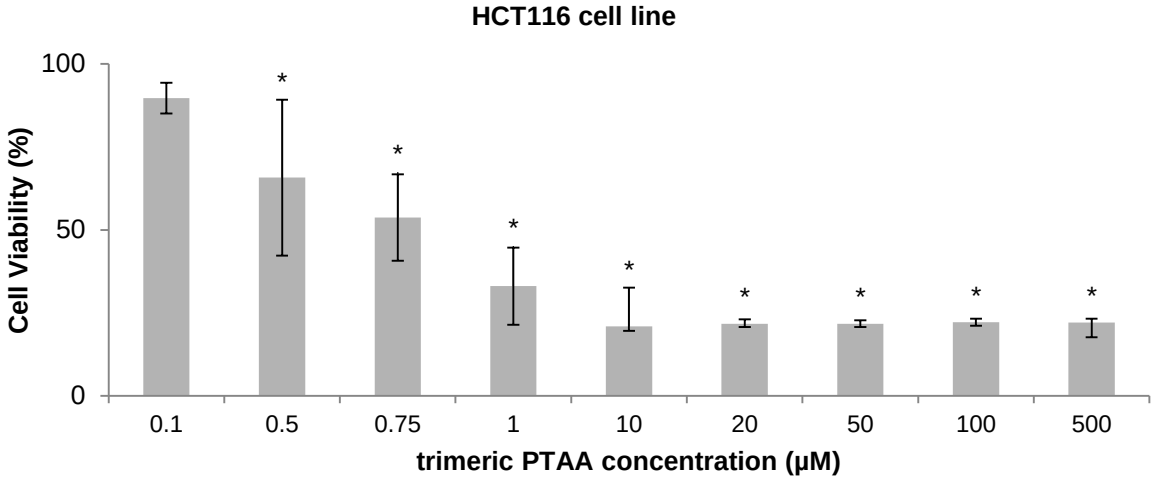

Figure 3.15 Cell viability assay in HCT116 cell line after 48 hours of treatment only with the tPTAA ligand of compound 4. Cell viability was assessed by MTS assay. The values shown correspond to media of three independent assays, excepting for 0.5, 0.75 and 500 µM. The error bars correspond to the standard error of the mean (*p<0.05 in relation to 0.1 µM of compound 4). Cell viability values were normalized to the control: (no added compounds; presence of DMSO 0.1%). Data provided by Master Joana Filipa Pires Silva.

Few communications that use trimeric PTAA have been reported. It is used mainly to identify and characterize amyloid deposits (Nilsson *et al*., 2010). The heterodisperse polythiophene acetic acid derivatives, polythiophene acetic acid (PTAA) and trimeric PTAA, emitted yellow-red fluorescence on binding to amyloid deposits, being luminescent-conjugated thiophene polymers spectroscopy a sensitive and powerful tool for identifying and characterizing amyloid deposits (Heilbronner *et al*., 2013; Nilsson *et al*., 2010).

Combined therapy of compound 4 and doxorubicin or cisplatin have also been performed due to the high antiproliferative potential of this compound in HCT116 tumor cell line (**Figure 3.16** and **Figure 3.17**). The best results were observed for the simultaneous administration of 4 and cisplatin

(see **Figure 3.17**) with a reduction of almost 3x in the percentage of cell viability compared to cisplatin alone (E bar compared to A bar in **Figure 3.16**).

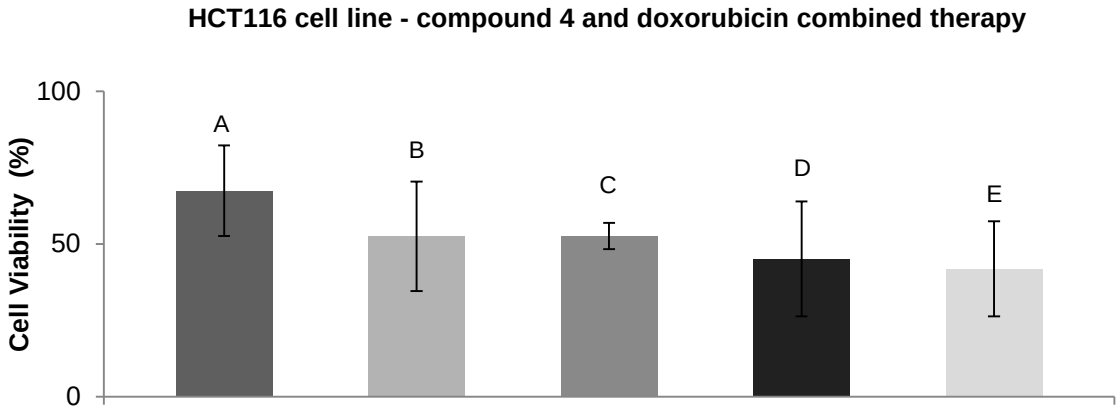

Figure 3.16 Cell viability in HCT116 cell line after combined therapy with compound 4 and doxorubicin in the following conditions (A) to (E): (A) 0.42 µM of doxorubicin for 48h, (B) 0.2 µM of compound 4 for 48h, (C) 0.42 µM of doxorubicin and afterwards 0.2 µM of compound 4 for more 24h and (D) vice versa, and the (E) simultaneous addition of doxorubicin (0.42 µM) and compound 4 (0.2 µM) for 48h. Cell viability was assessed using the MTS assay. The values shown correspond to media of three independent assays. The error bars correspond to the standard error of the mean (p>0.05, t-test). Cell viability values were normalized to the control cells (presence of DMSO 0.1%).

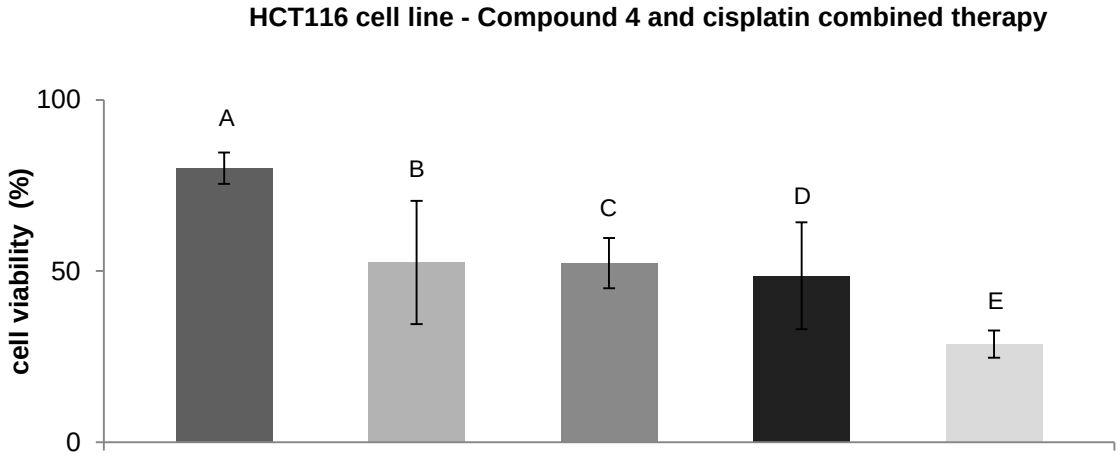

Figure 3.17 Cell viability assay in HCT116 cell line after combined therapeutics with compound 4 in the following conditions (A) to (E): (A) 15.3 µM of cisplatin, (B) 0.2 µM of compound 4, (C) 15.3 µM of cisplatin and afterwards 0.2 µM of compound 4 for more 24h and (D) vice versa, and the (E) simultaneous addition of cisplatin (15.3 µM) and compound 4 (0.2 µM). Cell viability is assessed by MTS assay. The values shown correspond to media of three independent assays. The error bars correspond to the standard error of the mean (p> 0.05, t-test). Cell viability values are normalized in relation to the control cells: (presence of DMSO 0.1%).

When tested in fibroblasts, compound 4 also promotes a high loss of cell viability (**Figure 3.18**). For this reason, it would be interesting to study compound 4 in a liposomal drug delivery system (Fernandes and Baptista, 2013).

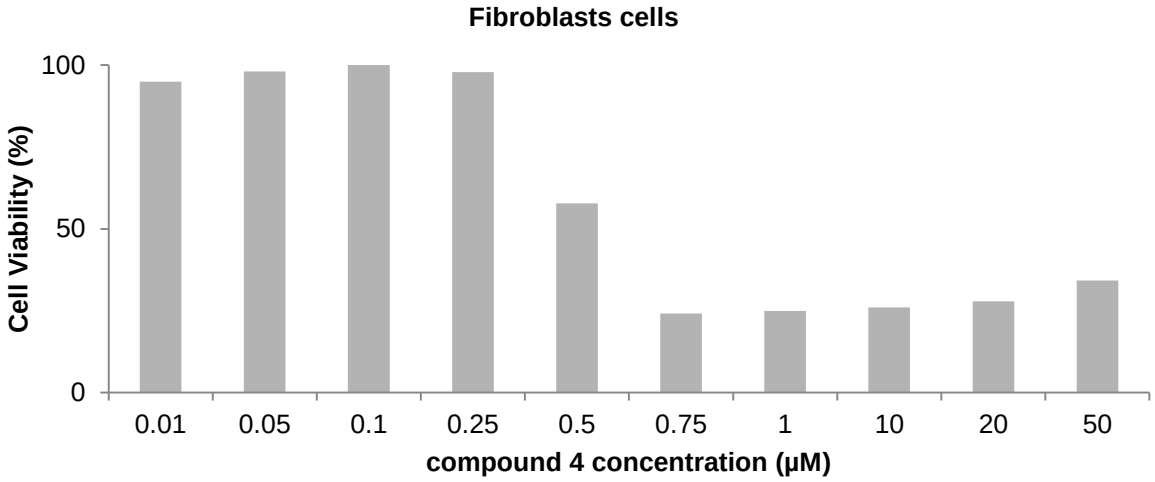

Figure 3.18 Cell viability in HCT116 cells after 48 hours of treatment with compound 4. Cell viability was assessed using the MTS assay. Cell viability values were normalized to the control cells (presence of DMSO 0.1%). Data provided by Master Joana Filipa Pires Silva.

3.2 Laser Flash photolysis

The Laser Flash photolysis studies were performed due to the possibility of formation of transient species by the rhenium compounds. This line of thinking was based on studies from Kastl and co-workers concerning the derivatives of a nontoxic luminescent probe of rhenium applied for biological imaging that was discovered to have antitumor properties when irradiated at a suitable wavelength (Kastl *et al.*, 2013). Photochemical activation also permits to achieve precise spatial and temporal control of the biological action of transition-metal complexes that behave as inactive "prodrugs" in the absence of light. In this way, transition-metal complexes could be used for the light-induced liberation of bioactive compounds from the metal coordination sphere as well as as to induce a direct action of the metal center (Schatzschneider *et al.*, 2010).

Flash photolysis is a commonly used fast reaction technique for photochemical reactions. The flash photolysis concept is very simple: a short pulse of light is used to interact with a sample that has been placed in the optical path of a spectrometer. The result of this interaction can be either a transient absorption or an emission process. The laser pulse contributes to the depletion of the ground state of the compound, and the detector will measure the number of counts, at the prescribed wavelength, with respect to time. The counts will decrease following a negative exponential law that can be characterized by a decay time τ.

When detecting the absorbance at the absorption wavelength corresponding to S_0 --> S_1, the flash creates a negative ΔOD due to the depletion of ground states, which will then decay towards 0 (equilibrium state). This decay corresponds to fluorescence and internal conversion phenomena, and it is consequently very fast. However, if the molecule studied has the capability to do intersystem crossing, some of the excited singlets will become triplets which will then decay ($^3T_1$ --> $^1S_0$) by phosphorescence, delayed fluorescence, and internal conversion, which are all slow phenomena. This can give the quantum yield of triplet formation by comparing the ΔOD that is recovered directly after the flash (mostly due to fluorescence and internal conversion) and the ΔOD slowly recovered (and thus assigned to triplet states coming back to ground state).

The objective of the experiments was the determination of the quantum yield of triplet formation for compound 2, and if it can originate transient species. For that purpose the transient absorption spectra for compound 2 in water and methanol were acquired. Two solvents of different polarity were used because is it known that the photochemical behavior is influenced by environment. The results are shown in **Figure 3.19**. The possibility of transient species formation in water (600 nm) was less clear in methanol.

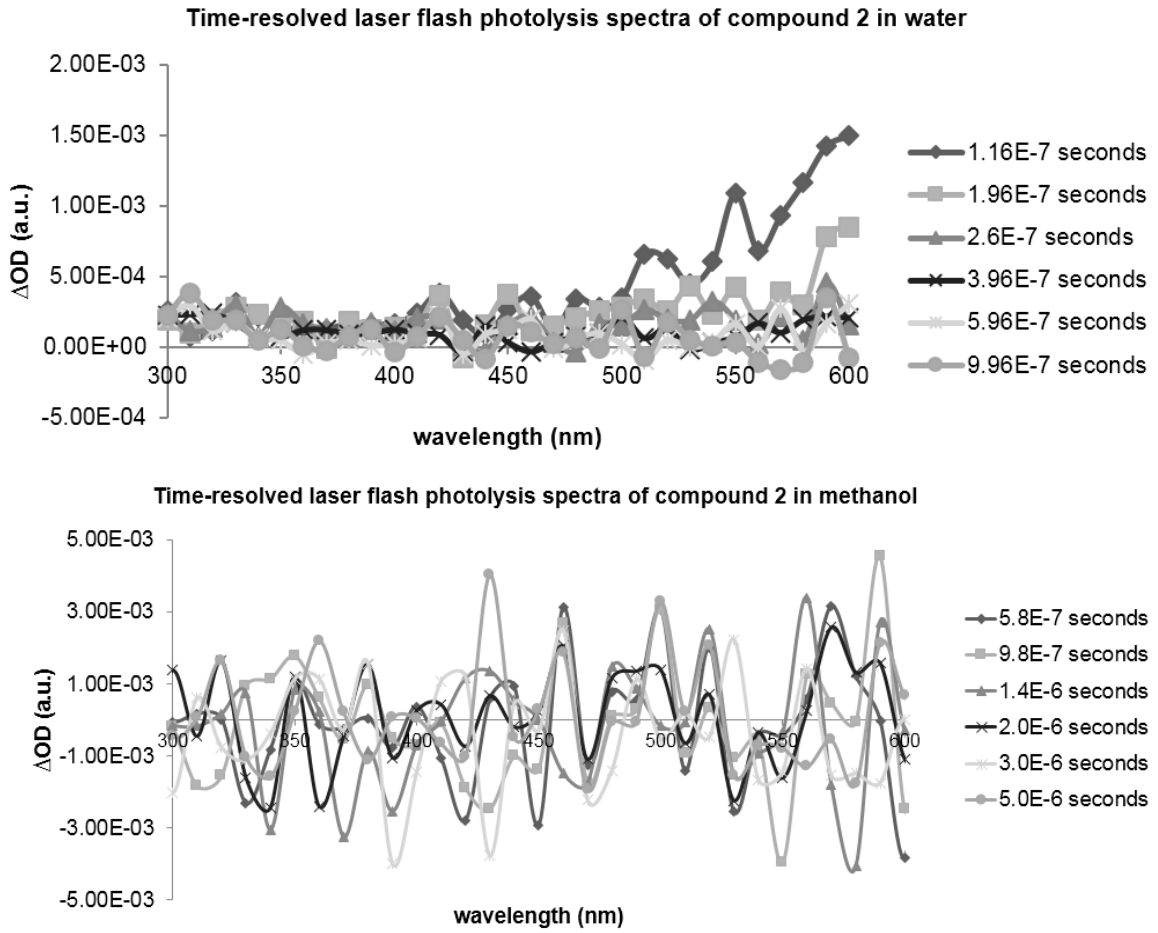

Figure 3.19 Transient absorption spectra of compound 2 in water (above) and in methanol (bottom). Laser Flash Photolysis experiments were carried out at room temperature. The concentrations of compound 2 were adjusted to yield an absorbance of 0.2 at the excitation wavelength (266 nm, laser enery around 10 J).The distilled water solution was deaerated for at least 5 minutes with oxygen-free nitrogen. Filters were placed in the light path to narrow the spectrum and remove wavelengths inferior to 305 nm. Transient absorption spectra were recorded after the laser pulse (ten shots at each wavelength, with an interval of ten nanometers).

Afterwards, an energy-transfer experiment was performed. This experiment consists in exciting another reference molecule that has the ability to transfer the energy from its T_1 excited states to the T_1 states of an acceptor molecule. This was accomplished by comparing the decays of pure donor molecule and a mixture of donor molecule and acceptor, which could gave the information on donor-to-acceptor energy transfer rate constant (ket) and consequently on the concentration of triplets in compound 2. Several criteria are necessary to have a good donor molecule: E_T (energy gap between T_1 and S_0) of the donor should be bigger than the E_T of the acceptor; the donor should have a quantum yield of triplet formation close to 1; the donor molecule should be soluble in water, what was more difficult because most of the photochemistry studies available in the reference book were conducted in organic solvents; the donor must have a singlet excitation energy corresponding to one of the laser frequency available; there must be a spectral region where the triplet of the acceptor absorb, but not those from the donor, otherwise the quenching effect may not be observed to its full scale.

The energy value corresponding to the highest energy peak observed in the 77K emission spectrum of compound 2 in methanol was measured previously. The highest energy peak

corresponds to the transition T_1 --> S_0 of the first vibrational states. Following these criteria, it was chosen benzophenone (see **Table 3.2**). The results are shown in **Figure 3.20**.

Table 3.2 The information of the benzophenone solvent for the designing of triplet-triplet energy transfer experiments in flash photolysis.

	λ_s^{0-0}	E_T	ϕ_T	λ_T	ε_T	τ_T
n/b	379	68.6	1.0	530	7220	6.9
p/nb	384	69.2	1.0	525	6250	50

Legend: The triplet energy, E_T is given in units of kcal/mol, and the singlet energy is given as an excitation wavelength, λ_s^{0-0} (nm). The triplet quantum yields, ϕ_T, and triplet lifetimes, τ_T (μs), triplet-triplet absorption wavelength, λ_T , molar absorption coefficient, ε_T ($M^{-1}cm^{-1}$), at that wavelength. To distinguish aromatic solvents for the pair of a given compound from nonaromatic solvents, "b" for "benzene-like" is used for aromatic solvents, and "nb" is used for other solvents. One or the other of these two symbols follow the "/" in the solvent column and refer only to the (λ_T, ε_T) column. The symbol preceding the "/" in the solvent column is a nonpolar/polar classification for the four properties, λ_s^{0-0}, E_T, ϕ_T and τ_T. Adapted from Murov *et al*., 1993.

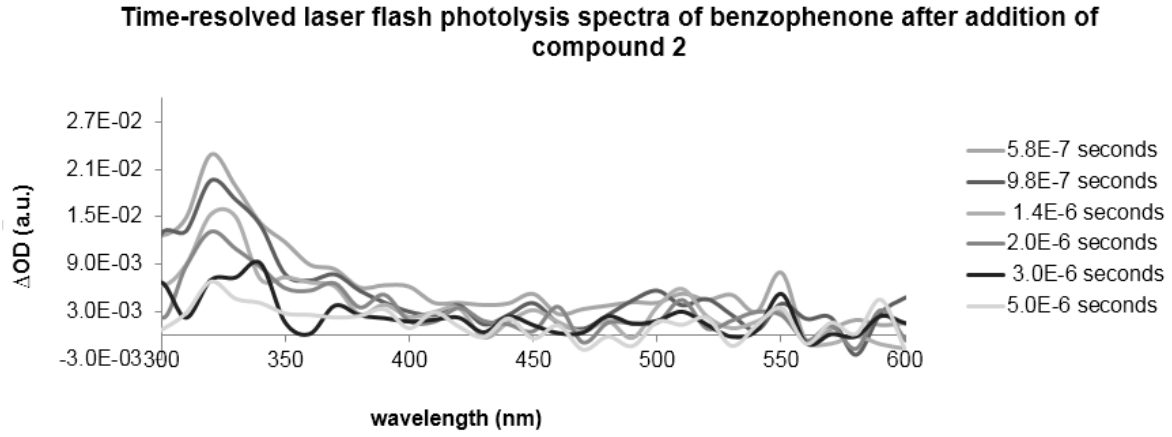

Figure 3.20 Transient absorption spectrum of benzophenone in water after the addition of compound 2 ($2.6x10^{-4}$ M). The volumes added during the titulation of benzophenone (10^{-5} mol/L) with compound 2 are described in the Table 2.3. Laser Flash Photolysis experiments were carried out at room temperature at the excitation wavelength of 266 nm and laser enery around 10 J. Filters were placed in the light path to narrow the spectrum and remove wavelengths inferior to 305 nm.

The time-resolved spectrum of benzophenone in water after the addition of compound 2 is the same of the benzophenone alone. No significative quenching effect was observed after the addition of compound 2 and the possibility of transient species formation was discarded. It could be said that the formation of transient species seen for compound 2 in water was due to solvated electrons in water as seen by other authors (Urbanek, J., 2014; Abel *et al*., 2012; Chen *et al.*, 2012).

DNA interaction assays

3.3 Study of the interaction between compounds and pUC 18 plasmid DNA

DNA unwinding properties of compounds 2 and 4 were further explored by electrophoretic mobility shift assay (EMSA) using pUC18 plasmid DNA.

Covalently closed circular DNA can assume different degrees of supercoiling ranging from the fully relaxed form to the fully supercoiled isoform. These isoforms can be separated as discrete bands using gel electrophoresis allowing the direct assessment of single or double strand breaks due to the presence of the compounds or the indirect determination of compound intercalation.

For the extracted plasmid a ratio Abs_{260}/Abs_{280} of 1.84 and a value Abs_{260}/Abs_{230} of 1.79 were obtained. The results of EMSA are shown in **Figures 3.21** and **3.22**. For compound 4, the relative percentages of plasmid DNA were not calculated because it was not possible to see all plasmid DNA isoforms. However, the results are very similar to compound 2. It can not be seen a decrease in the mobility of supercoiled DNA upon incubation with compound 2 and 4. In addition, the mobility of relaxed DNA (circular) for compound 2 is not alterated, eliminating the possibility of condensation of DNA helix due to DNA diadducts formed by the metal complexes. No perturbations of terciary structure of supercoiled DNA can be seen. The coalescence point for the two compounds at the range of concentrations tested, corresponding to the amount of intercalator molecules needed for complete removal of all supercoils from DNA (Palchaudhuri and Hergenrother, 2007), can not be determined.

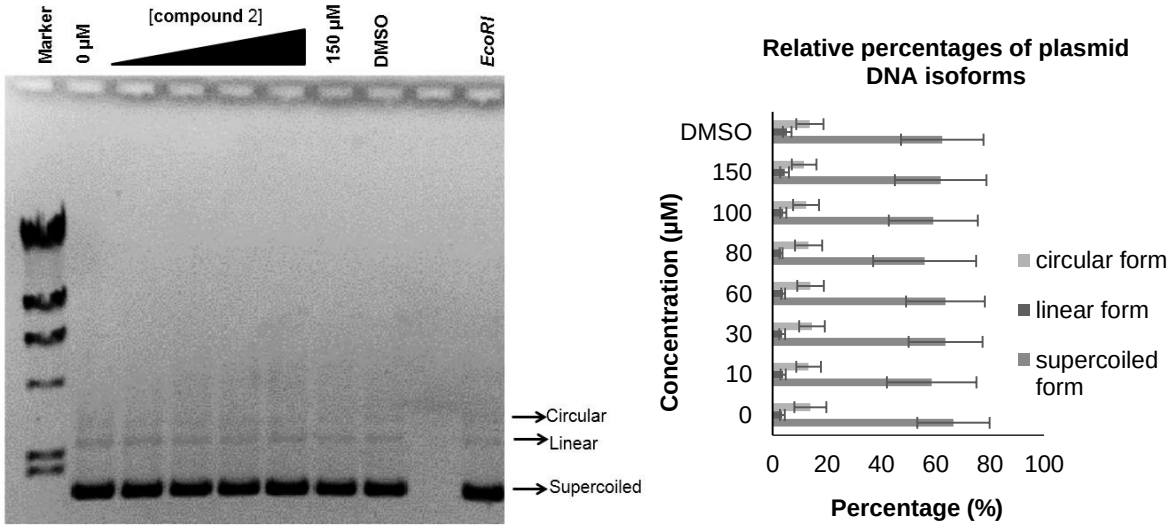

Figure 3.21 EMSA of 200 ng of pUC18 plasmid DNA after being exposed to compound 2 during 24 hours at 37ºC (left) and relative percentages of plasmid DNA isoforms per lane (3 independent assays). From left to the right on the first image: Marker is the DNA size marker λ DNA/HindIII, the concentrations (µM) of compound 2 used are 0, 10, 30, 60, 80, 100 and 150 µM, DMSO is the vehicular control lane with the DMSO volume corresponding to the maximum volume of compound 2 added, and the last lane is pUC18 linearized by *EcoRI* enzyme.

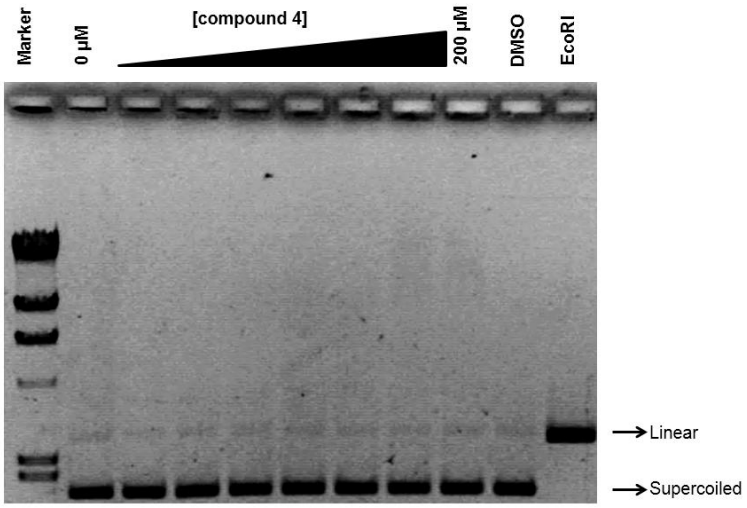

Figure 3.22 EMSA of 200 ng of pUC 18 after being exposed to the compound 4 during 24 hours at 37ºC. From left to the right: Marker is the DNA size marker λ DNA/HindIII, the concentrations (µM) of compound 4 used are 0, 10, 30, 60, 80, 100, 150 and 200 µM, DMSO is the vehicular control lane with the DMSO volume corresponding to the maximum volume of compound 4 added, and the last lane is pUC18 linearized by *EcoRI* enzyme.

3.4 DNA binding assays

DNA binding studies are important because many anticancer agents perform their action through binding to DNA leading to DNA damage in cancer cells, interrupting replication and transcription processes, and inducing apoptosis.

Generally, DNA-acting anticancer drugs can be classified into three categories: 1) drugs that form covalent linkages with DNA; 2) drugs that form noncovalent complexes with DNA by either intercalation or groove-binding and 3) drugs that cause DNA backbone cleavages (Hajian *et al*., 2009).

Rhenium is a metal able to induce adducts with nucleosides, like cisplatin, with cytotoxic properties on malignant cells (Collery *et al*., 2014). Re can bind to DNA adenine through the N1, N6 positions, or to guanine through the N7 position. Re can also induce Re-nucleotide adducts less stable than with cisplatin (Zobi *et al.*, 2007).

To assess the type of interaction of the Re compound 2, spectrophotometric studies with ct-DNA were done. The ratios Abs_{260}/Abs_{280} and Abs_{260}/Abs_{230} obtained for ct-DNA were 1.88 and 2.22, respectively.

The binding constant was calculated (see **Table 3.3**) and the absorption spectrum after 24-hour incubation at 37ºC is shown in **Figure 3.23**.

Table 3.3 Spectrophotometric assays of the interaction of compound 2 with calf-thymus DNA (ct-DNA). The data is represented as [DNA] x εa x εf versus [DNA] and then the ratio of the slope, 1/(εb-εf), to the intercept, 1/Kb(εb-εf) gives the binding constant, Kb, represented as Kb +/- SEM.

Assay number	Binding constant (Kb, M^{-1})	Mean (M^{-1})
1	$4.16x10^5$	
2	$3.64x10^5$	5.01 (+/- 1.12) $x10^5$
3	$7.23x10^5$	

Legend: εa is the apparent molar extiction coefficient, εf is the molar extiction coefficient of the compound and εb is the molar extinction coefficient of the complex bounded to DNA.

The UV-Visible spectrum of compound 2 with ct-DNA exhibits two major band at 235 nm and 260 nm. Compounds binding with DNA through intercalation usually results in hypochromism and bathochromism (Sirajuddin *et al*. , 2013). It can not be seen neither a hypsochromic or bathochromic shifts. However, a hypochromic effect exists. Additionally, based on the absorbance values obtained in the spectroscopic titration, the value obtained for *K*b was 5.01 (+/- 1.12)×$10^5 M^{-1}$. *K*b value is lower than those observed for typical classical intercalators, e.g. *K*b for ethidium bromide–DNA complex is equal to 7×10^7 M^{-1} (Ahmadi *et al*., 2011). Therefore, in addition to the results of the electrophoretogram (see **Figure 3.21**) it could be proposed that compound 2 interacts weakly with ct-DNA and has a non-covalent mode of binding. Furthermore, the low binding constant ~10^5 suggests that the interaction between the metal complex and DNA might not be intercalative in nature. More studies are needed in order to support the results, such as fluorescence measurements, viscosity measurements or even melting studies.

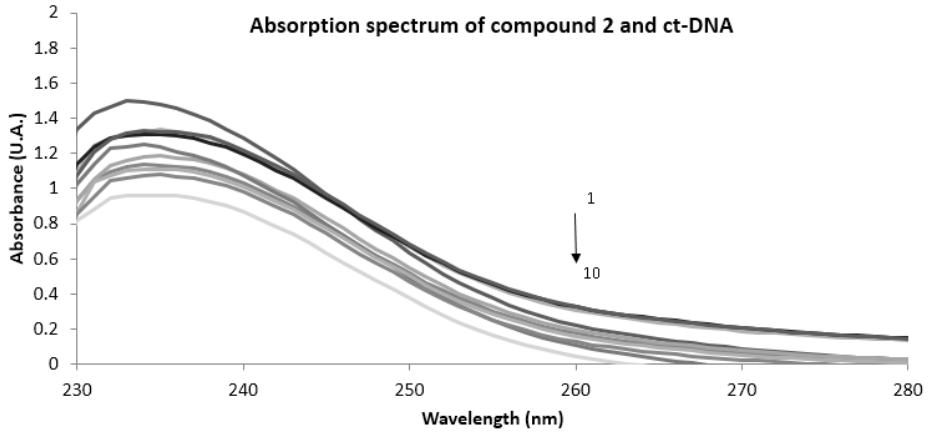

Figure 3.23 Absorption spectra of compound 2 (200 μM) with a range of ct-DNA concentrations from 1 to 10 (2.84 μM to 80.42 μM).

Despite our results, other authors have synthesized and characterized tricarbonyl rhenium complexes with intercalative binding behaviour (Olmon *et al*., 2011). Indeed, Ma and co-workers studied $Re(CO)_3$(2-appt)-Cl [2-appt is 2-amino-4-phenylamino-6-(2-pyridyl)-1,3,5-triazine], a rhenium complex that can participate in both hydrogen-bonding and π-π interactions. Results from spectroscopic titrations and viscosity showed a low binding constant (~10^4) and indicated that this metal complex interacts with DNA via groove binding (Ma *et al*., 2007).

While compound 2 with the hexamethylenetetramine (HMT) ligand does not present a strong interaction with DNA, some studies show that if this ligand alone is coadministrated with doxorubicin, it can potenciate its ability to interact with DNA. HMT is known to hydrolyze and release up to six molecules of formaldehyde in a pH-dependent manner. The capability of doxorubicin to form interstrand lesions in the absence or presence of formaldehyde releasing agent HMT was analysed by Swift and co-workers using gel electrophoresis. Doxorubicin in the absence of formaldehyde formed no interstrand lesions whereas doxorubicin in the presence of HMT readily formed interstrand lesions in a pH-dependent manner and the amount of these lesions increased with decreasing pH. In addition, doxorubicin-DNA interstrand lesions have been shown to be considerably more effective in triggering apoptosis and to be more cytotoxic than doxorubicin alone (Swift *et al*., 2003). It would be interesting to study the simultaneous incubation of doxorubicin and the compound 2 with DNA to see the Re metal influence.

3.5 Human Serum Albumin interaction assays

The main biological effect of Re is considered to be the formation of adducts with proteins or with DNA. The formation of stable covalent adducts with proteins was shown with lysozyme, with the binding of Re to His15 via the replacement of one coordinated water molecule, and confirmed by X-ray crystallography (Collery *et al*., 2014). The hypothesis of adducts formation with the DNA was not proven for the Re compound 2 (see Sections 3.3 and 3.4).

The interaction of compound 2 with Human Serum Albumin (HSA) was studied by fluorescence spectroscopy. HSA is a 66 kDa protein commonly present at concentrations of around 600 μM in human plasma. The formation of a complex between a drug and HSA decreases the concentration of unbound molecules in the plasma and thereby affects the drug's action. From the pharmacokinetic point of view, binding to albumin is beneficial only as it extends the length of time at which the free drug remains above its therapeutically efficacy concentration. For this reason, it is important to know the affinity of any drug for albumin (Buttar *et al*., 2010).

Spectrofluorimetry can provide precise information about protein-drug interactions. A diverse range of process can result in fluorescence quenching, including complex formation. The quenching produced by a quencher to a fluorescent molecule results from the collisional encounters between the fluorophore and the quencher, which is called collisional or dynamic quenching. Static quenching is due to complex formation (Montero *et al*., 1994).

One of the major problems with this technique is the inner-filter effect that is the absorption of light at both the excitation and emission wavelengths (Larsson *et al*., 2007). However, as is observed in **Figure 3.24**, this is not a problem to have into consideration. There is no sobreposition between the absorption band of compound 2 and the emission band of HSA when excited at 295 nm.

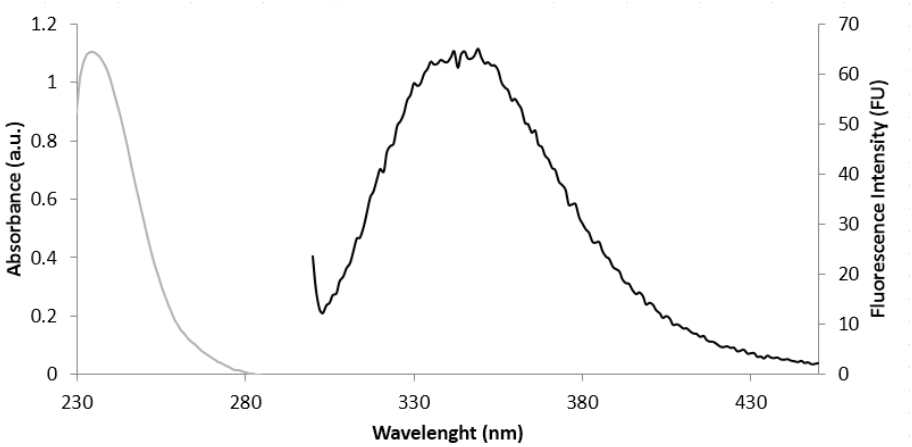

Figure 3.24 Fluorescence spectrum of HSA ($1.5x10^{-5}$M) on the right and absorption spectrum of compound 2 on the left (200 μM). The excitation wavelength used was 295 nm.

In **Figure 3.25** the fluorescence spectrum of HSA and compound 2 is shown. We can observe the quenching of HSA with increasing concentrations of compound 2 (**Figure 3.25**).

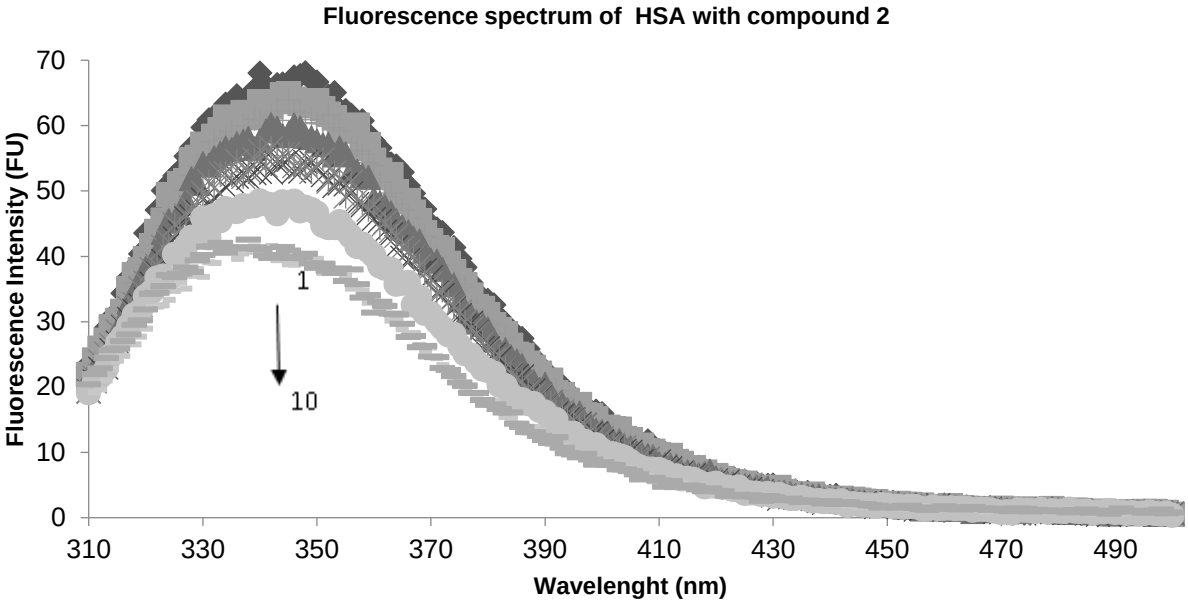

Figure 3.25 Fluorescence spectrum of HSA ($1.5x10^{-5}$M) with compound 2 from 1 to 10 (only HSA and $7.2x10^{-6}$M to $1.3x10^{-3}$M of compound 2 with HSA). The excitation wavelength was 295 nm.

Fluorescence quenching data was analyzed to obtain various binding parameters for the interaction of compound 2 and HSA. Quenching data were first analyzed using the Stern-Volmer equation F0/F = 1 + K [compound 2 concentration], being F the fluorescence of protein solution in presence of compound 2, and K is the Stern-Volmer constant. Fluorescence of the protein sample that contained only HSA in phosphate buffer is taken as 100% fluorescence (F0), while the phosphate buffer gave the 0% fluorescence.

Plotting F0/F versus [compound 2 concentration] two types of plots may be obtained. A linear Stern-Volmer plot indicates that only one type of quenching, dynamic, occurs. When the same fluorophore can be quenched both for collisions and by complex formation, an upward curvature is observed (Montero *et al*., 1994). In **Figure 3.26** can be seen a linear Stern-Volmer plot, and the Stern-Volmer constant is calculated in **Table 3.4**.

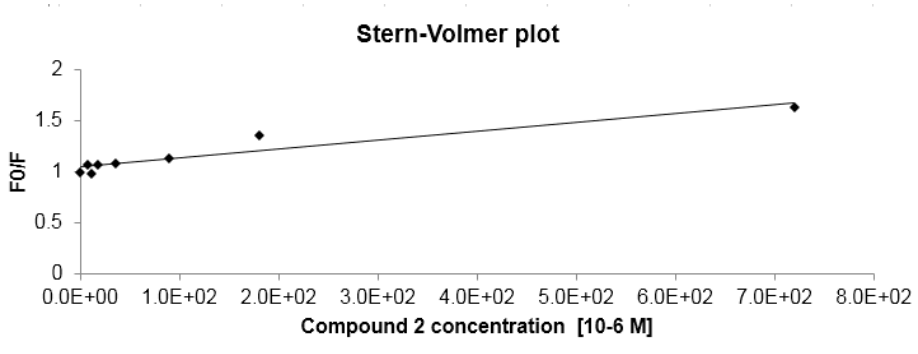

Figure 3.26 Stern-Volmer plot obtained from the titration of $1.5x10^{-5}$M of HSA with compound 2.

Table 3.4 Stern-Volmer constant for compound 2, represent as K +/- SEM.

	First assay	Second assay	Third assay	Mean
Stern-Volmer constant (M^{-1})	802.94	909.06	863.96	858.65 +/- 30.75

From the relative fluorescence values the fraction of the fluorescence that has been quenched, Q, is obtained as Q = (F0 - F)/100. With this parameter a new representation of Q versus [compound 2 concentration]/[HSA concentration] could be made (Montero *et al*., 1994). However, the limit quenching concentration can not be determined, since the maximal quenching was not achieved with the range of concentrations tested for compound 2. The reciprocal of fractional quenching versus the reciprocal of the free ligand concentration plot gave an average value of binding constant of the protein-quencher complex (Kd) of 3.10 (+/- 1.2) x 10^3 M^{-1}.

Table 3.5 HSA binding constant for compound 2, represent as K_d +/- SEM.

	First assay	Second assay	Third assay	Mean
Binding constant (M^{-1})	1.97x10^3	1.87x10^3	5.44x10^3	3.10 (+/- 1.2) x 10^3

It is shown that there was a relatively moderate interaction between compound 2 and HSA. The binding constant was reported to be 1.1 (±0.3)×10^4 M^{-1} (Agudelo *et al*., 2012) for doxorubicin to HSA by fluorescence methods and for Uracil, 5-Fluorouracil and 5-Chlorouracil was suggested a static quenching mechanism with a binding constant of ∼10^4 M^{-1} at 303 K that was considered in the range suitable for drug transportation (Bakkialakshmi *et al*., 2012). 5-Fluorouracil is one of the most used drug for the treatment of advanced colorectal cancer (Carethers, 2008).

3.6 Proteomic analysis

In order to identify the potencial biological targets of compound 2, the proteome of HCT116 cells exposed or not to the compound (IC_{50}) after 48 h was performed. Protein extracts were subjected to 2-DE electrophoresis, obtaining a total of 4 bidimensional gels, corresponding to the proteome duplicates in the presence or absence (0.1 % DMSO) of the compound.

2-DE electrophoresis is suitable for proteome analysis and it allows detecting large quantity of proteins in a single run. Notwithstanding, it is not suitable for low abundant proteins, affected by posttranslational modifications (Wang and Chiu, 2008).

Data analysis was carried out in three distinct stages. First, the capture of digitised gel images which provides quantitative data in the form of density maps. There is a linear correlation between the amount of protein in the gel and the amount of stain bound. To overcome gel-to-gel variation in staining intensity, the data have to be normalized, expressing each spot relative to the total image intensity of the gel. Then, a spreadsheet of matched spot data is created and the spots labeled. Quantitative analysis of the variation of abundance of protein spots was performed using Melanie 7.0 software. Protein identification was done by gel-by-gel comparison comparison between a reference gel with protein spots previously identified at the laboratory. The results are represented in **Figure 3.27**.

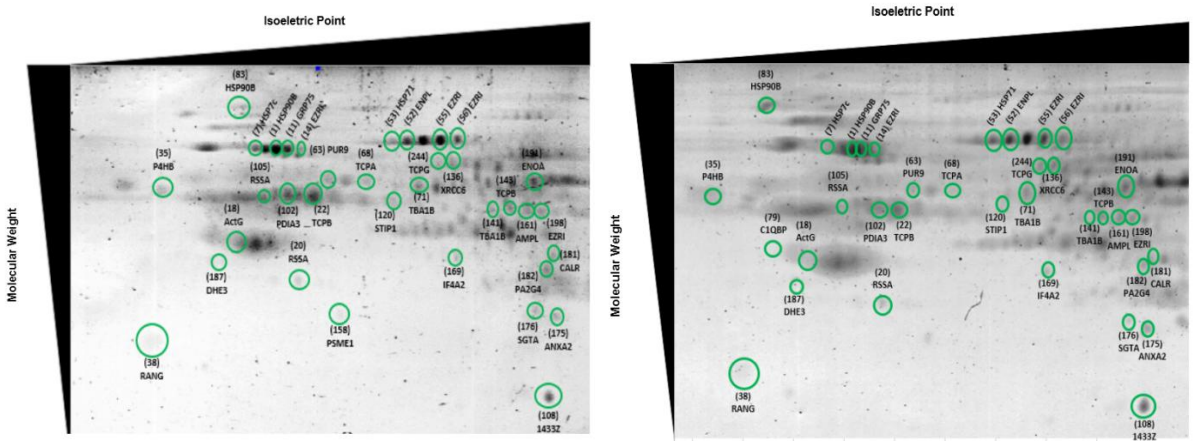

Figure 3.27 Image of the 2-DE gels of HCT116 cell line treated during 48 hours with 0.1% of DMSO (left) and 86.5 μM of compound 2 (right), stained with comassie blue R350. The marked spots correspond to the identified proteins with the respective landmark and abbreviation of the name. Gels are representatives from duplicate experiments.

From the 2-DE gels we were able to detect 34 spots (proteins and relative abundance): Endoplasmin (ENPL, 0.7), Tubulin alpha-1B chain (TBA1B, 0.6), Ran-specific GTPase-activating protein (RANG, 0.4), Heat shock cognate 71 kDa protein (HSP7C, 0.5), Bifunctional purine biosynthesis protein (PUR9, 0.67), T-complex protein 1 subunit gamma (TCPG, 0.67), Ezrin (EZRI, 1.7), 40S ribosomal protein SA (RSSA, 1.5), Actin Gamma 1 (ACTG, 0.8), chaperones such as HSP90B (0.96), HSP71 (0.9), TCPA (1.13), TCPB (0.98) , GRP75 (1.31), Small glutamine-rich tetratricopeptide repeat-containing protein alpha (SGTA, 0.68) prolyl 4-hydroxylase beta polypeptide (P4HB, 0.9), Glutamate dehydrogenase (DHE3, 3.3), Proliferation-associated protein 2G4 (PA2G4, 2.2), Proteasome activator subunit 1 (PMSE1, 1.3), Annexin A2 (ANXA2, 2.03), Eukaryotic initiation

factor 4A-II (IF4A2, 2.9), Stress-induced-phosphoprotein 1 (STIP1, 0.18), 14-3-3 protein zeta (1433z, 0.97), Calreticulin (CALR, 1.3), the mitochondrial Complement 1q-binding protein (C1qbp, 0.3), Protein disulfide isomerase family A member 3 (PDIA3, 1.3), Cytosol aminopeptidase (AMPL, 0.8) and Alpha-enolase protein (ENOA, 1.3).

It was considered biologically significant the relative abundance (compared to control) higher than 1.5 or smaller than 0.7 (reference). In this way, 15 known spots showed biologically significant relative abundance, and were previously identified in the laboratory by mass spectrometry (**Table 3.6**). From the identified spots, differences in protein abundace spots were not statistically significant (t-test, $p < 0.05$ was considered significant). This is due to insufficient number of replicates, which give a better estimation of variability. This variability come from the biological and technical phases (Chich *et al*., 2007; Wood *et al*., 2004).

It may be inferred that compound 2 interferes with proteins responsible for the maintenance of the cytoskeleton (**Table 3.6**), such as Tubulin alpha-1B chain (TBA1B), Ezrin (EZRI) and T-complex protein 1 subunit gamma (TCPG). For some of them there is a link with apoptosis.

Table 3.6 Proteins whose expression was significantly changed relatively to the control (more than 1.5-fold or less than 0.7-fold) in HCT116 cells exposed to 86.5 µM of compound 2. Proteins responsible for the maintenance of the cytoskeleton.

Landmark Number and Protein Name	Relative abundance	Function
(71)Tubulin alpha-1B chain (TBA1B)	0.6	Tubulin is the major constituent of microtubules. It binds two moles of GTP.
(143)T-complex protein 1 subunit gamma (TCPG)	0.67	Molecular chaperone; assists the folding of proteins upon ATP hydrolysis. Known to play a role, in vitro, in the folding of actin and tubulin.
(56)Ezrin (EZRI)	1.7	Probably involved in connections of major cytoskeletal structures to the plasma membrane.

Legend: adapted from: (71)http://www.uniprot.org/uniprot/P68363;(143)http://www.uniprot.org/uniprot/P49368;(56)http://www.uniprot.org/uniprot/P15311.

TBA1B, which was less abundant for cells exposed to compound 2, is the main component of the microtubules. As microtubules are highly involved in cellular growth, they are a potential target for cancer treatment. Some antimitotic agents inhibit cell proliferation by binding to microtubules and suppressing microtubule dynamics during the mitotic stage of the cell cycle (Dumontet and Jordan, 2010). Other advantage of this kind of compounds is that binding to tubulin and in this manner perturbing the microtubule stability and the function of the spindle apparatus, causes cancer cells to arrest and undergo apoptosis. Several microtubule inhibitors are in clinical trials (Aryapour *et al*., 2012).

Ezrin was more abundant for cell exposed to compound 2. EZRI is involved in the adhesion and organization of the cellular structure. Ezrin acts as a linker between the plasma membrane and the actin cytoskeleton and plays important roles in cell motility, invasion and metastasis (Leiphrakpam *et al*., 2014). Recently, Ezrin has been linked to Akt-mediated cell survival. It was reported that Akt2 phosphorylates Ezrin to activate it and phosphorylates X-linked inhibitor of apoptosis protein (XIAP) for

reducing its degradation conferring resistance to caspase activation and apoptosis. Transient knockdown using ezrin siRNA in colorectal cancer cells led to the downregulation of XIAP, which is critical for cell survival and tumor growth and for supporting the metastatic process *in vivo*. Ezrin knockdown also resulted in approximately 1.5 fold increase in cell death in colorectal cancer cells (Leiphrakpam *et al*., 2014).

T-complex protein 1 subunit gamma is a subunit in a large molecular chaperone known as chaperonin-containing tail-less complex polypeptide-1, which maintains cellular protein folding homeostasis by assisting the biogenesis of many proteins, including the fold of actin and tubulin, and non-cytoskeletal substrate proteins, including cyclin E, CDC20 and the Von Hippel-Lindau tumor suppressor (Lee *et al*., 2012). TCPG was less abundant in cells treated with compound 2 and this might be related to less abundance of TBA1B, the main component of microtubules.

In addition, increased expression of cytosolic chaperonin-containing t-complex polypeptide 1 in human colon carcinoma has been reported (Shi *et al*., 2013). Lee and collaborators demonstrate by proteomic analysis that *p53* loss in HCT116 colon cancer cells is associated with up-regulation of a phosphorylated TCPG variant. However, there is no direct evidence that TCPG plays a role in p53-regulated biological functions such as apoptosis, senescence and/or cell cycle regulation (Lee *et al*., 2012). The p53 plays an important role in the response to genotoxic stress and hypoxia (Vogelstein *et al*., 2000). In this way, TCPG abundance in cells exposed to compound 2 could also be related to p53 activity.

There are also alterations in the abundance of proteins related to cellular protection (**Table 3.7**) caused by compound 2, such as GRP94, ANXA2, HSP7C and related proteins.

Table 3.7 Proteins whose expression was significantly changed relatively to the control (more than 1.5-fold or less than 0.7-fold) in HCT116 cells exposed to 86.5 µM of compound 2. Proteins related to cellular protection.

Landmark Number and Protein Name	Relative abundance	Function
(52)Endoplasmin (ENPL/ GRP94)	0.7	Molecular chaperone. Functions in endoplasmic reticulum associated degradation (ERAD). Has ATPase activity.
(176)Small glutamine-rich tetratricopeptide repeat-containing protein alpha (SGTA)	0.68	Co-chaperone that binds directly to HSC70 and HSP70 and regulates their ATPase activity.
(120)Stress-induced-phosphoprotein 1 (STIP1)	0.18	Mediates the association of the molecular chaperones HSC70 and HSP90.
(7)Heat shock cognate 71 kDa protein (HSP7C)	0.5	Acts as a repressor of transcriptional activation. May have a scaffolding role in the spliceosome assembly as it contacts all other components of the core complex.
(175) Annexin A2 (ANXA2)	2.0	May be involved in heat-stress response.

Legend: adapted from:
(52)http://www.uniprot.org/uniprot/P14625;(176)http://www.uniprot.org/uniprot/O43765;(120)http://www.uniprot.org/uniprot/P31948;(7)http://www.uniprot.org/uniprot/P11142; (175) http://www.uniprot.org/uniprot/P07355.

The GRP94 or endoplasmin is the most abundant glycoprotein in the endoplasmic reticulum. It belongs to the family of the heat-shock proteins, and assists the folding and assembly of a wide range

of proteins. The depletion of the chaperone GRP94 makes worms sensitive to cisplatin (Natarajan *et al*., 2013). Authors explain that this could be due to elevated Endoplasmic Reticulum stress levels in *grp94* mutants. This could be explored to enhance the effects of cisplatin based cancer therapy. The expression of this endoplasmin in HCT116 cells treated with compound 2 was smaller than 0.7 compared to the control. However, the combined therapeutics of compound 2 and cisplatin was tested (**Figure 3.11**) without a significant sensitivity of colon cancer cell line to the therapeutic schedule chosen. This may be due to the higher levels of Ezrin that regulates cell survival signaling in colorectal cancer (Leiphrakpam *et al*., 2014).

The GRP94 also shows ATPase activity and plays an essential role in the cellular protection against different stress situations. GRP94 is dramatically up-regulated in colorectal cancer (animal models and human tumors), allowing the correct folding of several oncogenic products and a more aggressive tumour phenotype, metastasis and a poor evolution of the disease (Romay *et al*., 2011).

Small glutamine-rich tetratricopeptide repeat-containing (SGTA) protein alpha was less abundant in cells treated with compound 2. SGTA has also a role in Hsp70-mediated folding (Paul *et al*., 2014). Less abundance of SGTA is coherent with less abundance of Stress-induced-phosphoprotein 1 (STIP1) since it mediates the association of the molecular chaperone HSP7C. Heat shock cognate 71 kDa protein (HSP7C) is a constitutively expressed chaperone. The basal level of HSP7C in cisplatin-resistant cervix squamous cell carcinoma cells was up-regulated compared to cisplatin-sensitive cells, as reported by Castagna and co-workers (Castagna *et al*., 2004). In this way, the less abundance of HSP7C and SGTA caused by compound 2 is favorable to tumour cells death.

Annexin A2 (ANXA2) is more abundant in cells exposed to compound 2. ANXA2 is reported to be highly expressed in human colorectal cancer cell lines including HCT116 (Wang and Lin, 2014; Emoto *et al*., 2001) and is a marker for drug resistance (Wang and Lin, 2014). This could be an adaptive response to compound 2. On the other hand, ANXA2 is a cellular redox regulatory protein. It possesses a reactive cysteine residue (Cys-8) which is oxidized by H_2O_2 and subsequently reduced by the thioredoxin system, thereby enabling annexin A2 to participate in multiple redox cycles (Madureira and Waisman, 2013). Elevated levels of ANXA2 could mean that compound 2 induces oxidative stress in HCT116 cells, however the level of several heat shock proteins and other proteins involved in cellular protection didn't corroborate this possibility.

Other proteins affected by compound 2 are related to DNA synthesis, translation and other cellular functions (**Table 3.8**).

Table 3.8 Proteins whose expression was significantly changed relatively to the control (more than 1.5-fold or less than 0.7-fold) in HCT116 cells exposed to 86.5 µM of compound 2.

Landmark Number and Protein Name	Relative abundance	Function
(38)Ran-specific GTPase-activating protein (RANG)	0.4	Inhibits GTP exchange on Ran. May act in an intracellular signaling pathway which may control the progression through the cell cycle.
(79)Mitochondrial protein C1qbp	0.3	Involved in ribosome biogenesis, regulation of apoptosis, transcriptional regulation and pre-mRNA splicing.
(63)Bifunctional purine biosynthesis protein (PUR9)	0.67	Bifunctional enzyme that catalyzes 2 steps in purine biosynthesis.
(20)40S ribosomal protein SA (RSSA)	1.5	Assembly and/or stability of the 40S ribosomal subunit. Cell surface receptor for laminin. May play a role in cell fate determination and tissue morphogenesis.
(182)Proliferation-associated protein 2G4 (PA2G4)	2.2	Seems be involved in growth regulation.
(169)Eukaryotic initiation factor 4A-II (IF4A2)	2.9	ATP-dependent RNA helicase which is a subunit of the eIF4F complex involved in cap recognition and is required for mRNA binding to ribosome.
(187)Glutamate dehydrogenase (DHE3)	3.3	Mitochondrial glutamate dehydrogenase that converts L-glutamate into alpha-ketoglutarate.

Legend: adapted from:
(38)http://www.uniprot.org/uniprot/P43487;(79) http://www.uniprot.org/uniprot/Q07021;(63)http://www.uniprot.org/uniprot/P31939;(20)http://www.uniprot.org/uniprot/P08865;(182)http://www.uniprot.org/uniprot/Q9UQ80;(169)http://www.uniprot.org/uniprot/Q14240;(187)http://www.uniprot.org/uniprot/P00367.

Bifunctional purine biosynthesis protein was less abundant for cells exposed to compound 2. Cancer cells depend mainly on de novo purine pathway for synthesis of adenine and guanine, in contrast to normal cells that favor a salvage pathway. In this way, enzymes involved in the de novo pathway have become attractive candidates for rational anticancer drug design (Li *et al*., 2006).

Complement 1q-binding protein (C1qbp) was less abundant in cells treated with compound 2. It is reported to be upregulated in colon cancer cell lines and it contributes to the hyperproliferative, hypermigratory and cytoprotected phenotype of a cancer cell line (McGee *et al*., 2011).

Proliferation-associated protein 2G4 (PA2G4) was overexpressed in cells exposed to compound 2. PA2G4 induces cell cycle arrest possibly by repressing E2A activation of cell cycle related genes (Zhang *et al*., 2003). Compound 2 could trigger cell death by cell cycle arrest.

Glutamate dehydrogenase (DHE3) and Eukaryotic initiation factor 4A-II (helicase important for mRNA translation) were more abundant in cells exposed to compound 2 and these alterations could be an adaptive response. Glutamine has an important role in cell growth and energy metabolism. Glutamate dehydrogenase (GDH) participates in the second step of glutaminolysis converting glutamate to *α*-ketoglutarate (*α*-KG). Cancer cells are dependent on glutamine to maintain the tricarboxylic acid cycle (TCA) cycle (Zhao *et al*., 2013).

A translation-related protein, 40S ribosomal protein SA (RSSA), was up-regulated with compound 2 treatment. Downregulation of this protein may be related to the suppression of

translation. Moreover, RSSA is also known as a multidrug resistance-associated protein MGr1-Ag, and its downregulation can significantly enhance the cytotoxicity of antitumor drugs to cancer cells (Yao *et al*., 2009).

Ran-specific GTPase-activating protein (RANG) is considered a promising therapeutic target for aggressive B-cell lymphoma (Chang *et al*., 2013). This protein is also less abundant in the proteome of HCT116 cells treated with compound 2. Ran is a small GTPase that functions as a molecular switch by binding to either GTP or GDP. One essential regulator of this process is Ran-specific GTPase-activating protein, which also catalyzes the GTP hydrolysis of Ran. It has been found that Ran and Ran binding proteins are involved in a broad range of fundamental cellular processes including mitotic spindle assembly, cell death, cell proliferation, cell differentiation and malignant transformation. Moreover, the abrogation of RANG may lead to cell death (Schreier *et al*., 2014). This could be one inductor of cell death after treatment with compound 2.

To conclude, after 48h of treatment with compound 2, colorectal cancer cells are more sensitive and prone to cell death due to the relative abundance of the heat shock proteins, GRP94 and HSP7C, and also RANG protein, a small GTPase involved in many cellular processes. On the other hand, the altered abundance of TBA1B protein can consequently alter microtubule stability and the function of the spindle apparatus compromised causing cancer cells to arrest and undergo apoptosis. These results might be confirmed by detecting the protein levels or activity of downstream caspases, which are crucial for apoptosis induction, by western blotting or by enzyme assay, respectively (Sarastea *et al*., 2000). PA2G4 overexpression might indicate that compound 2 triggers cell death by cell cycle arrest. In addition, TCPG was less abundant in compound 2 treated cells what might be related to p53 activity and genotoxic stress response. Ezrin, RSSA and DHE3 were more abundant on colon cancer cells treated with the compound 2 that in control, what could be an adaptive response since Ezrin has been linked to Akt-mediated cell survival, RSSA with multidrug resistance and DHE3 with cancer cells growth.

Apoptotic potential assessment

3.7 Hoechst assay

To visualize nuclear changes and apoptotic body formation that are characteristic of apoptosis, HCT116 cells treated for 48h with compound 4 or compound 2 were stained with Hoechst 33285. This dye is known to penetrate the plasma membrane and stain DNA in cells without permeabilization (Kasibhatla *et al*., 2006). Cells are observed in a fluorescence microscope and counted in order to quantify the level of apoptosis. Cells are scored as apoptotic if their nuclei present chromatin condensation and marginalization or nuclear beading. In this assay, apoptotic cells have a stronger blue fluorescence compared with nonapoptotic cells.

Results are shown in **Figure 3.28** and **Figure 3.29**.

Vehicle control (0.1%DMSO)

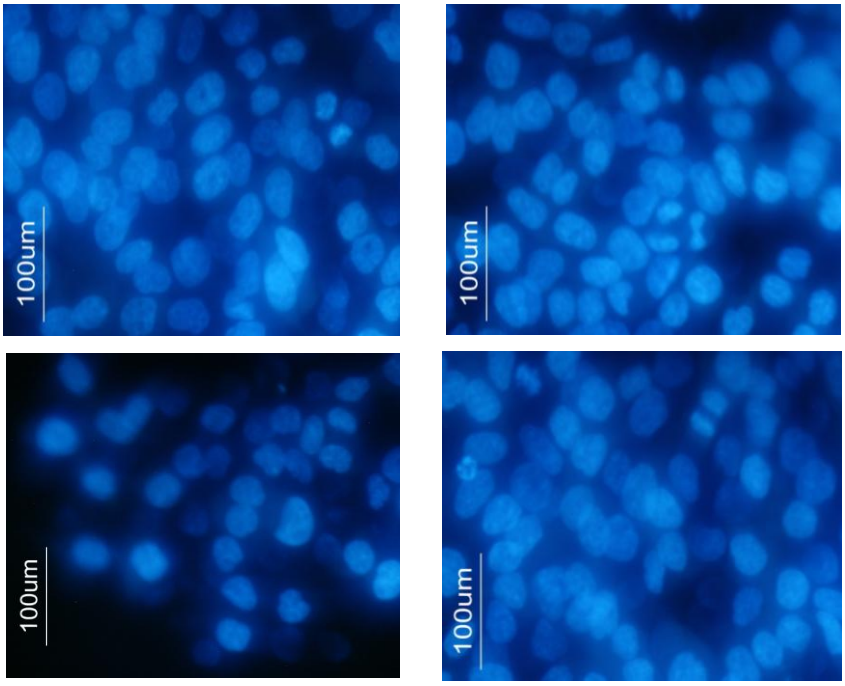

Figure 3.28 HCT116 cells (0.75 x 10^5 cells/mL) stained with Hoechst 33258 after treatment with DMSO (0.1% DMSO, 48 hours, control). Total magnification of 50x10x. Images are representative of two independent assays.

Compound 4 (0.2861 µM)

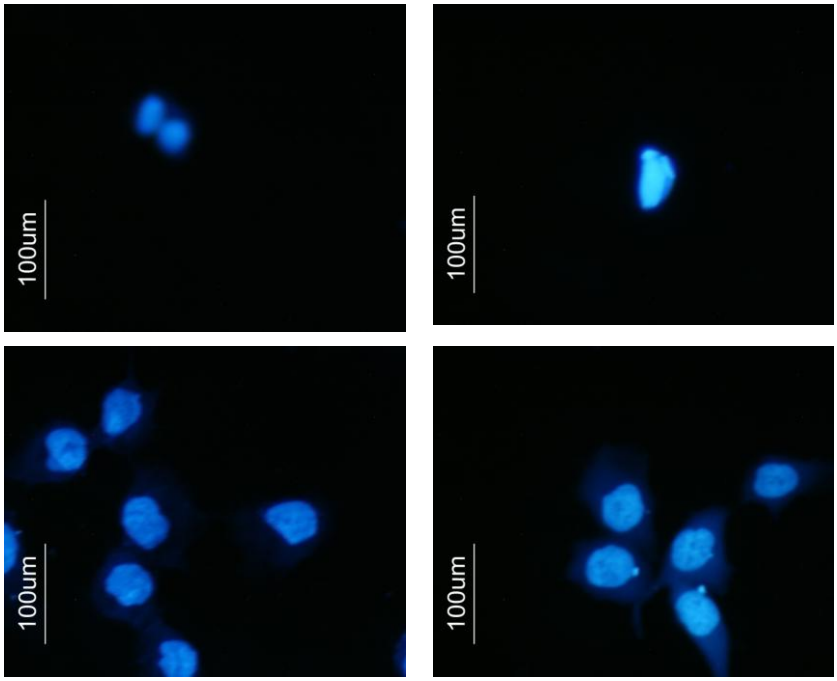

Compound 2 (86.5 µM)

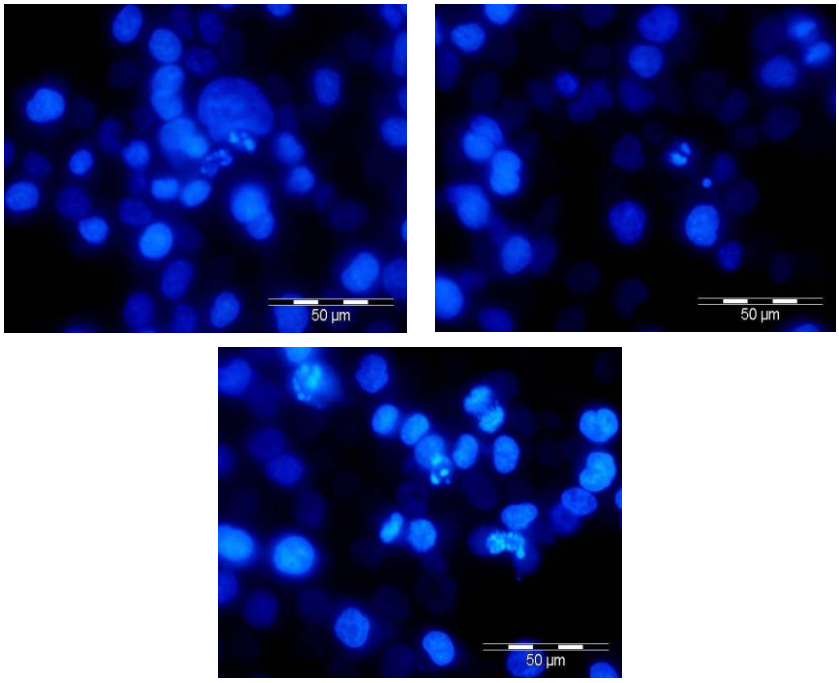

Figure 3.29 HCT116 cells (0.75 x 10^5 cells/mL) stained with Hoechst 33258 after treatment with compound 4 (above) and compound 2 (bottom). Total magnification of 50x10x. Images are representative of two independent assays.

In contrast to control cells, cells treated with the compounds (~IC_{50}) show more nuclear condensation and fragmentation (**Figures 3.28** and **3.29**). Compound 4 seems to be more effective in killing tumour cells than compound 2, what corroborates with the results of the cell viability assays. However, itseems to be an overestimation of cell death by compound 2 and underestimation by compound 4 compared to the cell viability assays. Apparently, apoptosis is not the main mechanism of cell death for compound 2 with 4.15 +/-1.16 % of apoptotic cells. However, apoptosis begins several hours before the appearance of morphologic features and the morphologic changes usually take place in less than 2 hours (Saraste and Pulkki, 2000).

Although apoptosis is an important mechanism of tumour cells death, a cancer therapy that acts solely by inducting apoptosis and had no intrinsic cytotoxicity would cause the death of more normal cells than cancer cells. Effective cancer therapies should have a direct toxic activity and inhibit vital processes such as DNA replication, microtubule function, and other targets. Some of these functions were apparently altered after 48-hour treatment with compound 2 (see Section 3.6). In addition, agents that inhibit apoptosis might be useful in conjunction with chemotherapy or radiotherapy to reduce dose-limiting side-effects due to apoptosis of normal cells (Gerl and Vaux, 2005). This may not be the case as some evidences of apoptosis are seen on the Hoeschst images. However the proteomic results showed a higher relative abundance for Ezrin after 48-hour treatment with compound 2, a protein that when is absent in colorectal cancer cells leads to the downregulation of X-linked inhibitor of apoptosis protein (see Section 3.6). This response could be inhibiting apoptosis.

3.8 Flow citometry

Flow citometry was used in this work to assess cell death. The principle of the assay is the simultaneous use of two markers, Anexin V in the presence of calcium ions (Brumatti et al., 2008) and dye propidium iodide (Brun et al., 2012), which bind to exposed phospholipid phosphatidylserine (PS) and DNA, respectively. This technique takes advantage of some earliest morphological changes that occur in the plasma membrane during apoptosis such as the translocation of the membrane phospholipid phosphatidylserine from the internal layer to the external layer of the cell membrane. To distinguish between apoptotic and necrotic cells, the fluorescent dye propidium iodide is used, since it can only enter necrotic cells across a damaged plasma membrane (Hingorani *et al*., 2011).

Analysis can result in three distinct cellular populations: early apoptotic cells if they are positive for Annexin V binding (Annexin V+, PI-), late apoptotic cells are positive for Annexin V and propidium iodide binding (Annexin V+, PI+), necrotic cells are negative for Annexin V binding and positive for propidium iodide binding (Annexin V-, PI+) and viable cells that are negative for both the markers (Annexin V-, PI-) (Hingorani *et al*., 2011).

Results for combined therapy with compound 2 and doxorubicin are in **Figure 3.30**.

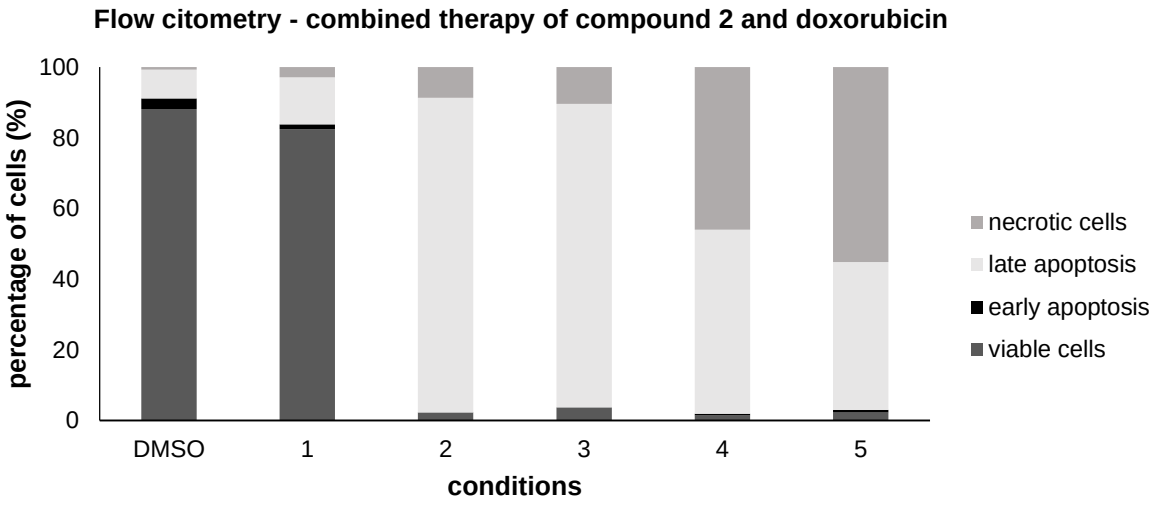

Figure 3.30 Evaluation of the apoptotic potential in HCT116 cells. Apoptosis was evaluated and quantified by flow cytometry analysis with annexin V-FITC and PI double staining. Cells were treated with 0.1% (v/v) DMSO (vehicle control) and (1) the compound 2 at 86.5 μM for 48 h, (2) 0.42 μM of doxorubicin for 48 h, (3) 0.25 μM of doxorubicin for 48 h, (4) 0.42 μM of doxorubicin and afterwards compound 2 at 86.5 μM for more 24h and (5) 0.25 μM of doxorubicin and afterwards compound 2 at 86.5 μM.

It is observed 88.2% of viable cells for DMSO (0.1%) control, being the number of apoptotic cells (11.1%) higher than necrotic cells (0.7%). This is similar to previous assays in the lab (Silva, 2012). The results (**Figure 3.30**) go in line with what is reported for doxorubicin cell death. Doxorubicin induces apoptosis via the activation of caspases and disruption of mitochondrial membrane potential (Gamen *et al.*, 2000). However, doxorubicin is able to induce cell death by apoptosis only at particular dose and treatment conditions and careful consideration of incubation period as well as doxorubicin concentrations used is of importance for achievement of apoptosis in treatment of colon cancer cells (Lüpertz *et al*., 2010). Results of combined therapy with either 0.25 or 0.42μM of doxorubicin and afterwards 86.5 μM of compound 2 showed a higher number of necrotic cells (55.1%) when used the lowest dose of doxorubicin, but a also a higher number of viable cells (2.31%) for the same concentration. The same outcome happens when HCT116 cells are exposed to 0.25 μM of doxorubicin alone (10.4% of necrotic cells) but the percentage of necrotic cells is higher in combined therapy with compound 2 (55.1%).

The fundamental characteristics of necrosis include cellular energy depletion, damage to membrane lipids, and loss of function of homeostatic ion pumps/channels. These events often potentiate each other and synergize to cause necrosis (Riccia and Zong, 2006). The proteomic analysis of cells exposed to compound 2 showed alterations in proteins related to cell growth and energy metabolism. Combined with doxorubicin it can potentiate the alterations of cells exposed to doxorubicin and increase the number of necrotic cells as shown in flow citometry.

Although early apoptosis is virtually seen for cells exposed to doxorubicin alone, when combined with compound 2 it increases (0.5% for condition 4 and 0.7% for 5, **Figure 3.30**). Cell death is not significant high in cells exposed to compound 2 (82.5% of viable cells). This could be due to the possible adaptive response seen in the proteomic analysis by Ezrin, RSSA and DHE3 overexpression on colon cancer cells treated with the compound 2. The percentage of viable cells is also higher than

achieved in the MTS assay (~50%). This might mean that its antiproliferactive effect is mainly due to cell cycle arrest and not due to apoptosis induction. This hypothesis was also raised in proteomic analysis due to PA2G4 overexpression.The results of flow citometry for early (1.4%) and late apoptosis (13.3%) of cells exposed to compound 2 are also coherent with the Hoechst staining assay in which a low number of apoptotic cells were seen (4.15 +/-1.16 %).

4 Conclusions

Cisplatin, oxaliplatin, related metallodrugs as well doxorubicin are extensively used in the treatment of a diversity of cancers. However these drugs are highly toxic and tumor becomes drug-resistance (Holohan *et al*., 2013). On the other hand, in addition to drug resistance there are also complicated side effects (Tacar *et al*., 2012). New metallic compounds which do not have the same mechanism of action of these drugs could fulfil these requirements.

The *in vitro* antiproliferative potential of three new rhenium compounds, in particular compounds 1 and 2 bearing the 1,3,5-triaza-7-phosphaadamantane (PTA) and the hexamethylenetetramine (HMT) ligands, respectively, compound 3 bearing the tris(pyrazol-1-yl)methanesulfonate (Tpms) and HMT ligands was evaluated using colorectal, chronic myelogenous leukemia, hepatocellular carcinoma, mammary gland adenocarcinoma, melanotic and non-small cell lung cancer cell lines, and human fibroblasts as the normal cell line. Compound 4 bearing the trimeric polythiophene acetic acid (tPTAA) ligand was also evaluated.

The rhenium compound 2 showed the best results on the colorectal cancer cell line, excepting the melanotic cell line, with a relative IC_{50} of 88.6 +/- 7.1. The melanotic cell line results were not considered due to possible interference of the dark colour in the colorimetric viability assay. Colorectal cancer is the third most common cancer in men (10 % of the total) and the second in women (9.2 % of the total) worldwide, and the deadliest type of cancer in Portugal (3797 deaths, 15.7% of the total) (IARC, 2012).

Being important to study drug combinations and administration schedules with more efficacy and less side-effects than the already existent (Yap *et al*., 2013), combined therapeutics with some of the most used anticancer drugs were performed.

Following this line of thinking, combined therapy of compound 2 and cisplatin or doxorubicin was performed in colorectal cancer cell line. The same schedule and conditions of treatment was tested for compound 4.

Platinum compounds are usually used in the FOLFOX therapeutics (5-FU, leucovorin, and oxaliplatin) for colorectal cancer patients (Carethers, 2008). Furthermore, Re has stabilizing properties of the membrane erythrocyte by an antioxidant effect and protect the erythrocytes against toxic agents that induce hemolysis. In this way, Re could be used in combination with other cytotoxic drugs, like cisplatin, in order to reduce side effects such as anemia and improve the antitumour potencial (Collery *et al*., 2004). The ligand of the compound 2, hexamethylenetetramine (HMT), was also studied as an adjuvant to radiation and cisplatin in the treatment of the solid tumours with promising results (Masunaga *et al*., 2010).

Other authors studied the administration *in vivo* of doxorubicin encapsulated into pegylated liposomes and the combination with hexamethylenetetramine (HMT), showing promising results (Masunaga *et al*., 2009).

These observations together justified the study of the rhenium compound 2 combined with cisplatin and doxorubicin on the colorectal cancer cell line.

The best results of the combined therapy were for compound 2 administration and 24 hours later doxorubicin treatment, and vice versa, with a reduction of ~1.5x in the percentage of cell viability in relation to doxorubicin alone. The best results for compound 4 were the simultaneous administration of 4 and cisplatin with a reduction of almost 3x of the percentage of cell viability for cisplatin alone.

Based on the absorbance values obtained in the spectroscopic titration with calf thymus DNA, the value obtained for the binding constant of compound 2 was 5.01 (+/- 1.12)×$10^5 M^{-1}$. This value is lower than those observed for typical classical intercalators, e.g. *K*b for ethidium bromide–DNA complex is equal to 7×10^7 M^{-1} (Ahmadi *et al*., 2011). Therefore, in addition to the results of the electrophoretogram with plasmid DNA was proposed that compound 2 interacts weakly with ct-DNA and has a non-covalent mode of binding. Furthermore, the low binding constant ~10^5 suggests that the interaction between the metal complex and DNA might not be intercalative in nature. More studies are needed in order to support the results, such as fluorescence measurements and viscosity measurements. However, this is an important result since it could indicate other form of action of the compound 2 different from the doxorubicin and cisplatin.

The fluorescence quenching assay of HSA showed a relatively moderate interaction between compound 2 and HSA with an average value of binding constant of the protein-quencher complex of 3.10 (+/- 1.2) x 10^3 M^{-1}. The binding constant reported by other authors to 5-Fluorouracil was of ~10^4 M^{-1} at 303 K that was considered in the range suitable for drug transportation (Bakkialakshmi *et al*., 2012).

Comparative proteomic analysis for compound 2 was assessed in the colorectal cancer cell line. After 48-hour treatment with compound 2 colon cancer cells apparently are more sensitive and prone to death due to the relative abundance of the heat shock proteins, GRP94 and HSP7C, affected and also RANG protein, a small GTPase involved in many cellular processes. Compound 2 might indirectly induce apoptosis since the relative abundance of the TBA1B protein was altered, and consequently microtubule stability and the function of the spindle apparatus can be compromised causing cancer cells to arrest and undergo apoptosis. On the other hand, Ezrin was more abundant on colorectal cancer cells treated with the compound 2 that in the control, what could be an adaptive response since Ezrin has been linked to Akt-mediated cell survival and apoptosis. When Ezrin is absent in colorectal cancer cells this leads to the downregulation of X-linked inhibitor of apoptosis protein (Leiphrakpam *et al*., 2014). This response could be inhibiting apoptosis. In addition, PA2G4 overexpression might indicate that compound 2 triggers cell death by cell cycle arrest.

Tumor cell death was evaluated by fluorescence microscopy and flow citometry. Compound 4 was more effective in killing tumour cells than compound 2, what corroborates the results of the cell viability assays. Nevertheless, it seems to be an overestimation of cell death for compound 2. Apparently, apoptosis is not the main mechanism of cell death for compound 2 with 4.15 +/-1.16 % of apoptotic cells by Hoechst staining and 1.4% of early apoptotic cells and 13.3% of late apoptotic cells in flow citometry. This goes in line with the proteomic results, in particular the higher abundance of Ezrin. In order to confirm these results other assays are needed such as western blott for specific proteins with a role in apoptosis.

5 References

Abel, B., Buck, U., Sobolewski, A. L., Domcke, W. 2012. On the nature and signatures of the solvated electron in water. Physical Chemistry Chemical Phycsis 14:22-34.

Abnet, C.C. 2007. Carcinogenic food contaminants. Cancer Investigation 25:189–196.

Adam, T. 2005. Purine de novo Synthesis – Mechanisms and Clinical Implications. Klinick· biochemie a metabolismus 13(34):177–181.

Agudelo, D., Bourassa, P., Bruneau, J., Bérubé, G., Asselin, E., Tajmir-Riahi, H. 2012. Probing the Binding Sites of Antibiotic Drugs Doxorubicin and *N*-(trifluoroacetyl) Doxorubicin with Human and Bovine Serum Albumins. Plos One 7(8): 1-13.

Ahmadi, S., Feizi, M., Dehghan, G., Dolatabadi, J. 2011. In Vitro Studies on Calf Thymus DNA interaction with Quercetin-Palladium (II) Complex. International Conference on Bioscience, Biochemistry and Bioinformatics 5:110-114.

Alberts, B., Johnson, A., Lewis, J., Raff, M., Roberts, K., Walter, P. 2008. Molecular Biology of the Cell. Garland Science, New York.

Apel, A., Zentgraf, H., Büchler, M.W., Herr, I. 2009. Autophagy-A double-edged sword in oncology. International Journal of Cancer 125(5):991-995.

Aryapour, H., Riazi, G.H., Ahmadian, S., Foroumadi, A., Mahdavi, M., Emami, S. 2012. Induction of apoptosis through tubulin inhibition in human cancer cells by new chromene-based chalcones. Pharmaceutical Biology 50(12):1551-1560.

Audisio, D., Gonnot, D., Radanyi, C., Renoir, J., Denis, S., Sauvage, F., Gauduchon, J., Brion, J., Messaoudi, S., Alami, M. 2014. Synthesis and Antiproliferative Activity of Novobiocin Analogues as Potential Hsp90 Inhibitors. European Journal of Medicinal Chemistry 83:498-507.

Badisa, R.B., Darling-Reed, S.F., Patrick, J.P., Cooperwood, S., Latinwo, L. M., Goodman, C.B. 2010. Selective Cytotoxic Activities of Two Novel Synthetic Drugs on Human Breast Carcinoma MCF-7 Cells. Anticancer Research 29(8): 2993–2996.

Bai, L., Wang, S. 2014. Targeting Apoptosis Pathways for New Cancer Therapeutics. Annual Review of Medicine Vol. 65: 139-155.

Bakkialakshmi, S., Chandrakala, D. 2012. A spectroscopic investigations of anticancer drugs binding to bovine serum albumin. Spectrochimica Acta Part A: Molecular and Biomolecular Spectroscopy 88:2-9.

Bao, Y., Hu, F.B., Giovannucci, E.L., Wolpin, B.M., Stampfer, M.J., Willett, W.C., Fuchs, C.S. 2013. Nut consumption and risk of pancreatic cancer in women. British Journal of Cancer 109(11):2911-2916.

Baeriswyl, V., Christofori, G. 2009. The angiogenic switch in carcinogenesis. Seminars in Cancer Biology 19(5):329-337.

Barras, D., Widmann, C. 2011. Promises of apoptosis-inducing peptides in cancer therapeutics. Current Pharmaceutical Biotechnology 12(8):1153-1165.

Berdasco, M., Esteller, M. 2010. Aberrant epigenetic landscape in cancer: how cellular identity goes awry. Developmental Cell 19(5):698-711.

Berman, D.W., Crump, K.S. 2008. A meta-analysis of asbestos-related cancer risk that addresses fiber size and mineral type. Critical Reviews in Toxicology 38:49-73.

Bertrand, H.C., Clède, S., Guillot, R., Lambert, F., Policar, C. 2014. Luminescence modulations of rhenium tricarbonyl complexes induced by structural variations. Inorganic Chemistry 53(12):6204-6223.

Bindea, G., Mlecnik, B., Galon, J. 2011. The prognostic impact of anti-cancer immune response: a novel classification of cancer patients. Seminars in Immunopathology 33:335–340.

Biswas, S.K., Mantovani, A. 2010. Macrophage plasticity and interaction with lymphocyte subsets: cancer as a paradigm. Nature Immunology (10):889-96.

Blank, M., Goodman, R. 2009. Electromagnetic fields stress living cells. Pathophysiology 16(2-3):71-78.

Blasco, M.A. 2005. Telomeres and human disease: ageing, cancer and beyond. Nature Reviews Genetics 6(8):611-622.

Bogaert, J., Prenen, H. 2014. Molecular genetics of colorectal cancer. Annals of Gastroenterology 27(1): 9–14.

Bravi, F., Bosetti, C., Filomeno, M., Levi, F., Garavello, W., Galimberti, S., Negri, E., La Vecchia, C. 2013. Foods, nutrients and the risk of oral and pharyngeal cancer. British Journal of Cancer 109(11):2904-2910.

Brumatti, G., Sheridan, C. e Martin, S.J. 2008. Expression and purification of recombinant annexin V for the detection of membrane alterations on apoptotic cells. Methods 44: 235-240.

Brun, P., Zavan, B., Vindigni, V., Schiavinato, A., Pozzuoli, A., Iacobellis, C. e Abatangelo, G. 2012. *In vitro* response of osteoarthritic chondrocytes and fibroblast-like synoviocytes to a 500-730 kDa hyaluronan amide derivative. Journal of Biomedical Materials Research Part B: Applied Biomaterials 100(8):2073-2081.

Buttar, D., Colclough, N., Gerhardt, S., MacFaul, P.A., Phillips, S.D., Plowright, A., Whittamore, P., Tam, K., Maskos, K., Steinbacher, S., Steuber, H. 2010. A combined spectroscopic and crystallographic approach to probing drug–human serum albumin interactions. Bioorganic & Medicinal Chemistry 18:7486–7496.

Cabeza, N.A., Garcia, A.R., Carretero, M. N., Martos, M., Expósito, J.R. 2005. Synthesis, characterization and antiproliferative behavior of tricarbonyl complexes of rhenium(I) with some 6-amino-5-nitrosouracil derivatives: Crystal structure Of fac-[ReCl(CO)3(DANU-N5,O4)](DANU = 6-amino-1,3-dimethyl-5-nitrosouracil). Journal of Inorganic Biochemistry 99:1637–1645.

Campisi, J. 2013. Aging, Cellular Senescence, and Cancer. Annual Review of Physiology 75:685–705.

Carethers J. M. 2008. Systemic treatment of advanced coloretal cancer: Tailoring therapy to the tumor. Therapeutic Advances in Gastroenterology 1(1):33-62.

Castagna, A., Antonioli, P., Astner, H., Hamdan, M., Righetti, S.C., Perego, P., Zunino, F., Righetti, P.G. 2004. A proteomic approach to cisplatin resistance in the cervix squamous cell carcinoma cell line A431. Proteomics 4: 3246-3267.

Chang, K., Chang, W., Chang, Y., Hung, L., Lai, C., Yeh, Y., Chou, Y., Chen, C. 2013. Ran GTPase-Activating Protein 1 Is a Therapeutic Target in Diffuse Large B-Cell Lymphoma. Plos One 8(11):1-12.

Chen, K., Huang, Y., Chen, J. 2013. Understanding and targeting cancer stem cells: therapeutic implications and challenges. Acta Pharmacologica Sinica 34: 732–740.

Chen, J., Kohler, B. 2012. Ultrafast nonradiative decay by hypoxanthine and several methylxanthines in aqueous and acetonitrile solution. Physical Chemistry Chemical Phycsis 14**:**10677-10682**.**

Chen, K.G., Leapman, R.D., Zhang, G., Lai, B., Valencia, J.C., Cardarelli, C.O., Vieira, W.D., Hearing, V.J., Gottesman, M.M. 2009. Influence of Melanosome Dynamics on Melanoma Drug Sensitivity. Journal of the National Cancer Institute 101:1259–1271.

Chen, Y., Ahsan, H. 2004. Cancer burden from arsenic in drinking water in Bangladesh. American Journal of Public Health. 12:741–744.

Cheng, X., Hochlowski,J., Tang, H., Hepp, D., Beckner, C., Kantor, S., Schmitt, R. 2003. Studies on repository compound stability in DMSO under various conditions. Journal of Biomolecular Screening 8(3):292-304.

Chich, J.F., David, O., Villers, F., Schaeffer, B., Lutomski, D., Huet, S. 2007. Statistics for proteomics: Experimental design and 2-DE differential analysis. Journal of Chromatography 849:261–272.

Cho, R.W., Clarke, M.F. 2008. Recent advances in cancer stem cells. Current Opinion in Genetics and Development 18(1):48-53.

Collado, M., Serrano, M. 2010. Senescence in tumours: evidence from mice and humans, Nature Reviews Cancer 10(1): 51–57.

Collery, P., Bastian, G., Santoni, F., Mohsen, A., Wei, M., Collery, T., Tomas, A., Desmaele, D., D'Angelo, J. 2014. Uptake and efflux of rhenium in cells exposed to rhenium diseleno-ether and tissue distribution of rhenium and selenium after rhenium diseleno-ether treatment in mice. Anticancer Research 34(4):1679-1689.

Collery, P., Mohsen, A., Kermagoret, A., D'Angelo, J., Morgant, G., Desmaele, D., Tomas, A., Collery, T., Wei, M., Badawi, A. 2012. Combination of three metals for the treatment of cancer: gallium, rhenium and platinum. 1. Determination of the optimal schedule of treatment. Anticancer Research 32(7):2769-2781.

Collery, P., Shtemenko, N., Shtemenko, A., Bourleaud, M., Etienne, J.C., Maymard, I., Loriquet, P. 2004. Supplementation by rhenium compounds instead of iron compounds during the treatment by erythropoietin of anemia in cancer patients. Metal Ions in Biology and Medicine 8:534-537.

Cooper, G.M. 2000. The Cell: A Molecular Approach. Sinauer Associates, Sunderland, United States of America.

Curto, M., Cole, B.K., Lallemand, D., Liu, C.H., McClatchey, AI. 2007. Contact-dependent inhibition of EGFR signaling by Nf2/Merlin. Journal of Cell Biology 177(5):893-903.

Daniel, C.R., Cross, A.J., Koebnick, C., Sinha, R. 2011. Trends in meat consumption in the USA. Public Health Nutrition 14: 575–583.

DeBerardinis, R.J., Lum, J.J., Hatzivassiliou G., Thompson, C.B. 2008. The biology of cancer: metabolic reprogramming fuels cell growth and proliferation. Cell Metabolism 7(1):11-20.

De Palma, M., Coussens, L.M. 2008. Immune Cells and Inflammatory Mediators as Regulators of Tumor Angiogenesis *In* Angiogenesis (W. D. Figg and J. Folkman eds) 1st ed., pp 225-237, Springer, Switzerland.

Desai, M.A., Mehta, S., Smith, K.R. 2004. Indoor smoke from solid fuels: Assessing the environmental burden of disease at national and local levels. Version April 10, 2014. http://www.who.int/quantifying_ehimpacts/publications/en/Indoorsmoke.pdf in World Health Organization, http://www.who.int/en/.

Dieckmann, S., Kastl, A., Wahler,K.,Vçlker, T., Kastl, L., Merkel, A.L., Vultur, A., Shannan, B., Harms, K., Ocker, M., Parak, W., Herlyn, M., Meggers, E. 2013. Rhenium Complexes with Visible-Light-Induced Anticancer Activity. ChemMedChem 8:924 – 927.

Dilworth, J.R., Parrot, S.J. 1998. The biomedical chemistry of technetium and rhenium. Chemical Society Reviews 27: 43-55.

Dirat, B., Bochet, L., Escourrou, G., Valet, P., Muller, C. 2010. Unraveling the obesity and breast cancer links: a role for cancer-associated adipocytes? Endocrine Development 19:45-52.

Dumontet, C., Jordan, M. 2010. Microtubule-binding agents: a dynamic field of cancer therapeutics. Nature Review Drug Discovery 9(10): 790–803.

Egeblad, M., Nakasone, E.S., Werb, Z. 2010. Tumors as organs: complex tissues that interface with the entire organism. Dev Cell. 18(6): 884–901.

Emoto, K., Yamada, Y., Sawada, H. 2001. Annexin II overexpression correlates with stromal tenascin-C overexpression: a prognostic marker in colorectal carcinoma. Cancer 92:1419–1426.

Fernandes, A.R., Baptista, P.V. 2013. Nanotechnology for Cancer Diagnostics and Therapy – An Update on Novel Molecular Players. Current Cancer Therapy Reviews 9(3):164-172.

Feron, O. 2009. Pyruvate into lactate and back: from the Warburg effect to symbiotic energy fuel exchange in cancer cells. Radiotherapy Oncology 92(3):329-333.

Ferrone, C., Dranoff, G. J. 2010. Dual roles for immunity in gastrointestinal cancers. Clinical Oncology 28(26):4045-4051.

Fidler, I.J. 2003. The pathogenesis of cancer metastasis: the 'seed and soil' hypothesis revisited. Nature Reviews 3:453–458.

Finkel, T., Serrano, M., Blasco. M., 2007. The common biology of cancer and ageing. Nature 448: 767-774.

Florea, A.M., Büsselberg, D. 2011. Cisplatin as an Anti-Tumor Drug: Cellular Mechanisms of Activity, Drug Resistance and Induced Side Effects. Cancers *3*(1):1351-1371.

Food and Drug Administration. 2011. PLATINOL® (cisplatin for injection, USP). Version July 10, 2014. http://www.accessdata.fda.gov/drugsatfda_docs/label/2011/018057s080lbl.pdf in the FDA approved drug products, http://www.accessdata.fda.gov/scripts/cder/drugsatfda/.

Frezza, M., Hindo, S., Ping Dou, Q. 2010. Novel Metals and Metal Complexes as Platforms for Cancer Therapy. Current Pharmaceutical Design 16(16):1813–1825.

Galluzzi, L., Kroemer, G. 2008. Necroptosis: A Specialized Pathway of Programmed Necrosis. Cell 135 (7):1161–1163.

Galluzzi, L., Kepp, O., Heiden, M.G.V., Kroemer, G. 2013. Metabolic targets for cancer therapy. Nature Reviews Drug Discovery 12: 829–846.

Gamen, S., Anel, A., Perez-Galan, P., Lasierra, P., Johnson, D., Pineiro, A. and Naval, J. 2000. Doxorubicin treatment activates a Z-VAD-sensitive caspase, which causes deltapsim loss, caspase-9 activity, and apoptosis in Jurkat cells.Experimental Cell Research, 258:223–235.

Garzon, R., Marcucci, G., Croce, C.M. 2010. Targeting microRNAs in cancer: rationale, strategies and challenges. Nature Reviews Drug Discovery 9:775-789.

Gerl, R., Vaux, D.L. 2005. Apoptosis in the development and treatment of cancer. Carcinogenesis 26(2):263-270.

Gong, H.C., Wang, S., Mayer, G., Chen, G., Leesman, G., Singh, S., Beer, D.G. 2011. Signatures of Drug Sensitivity in Nonsmall Cell Lung Cancer. International Journal of Proteomics 2011:1-13.

GraphPad Software. 2010. Relative vs. absolute IC_{50}. Version September 24, 2013. http://www.graphpad.com/support/faqid/1566/ in GraphPad http://www.graphpad.com/.

Grivennikov, S.I., Greten, F.R., Karin, M. 2010. Immunity, Inflammation, and Cancer. Cell 140(6):883–899.

Grossi, V., Peserico, A., Tezil, T., Simone, C. 2014. p38α MAPK pathway: A key factor in colorectal cancer therapy and chemoresistance. World Journal of Gastroenterology 20(29): 9744-9758.

Guerriero, J.L., Ditsworth, D., Fan, Y., Zhao, F., Crawford, H.C., and ZonG, W. 2008. Chemotherapy Induces Tumor Clearance Independent of Apoptosis. Cancer Research 68(23):9595-9600.

Gupta, G.P., Massagué, J. 2006. Cancer metastasis: building a framework. Cell 127(4):679-695.

Hajian, R., Shams, N., Parvin, A. 2009. DNA-binding Studies of Daunorubicin in the Presence of Methylene Blue by Spectroscopy and Voltammetry Techniques. Chinese Journal of Chemistry. 27:1055-1060.

Hanahan, D., Weinberg, R.A. 2011. Hallmarks of cancer: the next generation. Cell 144(5):646-674.

Hanson, R., Kirssa, R., McCaskilla, E., Huaa, E., Tongcharoensirikula, P., Olmstedb, S.L., Labareec, D., Hochberg, R.B. 2012. Targeting the Estrogen Receptor with Metal-carbonyl Derivatives of Estradiol. Bioorganic & Medicinal Chemistry Letters 22(4): 1670-1673.

Hartinger, C.G., Dyson, P.J. 2009. Bioorganometallic chemistry - from teaching paradigms to medicinal applications. Chemical Society Reviews 38(2):391-401.

Heilbronner, G., Eisele, Y., Langer, F., Kaeser, S.A., Novotny, R., Nagarathinam, A., Aslund, A., Hammarstro, P., Nilsson, K., Jucker, M. 2013. Seeded strain-like transmission of b-amyloid morphotypes in APP transgenic mice. European Molecular Biology Organization reports 14(11): 1017-1022.

Hingorani, R., Deng, J., Elia, J., McIntyre, C., Mittar, D. 2011. Detection of Apoptosis Using the BD Annexin V FITC Assay on the BD FACSVerse™ System. Version 6 September 2014. https://www.bdbiosciences.com/documents/BD_FACSVerse_Apoptosis_Detection_AppNote.pdf in the BD Biosciences, https://www.bdbiosciences.com/.

Ho, J., Lee, W.Y., Koh, K.J., Lee, P.P., Yaw-Kai Yan, Y. 2013. Rhenium (I) tricarbonyl complexes of salicylaldehyde semicarbazones: Synthesis, crystal structures and cytotoxicity. Journal of Inorganic Biochemistry 119:10-20.

Holohan, C., Schaeybroeck, S., Longley, D., Johnston, P. 2013. Cancer drug resistance: an evolving paradigm. Nature Reviews Cancer 13:714–726.

Horváth, I., Vígh, L. 2010. Cell biology: Stability in times of stress. Nature 463:436-438.

Hutter, J.J. 2010. Childhood leukemia. Journal of the American Academy of Pediatrics 31(6): 234–241.

Inspiralis. 2006. Anticancer agentes. Version July 10, 2014. http://www.inspiralis.com/go/anti_cancer_agents.php in the Technical Information, http://www.inspiralis.com/.

Internation Agency for Research on Cancer. 2003. IARC Handbooks on Cancer Prevention. World Health Organization, Geneva.

Internation Agency for Research on Cancer. 2008. World Cancer Report 2008. Version April 10, 2014. http://www.iarc.fr/en/publications/pdfs-online/wcr/2008/wcr_2008.pdf in the IARC publications, http://www.iarc.fr/index.php.

Internation Agency for Research on Cancer. 2012. GLOBOCAN 2012: Estimated Cancer Incidence, Mortality and Prevalence Worldwide in 2012. Version April 10, 2014. http://globocan.iarc.fr/Pages/fact_sheets_cancer.aspx in the Cancer Fact Sheets, http://www.iarc.fr/index.php.

Jackson, S.P., Bartek, J. 2009. The DNA-damage response in human biology and disease. Nature. 461(7267):1071-1078.

Jakupec, M.A., Galanski, M., Arion, V.B., Hartinger, C.G., Keppler, B.K. 2008. Antitumour metal compounds: more than theme and variations. Dalton Transactions 2:183-194.

Jemal A., Center, M.M., DeSantis, C., Ward, E.M. 2010. Global patterns of cancer incidence and mortality rates and trends. Cancer Epidemiology Biomarkers & Prevention 19:1893–1907.

Jones, R.G., Thompson, C.B. 2009. Tumor suppressors and cell metabolism: a recipe for cancer growth. Genes & Development 23:537–548.

Kandaswami, C., Lee, L., Lee, P. H., Hwang, J., Ke, F., Huang, Y., Lee, M. 2005. The Antitumor Activities of Flavonoids. In vivo 19:895-910.

Kasibhatla, S., Amarante-Mendes, G.P., Finucane, D., Brunner, T., Bossy-Wetzel, E., Green, D.R. 2006. Staining of suspension cells with hoechst 33258 to detect apoptosis. Cold Spring Harbor Protocols 2006:3-4.

Kennedy, S.R., Loeb, L.A., Herr, A.J. 2012. Somatic mutations in aging, cancer and neurodegeneration. Mechanisms of Ageing and Development 133(4):118-126.

Kennedy, K.M., Dewhirst, M.W. 2010. Tumor metabolism of lactate: the influence and therapeutic potential for MCT and CD147 regulation. Future Oncology 6(1):127-48.

Kitanovic, I., Can, S., Alborzinia, H., Kitanovic, A., Pierroz, V., Leonidova, A., Pinto, A., Spingler, B., Ferrari, S., Molteni, R., Steffen, A., Metzler-Nolte, N., Wölfl, S., Gasser, G. 2014. A deadly organometallic luminescent probe: anticancer activity of a ReI bisquinoline complex. Chemistry 20(9):2496-2507.

Klein, M., Lotem, M., Peretz, T., Zwas, S.T., Mizrachi, S., Liberman, Y., Chisin, R., Schachter, J., Ron, I.G., Iosilevsky, G., Kennedy, J.A., Revskaya, E., Kater, A.W., Banaga, E., Klutzaritz, V., Friedmann, N., Galun, E., DeNardo, G. L., DeNardo, S. J., Casadevall, A., Dadachova, E., Thornton, G. B. 2013. Safety and Efficacy of 188-Rhenium-Labeled Antibody to Melanin in Patients with Metastatic Melanoma. Journal of Skin Cancer 2013: 1-8.

Kobayashi, S., Boggon, T. J., Dayaram, T. 2005. HER1 mutation and resistance of non-small-cell lung cancer to gefitinib.The New England Journal of Medicine 352(8):786–792.

Krewski, D., Lubin, J.H., Zielinski, J.M., Alavanja, M., Catalan, V.S., Field, R.W., Klotz, J.B., Letourneau, E.G., Lynch, C.F., Lyon, J.I. 2005. Residential radon and risk of lung cancer: A combined analysis of 7 North American case-control studies. Epidemiology 16:137-138.

Krysko, O., Love, Aaes, T., Bachert, C., Vandenabeele, P., Krysko, D.V. 2013. Many faces of DAMPs in cancer therapy. Cell Death and Disease 4:1-7.

Kroemer, G., Galluzzi, L., Kepp, O., Zitvogel, L. 2013. Immunogenic cell death in cancer therapy. Annual Review of Immunology 31:51–72.

Larsson, T., Wedborg, M., Turner, D. 2007. Correction of inner-filter effect in fluorescence excitation-emission matrix spectrometry using Raman scatter. Analytica Chimica Acta 583(2):357–363.

Lecina, J., Cortés, P., Llagostera, M., Piera, C., Suades, J. 2014. New rhenium complexes with ciprofloxacin as useful models for understanding the properties of [99mTc]-ciprofloxacin radiopharmaceutical. Bioorganic and Medicinal Chemistry 22(13):3262-3269.

Lee, S., Chan, J. 2012. Proteomic Identification of Chaperonin-containing Tail-less Complex Polypeptide-1 Gamma Subunit as a p53-responsive Protein in Colon Cancer Cells. Cancer Genomics and Proteomics 9(2):101-108.

Leiphrakpam, P., Rajput, A., Mathiesen, M., Agarwal, E., Lazenby, A., Are, C., Brattain, M., Chowdhury, S. 2014. Ezrin expression and cell survival regulation in colorectal cancer. Cellular Signaling 26(5):868-879.

Levine, B., Kroemer, G. 2008. Autophagy in the pathogenesis of disease. Cell 132(1):27-42.

Li, S., Tong, Y., Xie, X., Wang, Q., Zhou, H., Han, Y., Zhang, Z., Gao, W., Li, S., Zhang, X., Bi, R. 2006. Octameric Structure of the Human Bifunctional Enzyme PAICS in Purine Biosynthesis. Journal of Molecular Biology 366: 1603-1614.

Lisiak, N., Totoń, E., Rybczyńska, M. 2014. Autophagy, new perspectives in anticancer therapy. Postepy Hig Med Dosw 68(0):925-35.

Luo, J., Solimini, N.L., Elledge, S.J. 2009. Principles of cancer therapy: oncogene and non-oncogene addiction. Cell. 136(5):823-37.

Lüpertz, R., Wätjen,W., Kahl, R., Chovolou, Y. 2010. Dose- and time-dependent effects of doxorubicin on cytotoxicity, cell cycle and apoptotic cell death in human colon cancer cells Toxicology 271(3):115–121.

Ma, D.L., Che, C.M., Siu, F.M., Yang, M., Wong, K.Y. 2007. DNA binding and cytotoxicity of ruthenium(II) and rhenium(I) complexes of 2-amino-4-phenylamino-6-(2-pyridyl)-1,3,5-triazine. Inorganic Chemistry 46(3):740-749.

Madsen, C.D., Sahai, E. 2010. Cancer dissemination–lessons from leukocytes. Developmental Cell 19:13–26.

Madureira, P.A., Waisman, D.M. 2013. Annexin A2: The Importance of Being Redox Sensitive. International Journal of Molecular Sciences 14(2): 3568–3594.

Martínez-Lillo, J., Mastropietro, T.F., Lappano, R., Madeo, A., Alberto, M.E., Russo, N., Maggiolini, M., De Munno, G. 2011. Rhenium (IV) compounds inducing apoptosis in cancer cells. Chemical Communications 47(18):5283-5285.

Martins, L., Alegria, E.C., Smolenski, P., Kuznetsov, M.L., Pombeiro, A.J. 2013. Oxorhenium Complexes Bearing the Water-Soluble Tris(pyrazol-1-yl)methanesulfonate, 1,3,5-Triaza-7-

phosphaadamantane, or Related Ligands, as Catalysts for Baeyer−Villiger Oxidation of Ketones. Inorganic Chemistry 52: 4534−4546.

Martins, P., Marques, M., Coito, L., Pombeiro, A.J.L., Baptista, P.V., Fernandes, A.R. 2014. Organometallic Compounds in Cancer Therapy: Past Lessons and Future Directions. Anti-cancer Agents in Medicinal Chemistry 14. PMID: 25173559.

Masunaga, S., Tano, K., Nakamura, J., Watanabe, M., Kashino, G., Takahasi, A., Tanaka, H., Suzuki, M., Ohnishia, K., Kinashi, Y., Liu, Y., Ohnishi, T., Ono, K. 2010. Usefulness of Hexamethylenetetramine as an Adjuvant to Radiation and Cisplatin in the Treatment of Solid Tumors: its Independency of p53 Status. Journal of Radiation Research 51: 27-35.

Masunaga, S., Kono, K., Nakamura, J., Tano, K., Yoshida, H., Watanabe, M., Kashino, G., Suzuki, M., Kinashi,Y., Liu, Y., Ono, K. 2009. Usefulness of hexamethylenetetramine in combination with chemotherapy using free and pegylated liposomal doxorubicin in vivo, referring to the effect on quiescent cells. Oncology Reports 21(5):1307-1312.

Matchett, K.B., McFarlane, S., Hamilton, S.E., Eltuhamy, Y.S., Davidson, M.A., Murray J.T., Faheem, A.M., El-Tanani, M. 2014. Ran GTPase in Nuclear Envelope Formation and Cancer Metastasis. Advances in experimental medicine and biology 773:323-351.

McGee, A., Douglas, D.L., Yayun Liang, Y., Hyder, S.M., Baines, C. 2011. The mitochondrial protein C1qbp promotes cell proliferation, migration and resistance to cell death. Cell Cycle 10(23):4119-4127.

McGowan, E.M., Alling, N., Jackson, E.A., Yagoub, D., Haass, N.K. 2011. Evaluation of Cell Cycle Arrest in Estrogen Responsive MCF-7 Breast Cancer Cells: Pitfalls of the MTS Assay. Plos One 6(6):1-8.

Mester, J., Redeuilh, G. 2008. Proliferation of Breast Cancer Cells: Regulation, Mediators, Targets for Therapy. Current Medicinal Chemistry - Anti-Cancer Agents 8(8):872-885.

Miranda, S., Vergara, E., Mohr, F., Vos, D., Cerrada, E., Mendia, A., Laguna, M. 2008. Synthesis, Characterization, and in Vitro Cytotoxicity of Some Gold(I) and Trans Platinum(II) Thionate Complexes Containing Water-Soluble PTA and DAPTA Ligands. X-ray Crystal Structures of [Au($SC_4H_3N_2$)(PTA)],*trans*-[Pt($SC_4H_3N_2$)$_2$(PTA)$_2$], *trans*-[Pt(SC_5H_4N)$_2$(PTA)$_2$],and *trans*-[Pt(SC_5H_4N)$_2$(DAPTA)$_2$]. Inorganic Chemistry 47:5641.

Mojarad, E.D., Kuppen, P.J.K., Aghdaei, H.A., Zali, M.R. 2013. The CpG island methylator phenotype (CIMP) in colorectal cancer. Gastroenterology Hepatology from Bed to Bench 6(3):120–128.

Montero, M., Hernández, J., Estelrich, J. 1994. Fluorescence quenching of albumin. A spectrofluorimetric experiment. Biochemical Education 18(2):99-102.

Multhoff, G., Hightower, L. E. 2011. Distinguishing integral and receptor-bound heat shock protein 70 (Hsp70) on the cell surface by Hsp70-specific antibodies. Cell Stress and Chaperones 16:251–255.

Murdoch, C., Muthana, M., Coffelt, S.B., Lewis, C.L. 2008. The role of myeloid cells in the promotion of tumour angiogenesis. Nature Reviews Cancer 8: 618-631.

Murov, S., Carmichael, I., Hug, G. 1993. Handbook of Photochemistry. CRC Press, United States of America.

Nagy, J.A., Chang, S., Dvorak, M.D. 2010. Heterogeneity of the Tumor Vasculature. Seminars in Thrombosis and Hemostasis 36(3): 321–331.

Natarajan, B., Gaur, R., Hemmingsson, O., Kao, G., Naredi, P. 2013. Depletion of the ER chaperone ENPL-1 sensitizes *C. elegans* to the anticancer drug cisplatin. Worm 2(1):1-8.

Negrini, S., Gorgoulis, V.G., Halazonetis, T.D. 2010. Genomic instability — an evolving hallmark of cancer. Nature 11:220-228.

Nilsson, K., Ikenberg, K., Åslund, A., Fransson, S., Konradsson, P., Röcken, C., Moch, H., Aguzzi, A. 2010. Structural Typing of Systemic Amyloidoses by Luminescent-Conjugated Polymer Spectroscopy. The American Journal of Pathology 176(2):563–574.

Olmon, E.D., Hill, M.G., Barton, J.K. 2011. Synthesis and Characterization of Tricarbonyl Rhenium Complexes. Journal of American Chemical Society 133:13718.

Paez, J.P., Janne, P.A., Lee, J.C. 2004. HER1mutations in lung cancer: correlation with clinical response to gefitinib therapy. Science 304(5676):1497–1500.

Palchaudhuri, R. e Hergenrother 2007. DNA as a target for anticancer compounds: methods to determine the mode of binding and the mechanism of action. Current Opinion in Biotechnology 18: 497-503.

Parker, A.M., Kavallaris, M., McCarroll, J. 2014. Microtubules and Their Role in Cellular Stress in Cancer. Frontiers in Oncology 4:153-154.

Parson, C., Smith, V., Krauss, C., Banerjee, H.N., Reilly, C., Krause, J.A., Wachira, J.M., Giri, D., Winstead, A., Mandal, S.K. 2013. The Effect of Novel Rhenium Compounds on Lymphosarcoma, PC-3 Prostate and Myeloid Leukemia Cancer Cell Lines and an Investigation on the DNA Binding Properties of One of these Compounds through Electronic Spectroscopy. Journal of Bioprocessing & Biotechniques 4(1): 1-5.

Parson, C., Smith, V., Krauss, C., Banerjee, H.N., Reilly, C., Krause, J.A.,Wachira, J.M., Giri, D., Winstead, A., Mandal, S.K. 2013. Anticancer Properties of Novel Rhenium Pentylcarbanato Compounds against MDA-MB-468(HTB-132) Triple Node Negative Human Breast Cancer Cell Lines. British Journal of Pharmaceutical Research 4(3): 362-367.

Pasquier, E., Kavallaris, M. 2008. Microtubules: A dynamic target in cancer therapy. International Union of Biochemistry and Molecular Biology Life 60(3):165-170.

Paul, A., Garcia, Y.A., Zierer, B.,Patwardhan, C., Gutierrez, O., Hildenbrand, Z., Harris, D.C., Balsiger, H.A., Sivils, J.C., Johnson, J.L., Buchner, J., Chadli, A., Cox, M.B. 2014. The Cochaperone SGTA (Small Glutamine-rich Tetratricopeptide Repeat-containing Protein Alpha) Demonstrates Regulatory Specificity for the Androgen, Glucocorticoid, and Progesterone Receptors. Journal of Biological Chemistry 289(22):15297-15308.

Pavia, M., Bianco, A., Pileggi, C., Angelillo, I.F. 2003. Meta-analysis of residential exposure to radon gas and lung cancer. Bulletin of the World Health Organization 81:732–738.

Peinado, H., Portillo, F., Cano, A. 2004. Transcriptional regulation of cadherins during development and carcinogenesis. The International Journal of Developmental Biology 48(5-6):365-375.

Pettinari, C., Marchetti, F. Lupidi, G., Quassinti, L., Bramucci, M., Petrelli, D.,Vitali, L.A., Silva, M.F., Martins, L., Smolenski, P., Pombeiro, A.J.L. 2011. Synthesis, Antimicrobial and Antiproliferative Activity of Novel Silver(I) Tris(pyrazolyl)methanesulfonate and 1,3,5-Triaza-7-phosphadamantane Complexes. Inorganic Chemistry 50:11173−11183.

Pietras, K., Ostman, A. 2010. Hallmarks of cancer: interactions with the tumor stroma. Experimental Cell Research 316(8):1324-1331.

Pracht, M., Edeline, J., Lepareur, N., Lenoir, L., Ardisson, V., Clement, B., Raoul, J.L., Audrain, O., Boucher, E., Garin, E. 2013. In vitro demonstration of synergy/additivity between (188) rhenium and sorafenib on hepatoma lines: preliminary results. Anticancer Research 33(9):3871-3877.

Qian, B.Z., Pollard, J.W. 2010. Macrophage diversity enhances tumor progression and metastasis. Cell 141(1):39-51.

Rasanen, K., Vaheri, A. 2010. Experimental Cell Research 316:2713–2722.

Riss, T., Moravec, R., Niles, A., Benink, H., Worzella, T., Minor, L. 2013. Cell viability assays. Version April 10, 2014. http://www.ncbi.nlm.nih.gov/books/NBK144065/pdf/mttassays.pdf in the The National Center for Biotechnology Information http://www.ncbi.nlm.nih.gov/.

Riccia, M.S., Zong, W. 2006. Chemotherapeutic Approaches for Targeting Cell Death Pathways. The oncologist 11(4):342-357.

Robertson, A., Allen, J., Laney, R., Curnow, A. 2013. The cellular and molecular carcinogenic effects of radon exposure: a review.

Romay, L., Portela, S., Cuevas, E., Gil-Martín, E., Fernández-Briera, A. 2011. Identification of α(1,6)fucosylated proteins differentially expressed in human colorectal cancer. BioMed Central Cancer 11:508-509.

Rosca, E.V., Koskimaki, J.E., Rivera, C.G., Pandey, N.B., Tamiz, A.P., Popel, A.S. 2011. Anti-angiogenic peptides for cancer therapeutics. Current Pharmaceutical biotechnology 8:1101-1116.

Sabeh, F., Shimizu-Hirota, R., Weiss, S.J. 2009. Protease-dependent versus -independent cancer cell invasion programs: three-dimensional amoeboid movement revisited. Journal of Cell Biology 185(1):11-19.

Saraste, A., Pulkki, K. 2000. Morphologic and biochemical hallmarks of apoptosis. Cardiovascular Research 45: 528–537.

Schatzschneider, U. 2010. Photoactivated Biological Activity of Transition-Metal Complexes. European Journal of Inorganic Chemistry 2010: 1451–1467.

Schreier, V., Pethő, L., Orbán, E., Marquardt, A., Petre, B., Mező, G., Manea, M. 2014. Protein Expression Profile of HT-29 Human Colon Cancer Cells after Treatment with a Cytotoxic Daunorubicin-GnRH-III Derivative Bioconjugate. Plos One 9(4):1-6.

Scolaro, C., Geldbach, T.J., Rochat, S., Dorcier, A., Gossens, C., Bergamo, A., Cocchietto, M., Tavernelli, I., Sava, G., Rothlisberger, U., Dyson, P.J. 2006. Influence of hydrogen-bonding substituents on the cytotoxicity of RAPTA compounds. Organometallics 25:756‑765.

Scolaro, C., Bergamo, A., Brescacin, L., Delfino, R., Cocchietto, M. G., Laurenczy, T.J., Geldbach, G., Sava, P.J., Dyson, J. 2005. In Vitro and in Vivo Evaluation of Ruthenium(II)−Arene PTA Complexes. Journal of Medicinal Chemistry 48:4161-4162.

Semenza GL. 2008. Tumor metabolism: cancer cells give and take lactate. Journal of Clinical Investigation 118(12):3835-3827.

Sethi, T., El-Ghamry, M., Kloecker, G. 2012. Radon and lung cancer. Clinical Advances in Hematology and Oncology 10:157–164.

Shanker, M., Jin, J., Branch, C.D., Miyamoto, S., Grimm, E.A., Roth, J.A., Ramesh, R. 2011. Tumor suppressor gene-based nanotherapy: from test tube to the clinic. Journal of Drug Delivery 2011: 1-10.

Shtemenko, A., Shtemenko, N., Oliyvnyk, S.A., Zelenuk, M.A. 2002. Lyposome forms of rhenium cluster compounds in models of haemolytic anemia. Metal Ions in Biology and Medicine 7:558-561.

Shi, Y., Deng, X., Zhan, Q., Shen, B., Jin, X., Zhu, Z., Chen, H., Li, H., Peng, C. 2013. A Prospective Proteomic-Based Study for Identifying Potential Biomarkers for the Diagnosis of Cholangiocarcinoma. Journal of Gastrointestinal Surgery 17:1584–1591.

Shimoda, M., Mellody, K.T., Orimo, A. 2010. Carcinoma-associated fibroblasts are a rate-limiting determinant for tumour progression. Seminars in Cell and Developmental Biology 21(1):19-25.

Silva, J.P. 2012. Caracterização do Potencial Citotóxico e Mecanismos de Acção de um Complexo de Platina de Configuração *trans* em Células Animais. Master Thesis. Faculty of Science and Technology, Universidade Nova de Lisboa.

Singh, A., Settleman, J. 2010. EMT, cancer stem cells and drug resistance: an emerging axis of evil in the war on cancer. Oncogene 29(34):4741-4751.

Sirajuddin, M., Ali, S., Badshah, A. 2013. Drug–DNA interactions and their study by UV–Visible, fluorescence spectroscopies and cyclic voltammetry. Journal of Photochemistry and Photobiology 124: 1–19.

Smilkov, K., Janevik, E., Guerrini, R., Pasquali, M., Boschi, A., Uccelli, L., Domenico, G., Duatti, A. 2014. Preparation and first biological evaluation of novel Re-188/Tc-99m peptide conjugates with substance-P. Applied Radiation and Isotopes 92C:25-31.

Subramanya, D., Grivas, P.D. 2008. HPV and cervical cancer: updates on an established relationship. Postgraduate Medical Journal 120(4):7-13.

Sun, B., Karin, M. 2014. The therapeutic value of targeting inflammation in gastrointestinal cancers. Trends in Pharmacological Sciences 35(7):349-357.

Steeg, P., Theodorescu, D. 2008. Metastasis: a therapeutic target for cancer. Nature Clinical Practice Oncology 5(4): 206–219.

Swift, L. P., Cutts, S. M., Rephaeli, A., Nudelman, A., Phillips, D. R. 2003. Activation of adriamycin by the pH-dependent formaldehyde-releasing prodrug hexamethylenetetramine. Molecular Cancer Therapeutics 2(2):189-198.

Tacar, O., Sriamornsak, P., Dass, C. 2012. Doxorubicin: an update on anticancer molecular action, toxicity and novel drug delivery systems. Journal of Pharmacy and Pharmacology 65(2)157–170.

Todosi, A.M., Gavrilescu, M.M., Aniţei, G.M., Filip, B., Scripcariu, V. 2012. Colon cancer at the molecular level--usefulness of epithelial-mesenchymal transition analysis. Revista medico-chirurgicala a Societatii de Medici si Naturalisti din Iasi's 116(4):1106-1111.

Urbanek, J. 2014. Multiphoton Ionization and Recombination Dynamics in Liquid-to-Supercritical Ammonia. PhD thesis. Fakultät der Rheinischen Friedrich-Wilhelms-Universität Bonn.

Valastyan, S., Weinberg, R.A. 2011. Tumor metastasis: molecular insights and evolving paradigms. Cell 147(2):275-292.

Vincent, T., DeVita, J., Edward, Chu. 2008. A History of Cancer Chemotherapy. Cancer Research. 68(21):8643-8653.

Vock, C.A., Renfrew, A.K., Scopelliti, R., Juillerat-Jeanneret, L., Dyson, P.J. 2008. European Journal of Inorganic Chemistry. 2008(10):1661–1671.

Vogelstein, B., Lane, D., and Levine, A. J. 2000. p53: The Most Frequently Altered Gene in Human Cancers. Nature 408:307–310.

Wang, C. and Lin, C. 2014. Annexin A2: Its Molecular Regulation and Cellular Expression in Cancer Development. Disease Markers 2014:1-10.

Wang, H.Y., Lin, W.Y., Chen, M.C., Lin, T., Chao, C.H., Hsu, F.N., Lin, E., Huang, C.Y., Luo T.Y., Lin, H. 2013. Inhibitory effects of Rhenium-188-labeled Herceptin on prostate cancer cell growth: a possible radioimmunotherapy to prostate carcinoma. International Journal of Radiation and Biology 89(5):346-355.

Wang, Y., Chiu, J. 2008. Proteomic Approaches in Understanding Action Mechanisms of Metal-Based Anticancer Drugs. Metal-Based Drugs 2008:1-9.

Wang, Y., Miao, Z. 2013. Marine-Derived Angiogenesis Inhibitors for Cancer Therapy. Marine Drugs 11(3):903-933.

White, E., DiPaola, R.S.2009. The double-edged sword of autophagy modulation in cancer. Clinical Cancer Research 15(17):5308-5316.

Winslow, T. 2014. Colon Cancer Treatment. Version 4 September 2014. http://www.cancer.gov/cancertopics/pdq/treatment/colon/Patient/page2#Keypoint11 in National Cancer Institute, http://www.cancer.gov/.

World Health Organization. 2011. Global Health and Aging. Version September 24, 2013. http://www.who.int/ageing/publications/global_health.pdf in the Ageing and Life Course Publications, http://www.who.int/en/.

World Health Organization. 2013. Cancer prevention. Version August 27, 2013. http://www.who.int/cancer/prevention/en/ in Cancer, http://www.who.int/cancer/en/.

Wood, J., White, I.R., Cutler, P. 2004. A likelihood-based approach to defining statistical significance in proteomic analysis where missing data cannot be disregarded. Signal Processing 84(10):1777-1788.

Wu., W., Zhao, S. 2013. Metabolic changes in cancer: beyond the Warburg effect. Acta Biochimica et Biophysica Sinica 45(1): 18-26.

Wuest, F., Bouvet, V., Mai, B., LaPointe, P. 2012. Fluorine- and rhenium-containing geldanamycin derivatives as leads for the development of molecular probes for imaging Hsp90. Organic & Biomolecular Chemistry 10(33):6724-6731.

Yap, T. A., Omlin, A., De Bono, J. S. 2013. Development of therapeutic combinations targeting major cancer signaling pathways. Journal of Clinical Oncology 31:1592–1605.

Yao, Y., Jia, X., Tian, H., Jiang, Y., Xu, G., Qian, Q., Zhao, F. 2009. Comparative proteomic analysis of colon cancer cells in response to Oxaliplatin treatment. Biochimica et Biophysica Acta 1794: 1433-1440.

Yumata, N.C. 2010. Reactivity of Rhenium(III) and Rhenium(V) with multidentate NN- and NO-Donor Ligands. MSc degree. Faculty of Science, Nelson Mandela Metropolitan University.

Zeestraten, E., Benard, A., Reimers, M.S., Schouten, P., Liefers, G.J., van de Velde, C., Kuppen, P.J.K. 2013. The prognostic Value of the Apoptosis pathway in colorectal Cancer: A Review of the Literature on Biomarkers Identified by Immunohistochemistry.Biomarkers in Cancer 2013(5):13-29.

Zhao, Y., Butler, E.B.,Tan, M. 2013. Targeting cellular metabolism to improve cancer therapeutics. Cell Death and Disease 4:1-10.

Zhang, Y., Woodford, N., Xia, X., Hamburger, A.W. 2003. Repression of E2F1-mediated transcription by the ErbB3 binding protein Ebp1 involves histone deacetylases Nucleic Acids Research 31:168.

Zobi, F., Blacque, O., Sigel, R.K., Alberto, R. 2007. Binding interaction of $[Re(H_2O)_3(CO)_3]+$ with the DNA fragment d(CpGpG). Inorganic Chemistry 46: 10458-10460.

6 Annex

Table 6.1 Lysis Buffer constitution.

Lysis Buffer	
Stock	**Final concentration**
phosphate inhibitor[1] (10x)	1x
protease inhibitor[2] (5x)	1x
NP-40[3] (10%, v/v)	2% (v/v)
Dithiothreitol[4] (10%)	0.1%
Phenylmethanesulfonyl fluoride[5] (10%)	0.1%
Tris-NaCl EDTA buffer pH 8.2[6] (5.5x)	1x

Legend: [1]PhosStop, Roche, Basel, Switzerland; [2]Complete Mini, Roche, Basel, Switzerland; [3]Thermo Scientific, Waltham, United States of America; [4] Promega, Madison, United States of America; [5]Sigma, St. Louis, United States of America; [6]150mM NaCl (VWR, Radnor, Pennsylvania), 50mM Tris (Sigma, St. Louis, United States of America) and 5mM EDTA (Sigma, St. Louis, United States of America).

Table 6.2 Rehidration Buffer constitution.

Rehidration Buffer	
Stock	**Final concentration**
Urea[1]	7 M
thioreia[2]	2 M
Chaps detergent [3] (10%)	2%
phosphate inhibitor [4] (10%)	1%
protease inhibitor [5] (5x)	1x
blue bromophenol [6]	traces

Legend: [1]Sigma, St. Louis, United States of America; [2]Sigma, St. Louis, United States of America; [3]GE healthcare, Wilmington, United States of America; [4]PhosStop, Roche, Basel, Switzerland; [5]Complete Mini, Roche, Basel, Switzerland and [6]Riedel-de Haën, Saint Louis, United States of America.Buffer stored in aliquots of 500 µL at -20ºC until use.

Table 6.3 SDS loading buffer constitution.

SDS loading buffer	
Concentration stock	**Final concentration**
glycerol[1]	40%
SDS[2]	8%
Tris-HCl[3]	200 mM

Legend: [1] Panreac, Barcelona, Spain; [2] Riedel-de Haën, Saint Louis, United States of America and [3] Merck, Whitehouse Station, United States of America.

Table 6.4 Poliacrilamide gels constitution.

Poliacrilamide gels		
	Separation gel	**Stacking gel**
Stock	**Volumes**	**Volumes**
Acrylamide/bisacrilamide [(1)]	4 mL	620 µL
Distilled water	3.5 mL	3.13 mL
Tris-HCl 1.5M pH 8.8[(2)]	2.5 mL	----
Ammonium persulfate (10%)[(3)]	75 µL	50 µL
Tetramethylethylenediamine[(4)]	10 µL	5 µL
Tris-HCl 0.5M pH 6.8[(2)]	---	1.25 mL

Legend: Recipe for two 12% poliacrilamide separation gels and two 3.7% stacking gels. [(1)]30%, Merck, Darmstadt, Germany;[(2)]Calbiochem, Darmstadt, Germany; [(3)]Biorad, California, United States of America; [(4)] Sigma, Saint Louis, United States of America.

Table 6.5 Electrophoresis buffer. Electrophoresis buffer (10x, pH 8.6-8.8) is prepared in a more concentrated solution and then diluted 10x with 0.1% of SDS (20%, p/v) [(3)] and Milli-Q water up to 1000 mL.

Electrophoresis buffer (10x)	
Solution	**Concentration or volume**
glycerol[(1)]	1.92 M
Tris base[(2)]	250 mM
Milli-Q water	500 mL

Legend: [(1)] Panreac, Barcelona, Spain; [(2)] Calbiochem, Darmstadt, Germany.

Table 6.6 Staining solution for proteomic gels.

Staining solution	
PhasTGel™ Blue R [(1)]	three tablets
acetic acid (10%, v/v)[(2)]	1 L
Milli-Q water	500 mL

Legend: [(1)]GE Healthcare, Wilmington, United States of America; [(2)]Panreac, Barcelona, Spain.

Table 6.7 Equilibration solution for proteomic strips.

Equilibration solution	
Solution	**Concentration**
Tris-HCl pH 8.8 [(1)]	70 mM
urea[(2)]	6 M
Glycerol[(3)]	30% (v/v)
SDS[(4)]	2% (p/v)
Bromophenol blue[(5)]	traces

Legend: [(1)]Calbiochem, Darmstadt, Germany, [(2)]Scharlau, Barcelona, Spain; [(3)]Panreac, Barcelona, Spain; [(4)] Riedel-de Haën, Saint Louis, United States of America and [(5)]Riedel-de Haën, Saint Louis, United States of America.